

**KERNFORSCHUNGSZENTRUM  
KARLSRUHE**

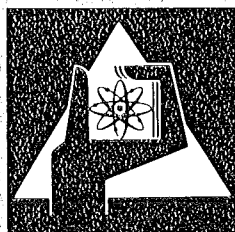
Oktober 1975

KFK 2193

Institut für Reaktorentwicklung  
Projekt Schneller Brüter

**Results of Measurements of Thermal Interaction  
between Molten Metal and Water**

W. Zyszkowski



**GESELLSCHAFT  
FÜR  
KERNFORSCHUNG M.B.H.**

**KARLSRUHE**

Als Manuskript vervielfältigt

Für diesen Bericht behalten wir uns alle Rechte vor

GESELLSCHAFT FÜR KERNFORSCHUNG M. B. H.  
KARLSRUHE

Institut für Reaktorentwicklung  
Projekt Schneller Brüter

Results of measurements of thermal interaction  
between molten metal and water

W. Żyszkowski\*

Gesellschaft für Kernforschung mbH, Karlsruhe

---

\*Delegate from the Institute of Nuclear Research, Świerk near  
Warsaw, Poland.



The author takes pleasure to thank Professor Dr. D. Smidt, Director of the Institut für Reaktorentwicklung, Kernforschungszentrum Karlsruhe, and colleagues of the Institut, particularly to Mr. H. Will, for their help in performing this study.

The author also thanks the colleagues of the Institut für Metal- und Festkörperforschung, Kernforschungszentrum Karlsruhe and of Karlsruhe University for their help in carrying out many supplementary studies.

The author gratefully acknowledges the Alexander von Humboldt-Foundation for the fellowship granted to him and the Kernforschungszentrum Karlsruhe for the technical facilities made available.

Abstract

The report describes results of an experimental investigation into thermal interaction of molten metals with water. The experiments were performed in two stages: The aim of the first stage was to study the general character of thermal interaction between molten metal and water and to measure the Leidenfrost temperature of the inverse Leidenfrost phenomenon. The second stage was directed to the experimental study of the triggering mechanism of thermal explosion.

The experimental material gathered in this study includes:

1. transient temperature measurements in the hot material and in water,
2. measurements of pressure and reactive force combined with thermal explosion,
3. high-speed films of thermal interaction,
4. investigation results of thermal explosion debris (microscopic, mechanical, metallographical and chemical).

The most significant observation is, that small jets from the main particle mass occurring 1 to 10 msec before, precede thermal explosion.

Zusammenfassung

Ergebnisse von Versuchen bezüglich der thermischen Wechselwirkung von geschmolzenem Metall und Wasser

Der Bericht beschreibt Ergebnisse von experimentellen Untersuchungen der thermischen Wechselwirkung von geschmolzenem Metall mit Wasser.

Die Versuche wurden in zwei Serien durchgeführt: Ziel der ersten Versuchsserie war das Studium des generellen Charakters der thermischen Wechselwirkung zwischen geschmolzenem Metall und Wasser und die Ermittlung der Leidenfrost-Temperatur des inversen Leidenfrost-Phänomens. Im zweiten Stadium waren die Arbeiten gerichtet auf das experimentelle Studium des Auslösemechanismus der thermischen Explosion.

Das in dieser Arbeit beschriebene Material beinhaltet:

1. Transiente Temperaturverläufe im heißen Material und in Wasser.
2. Messungen des Druckes und der Reaktionskraft in Verbindung mit der thermischen Explosion.
3. Hochgeschwindigkeits-Filmaufnahmen der thermischen Wechselwirkung.
4. Ergebnisse von Nachuntersuchung der Explosionsprodukte (Mikroskopisch, mechanisch, metallographisch und chemisch).

Die bedeutendste Beobachtung ist, daß kleine "jets" vom heißen Partikel 1 bis 10 msec vor der thermischen Explosion auftreten.

Contents

1. Introduction	1
2. Experimental technique	3
3. Results of measurements and description of the phenomena observed	10
3.1 Normal course of heat transfer	23
3.1.1 Film boiling	36
3.1.2 Transplosion and the following phenomena	40
3.2 Thermal explosion	45
3.2.1 Thermal explosion a short distance below the cold liquid surface	45
3.2.2 Thermal explosion at the bottom of the vessel	47
3.3 Special effects	72
3.3.1 Hydrodynamic partition	72
3.3.2 "Jets"	72
3.3.3 "Empty Shell"-particles	73
4. Conclusions	77
5. References	78
6. Appendixes	81

## 1. Introduction

Fast reactor safety requires to consider accidents which are e.g. caused by a local blockage of several flow channels inside a subassembly. Such flow disturbances may lead to fuel melting and an explosive energy release, if molten fuel and sodium are coming in contact. The energy release mechanism during such a molten-fuel-coolant-interaction (MFCCI) is not yet understood sufficiently. Caldarola gave an excellent review of current research effort in this field [1].

The aim of this study was to examine the events which may occur during a thermal interaction of a hot molten substance and a cold liquid.

In particular these are

- measurement of the Leidenfrost temperature of the inverse Leidenfrost phenomenon.
- recording of temperatures, pressure and reaction force during the thermal interaction.
- filming of the events.
- postexperiment examination of the solidified particles.

The results and their interpretation in comparison with a theoretical effort should lead to an answer of the question under which conditions a thermal explosion is possible and what is its maximum energy release.

In this report only the experimental facts of simulation experiments are given. With respect to a simple handling most of the experiments were made with copper and water. The details of the experimental technique are given in the following chapter.

Preliminary results of the study were presented at conferences [13, 14, 15, 18] and described in a paper [17]. Preliminary results of the copper-sodium thermal interaction are given in [11]. Final results of the Leidenfrost temperature measurements will be summarized in [18]. Concepts of the theoretical interpretation of the thermal explosion phenomenon can be found in [15, 16, 17]. Details of a hypothesis on the mechanism of thermal explosion will be given in [19].

A sound film showing several thermal explosions taken with a high-speed camera provides supplementary material to the foregoing descriptions [12].

In series of tests, the following types of thermal interaction can be specified:

1. Normal course of thermal interaction.
2. Thermal explosion.
3. Intermediate courses.

Normal course considers quiet heat transfer between the hot material and the cold liquid. Thermal explosion considers violent interaction of hot and cold substances and can be divided into the following two processes:

1. Fragmentation of the hot material.
2. Vapour explosion of the cold liquid.

The foregoing processes will be described in more detailed in the next sections.

## 2. Experimental technique

Thermal interaction was realized for small amounts of molten metal or other "hot material" interacting with the "cold liquid" - water or other substance - which is used as a coolant in reactor technology as e.g. liquid sodium.

The initial temperatures of the interacting substances were varied, the temperature histories during thermal interaction recorded, and sometimes the phenomena filmed.

A levitation coil as well as a small vessel with thermocouples in its bottom, a high speed camera and recording equipment were used (fig. 1).

Small metal particles of a defined mass were molten and heated to a determined temperature in the levitation coil. The power supplied to the coil was 10 kW in the maximum (see Appendix 1) at 0.6 MHz. The advantage of the method is that no crucible is needed. The problem consists in developing a coil design that will allow both efficient heating and stable levitation of the particle [5]. The theoretical treatment of the levitation of a liquid mass is limited [5, 6] and the experimental procedure was preferred in these tests. The levitation coil was constructed on a design given in [1, 2] (Appendix 1).

The small metal particle was suspended at a thin wire or at a thermocouple in the levitation coil. The levitation condition began after melting of the particle, subsequently, a mechanical support was not necessary. The temperature of the particle increased without any contact with its surroundings and the levitation time determined its final value (This method was normally used for temperature approximation of the metal particle in the levitation coil). In the levitation coil, the following metals were molten: Ag, Al, Au, Cu, Fe, Pb, Sn, Zn and stainless steel.

The hot molten metal particle dropped into the vessel containing the cold liquid upon interruption of the current in the levitation coil. This resulted in thermal interaction of both substances.

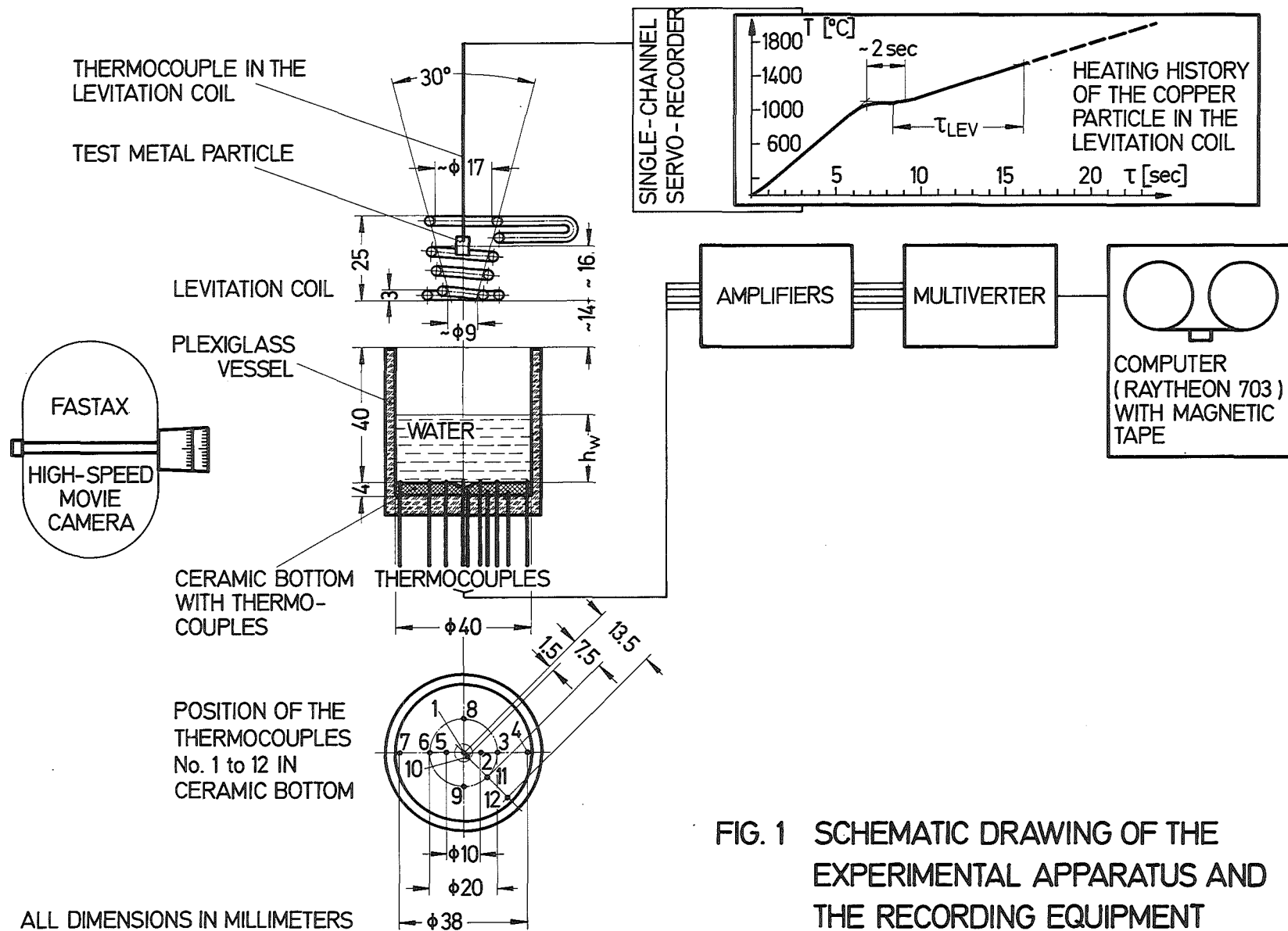


FIG. 1 SCHEMATIC DRAWING OF THE EXPERIMENTAL APPARATUS AND THE RECORDING EQUIPMENT

In the experiments with water, a plexiglass vessel was used to allow observation of the phenomena. The bottom of the vessel was made from a ceramic (Thermostix 2000) in which several thermocouples were installed. Thermocouple No. 1, placed in the centre of the bottom (Fig. 2), measured the temperature history of the metal particle. Other thermocouples usually measured the temperature of the water or the hot metal temperature, if the particle touched temporarily the additional thermocouple.

In the experiments with sodium stainless steel was chosen as the construction material for the vessel. In the centre of the bottom, a small plate of 10 mm O.D., made from tungsten was employed in the high temperature range.

Standard chromel-alumel thermocouples of the grounded-type and of 0.5 mm O.D. surrounded by a steel sheath (4301) with  $MgO$  insulating material were used in the experiments with water. The thermometric lag of these thermocouples were of the order of magnitude of 6 - 15 msec measured in sodium [8]. W-W26Rh - thermocouples were tested for the high temperature range, but the large thermometric lag made the interpretation difficult.

Signals from the thermocouples were recorded by a high-speed digitising system based on the Raytheon 703 Computer. A 500 Hz scanning frequency was used in the preliminary measurements. In the second stage of experiments, a 1 kHz scanning frequency was chosen for temperature measurements and 20 kHz (or 80 kHz for some tests) for pressure and force measurements. The integrated standard system SEDAP served for experimental data processing [20]. Signals from the thermocouple in the levitation coil (of the same type as at the bottom of the vessel) were indicated by a single-channel servo-recorder and recorded on a paper tape. Photographic data were obtained using a Fastax high-speed camera (up to 8000 frames per sec.)

A block diagram of the experimental arrangement is shown in Fig. 1.

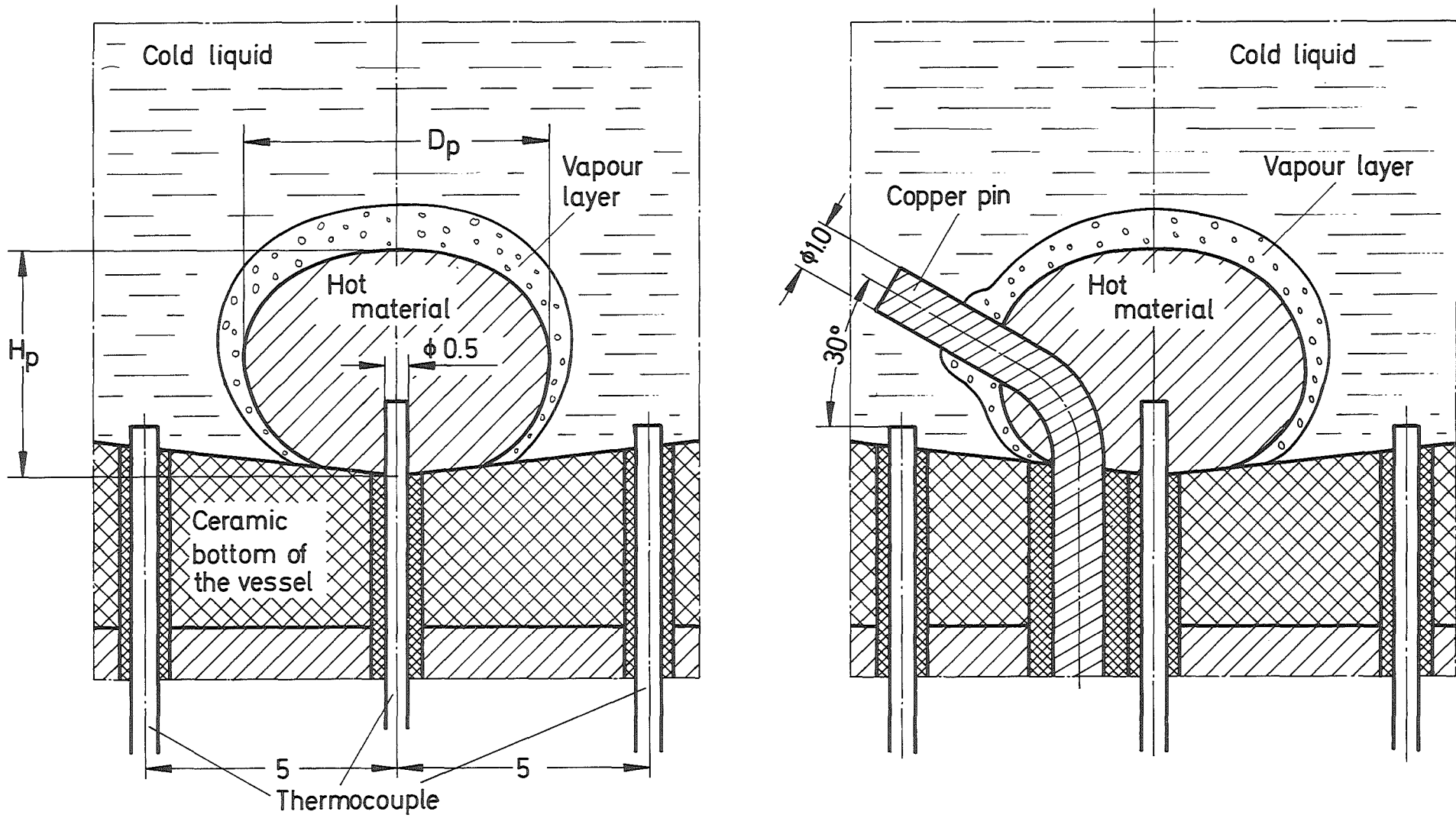


Fig. 2 Model of the hot material particle on the bottom of the experimental vessel.

In the experiments with an inert gas atmosphere (for some tests with water and for all tests with sodium), a simple vacuum-tight safety vessel was used. In principle, the same measurement technique was used. Argon, nitrogen, and "vacuum" were used as inert gas atmosphere. (Table 1).

The measurement technique was improved in the second stage of experiments and additional variables were recorded to complete the experimental data related to thermal explosion. The frequency of occurrence of thermal explosions was increased by use of a "triggering pin". This pin of 1- 1.35 mm O.D. was installed into the bottom of the vessel before thermal interaction. It promoted the "direct contact" between the molten hot material and the cold liquid (Fig. 2). A "thermal bridge" was generated and it increased the heat transfer rate between the two substances.

Alloys were also used as the hot material. Measurements based on this method were, however, limited in number. Only a few experiments were made with the (Ag+Cu)/water system.

In the second stage of this study, the following investigations were performed in addition to the transient temperature measurements:

1. Transient pressure and reactive force measurements using piezoelectric gauges (Kistler with a resonant frequency of 130 kHz and 80 kHz). 20 kHz scanning frequency were used.

2. Particle size analysis of thermal explosion debris. Meshes of: 10, 30, 50, 80, 100, 200, 500 and 800  $\mu\text{m}$  were used.

3. Metallographic investigation of:

- 3.1. Particles after normal course of thermal interaction, and

- 3.2. The formation of the debris of weak thermal explosion. Particles were cut, polished and studied with an optical microscope. (The debris of a strong explosion were too small for a postexperiment examination).

4. Microscopic study of thermal explosion debris with the scanning electron microscope.

Table 1. Specification of the experimental conditions

Specification		Experimental conditions	Remarks and main parameters investigated
Hot Material "HM"	Kind	Ag, Al, Au, Cu, Fe, Nb, Pb, Sn, Zn, SS	Cu
	Initial temp. [°C]	melting point to 1800 (to 2400)	Melting point to 7500
	Mass [g]	0.4 to 2	~0.5
Cold Liquid "CL"	Kind	water, sodium, ice (H <sub>2</sub> O, CO <sub>2</sub> + H <sub>2</sub> O, CO <sub>2</sub> ), N <sub>2</sub> liquid	water
	Volume [cm <sup>3</sup> ]	2 to 50	20, 25, 30
	Initial temp. [°C]	15 to 82 and temperature of ice and of liquid nitrogen	~ 20
Gas atmosphere		air argon (40 to 760 torr), nitrogen (300, 500 torr)	air
Interaction zone	Geometry	Cylindrical: Ø 40x40, Ø 30x35, Ø 20x25; Half-spherical: R <sub>S</sub> =20, R <sub>S</sub> =10	Cyl. Ø 40x40; Upper half of the sphere
	Bottom material	Ceramic (Thermostix 2000, Alumina), Graphit, Asbestos, Mica, Tungsten	Thermostix 2000
Initial "HM"- "CL" distance [mm]		15 to 80	30
Number of	tests	542	522 with water
	explosions observed	68	61 in water and air

5. Chemical analysis to determine the oxide content in the particle. Particles were analysed after normal course and the formation of thermal explosion debris.

6. Determination of the total surface of the thermal explosion debris by means of the nitrogen adsorption method.

### 3. Results of measurements and description of the phenomena observed.

Various hot material/cold liquid systems were considered in this study. The aim was to choose a system which allowed one to study various types of thermal interaction in a broad range of temperatures. Photographic results of this study are given in Fig. 3. Particles of various forms can be seen as a function of the hot material and of the course of interaction.

The copper/water system was found to be suited for the detailed study. Copper particles allowed to attain a favourable ratio between the levitation force and the power input to the particle in the levitation coil. The melting point of copper ( $1083^{\circ}\text{C}$ ) was advantageous for studying all basic regimes of boiling. Temperatures were recorded by standard thermocouples. The occasional occurrence of thermal explosion draws the attention to the cause and mechanism of this phenomenon. In the series of tests, technically pure copper particle (E-Cu 99.9 DIN 1708) weighting about 0.5 - 1.5 g were heated to  $1800^{\circ}\text{C}$  at the maximum. For various copper particles, the shut-off temperature (or levitation time) in the levitation coil, the temperature of the water from about 10 to  $80^{\circ}\text{C}$ , the volume of the water from 5 to  $50\text{ cm}^3$ , and the distance between the levitation coil and the bottom of the plexiglass vessel from about 40 to 80 mm were varied. The experimental conditions are summarized in Table 1.

The phases of heating and cooling which the individual metal particle passed in the experiments, were normally:

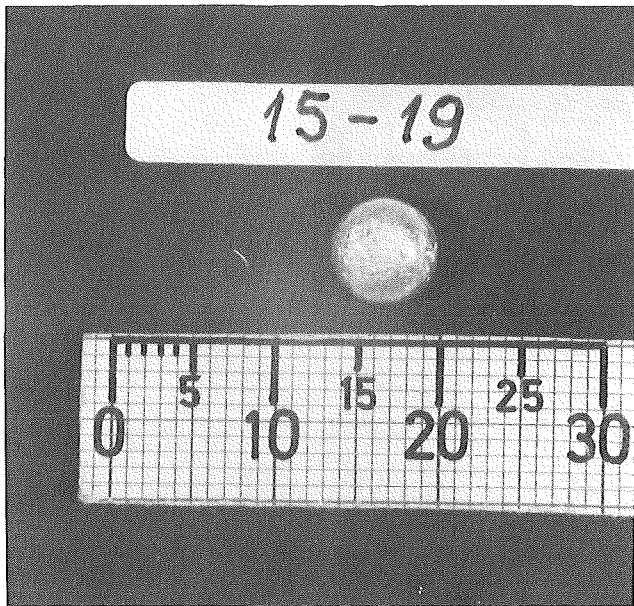
1. Heating above its melting point in the levitation coil,
2. Fall in air (or inert gas),
3. Entry into and fall in the water (or other liquid),
4. Contact with the bottom of the vessel,
5. Cooling and equalization of the metal temperature with the ambient temperature.

Each of the foregoing phases influenced the character of thermal interaction.

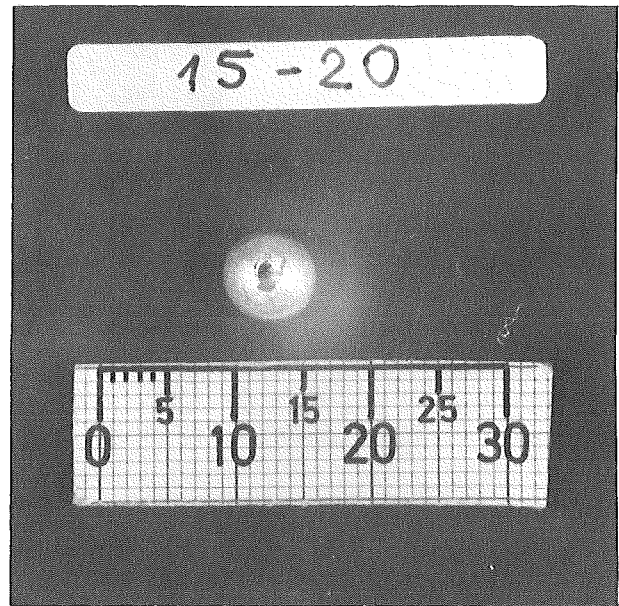
FIG. 3 PARTICLES OF VARIOUS METALS AFTER THERMAL INTERACTION WITH COLD LIQUID ( WATER OR SODIUM )

I. Ag/H<sub>2</sub>O - THERMAL INTERACTION; "NORMAL" COURSE

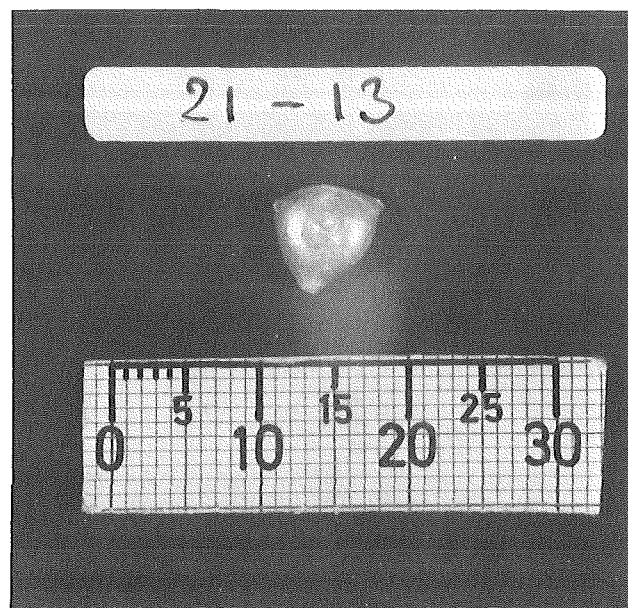
a)



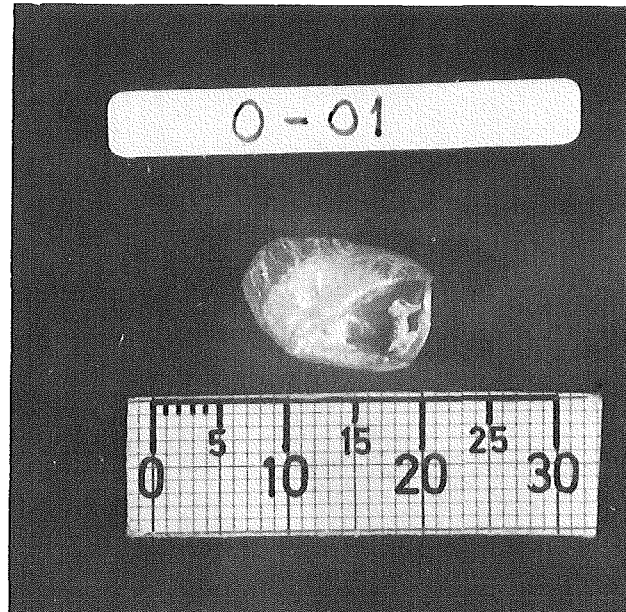
b)



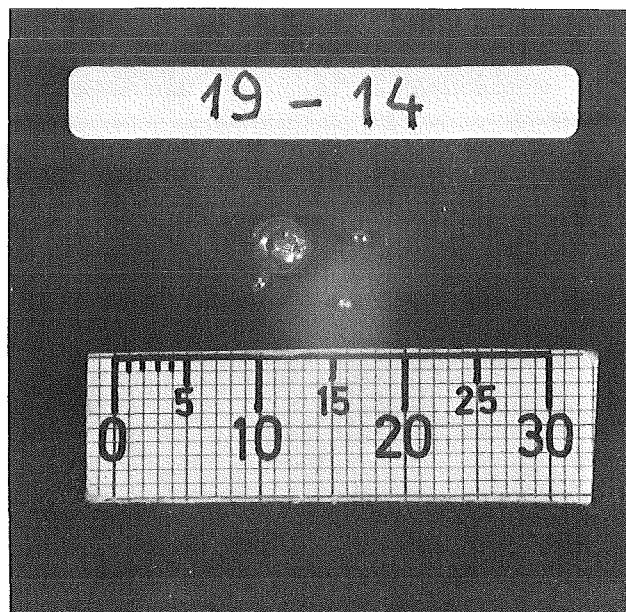
c)



II. Al/H<sub>2</sub>O - THERMAL INTERACTION; "EMPTY SHELL"

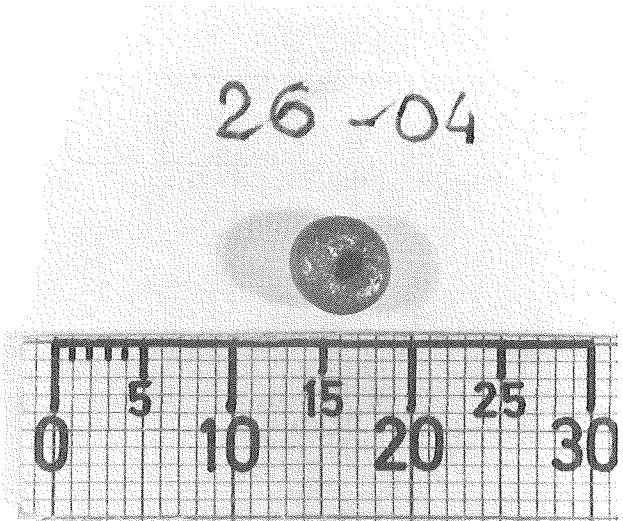
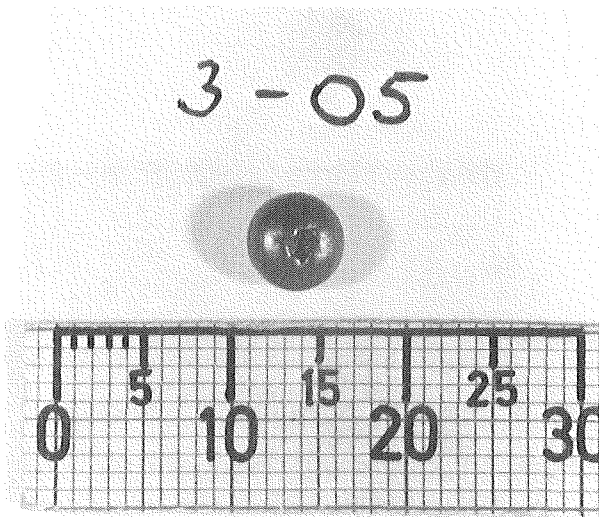


III. Au/H<sub>2</sub>O - THERMAL INTERACTION; HYDRODYNAMIC PARTITION AND A SOLIDIFIED "JET"

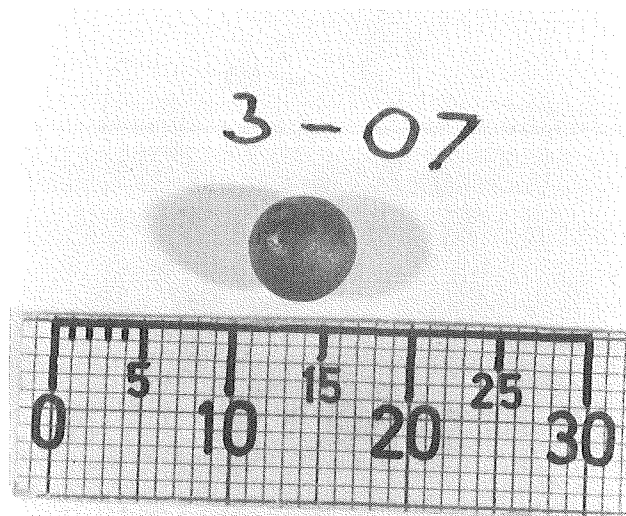


IV. Cu/H<sub>2</sub>O- THERMAL INTERACTION

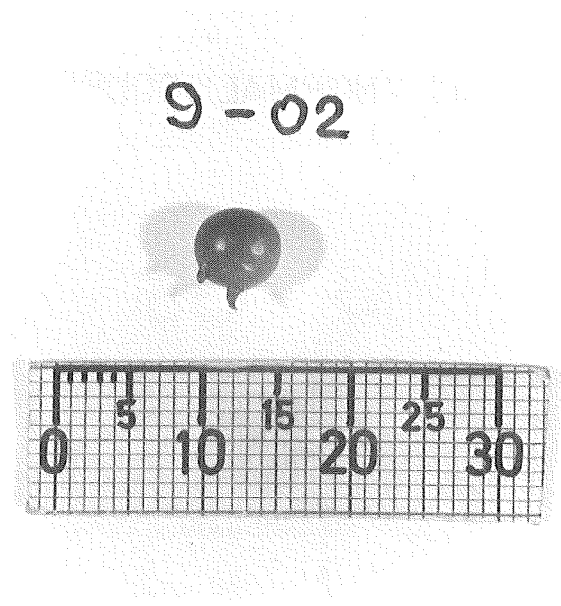
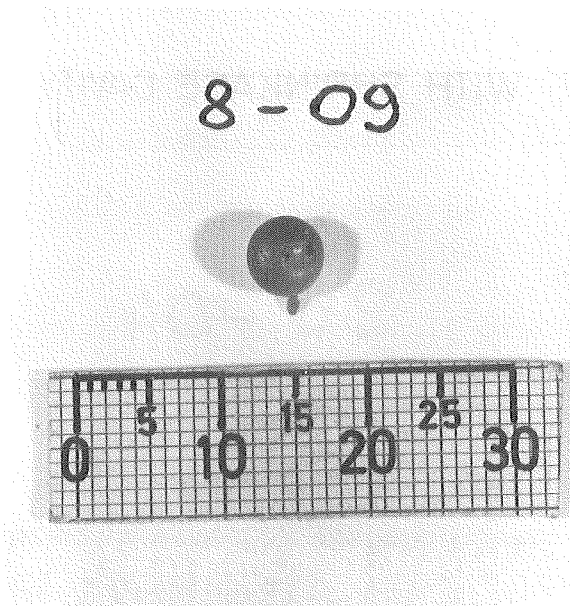
a) "NORMAL" COURSE ; PARTICLE WITH SHRINKAGE CAVITY



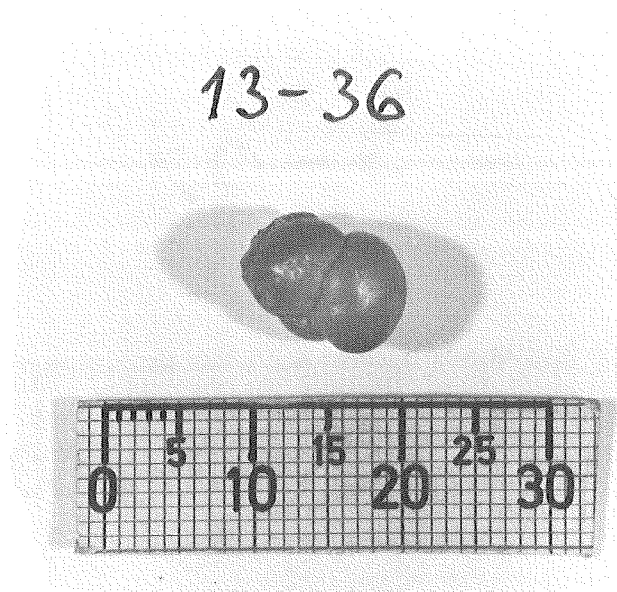
b) "NORMAL" COURSE ; PARTICLE WITHOUT SHRINKAGE CAVITY



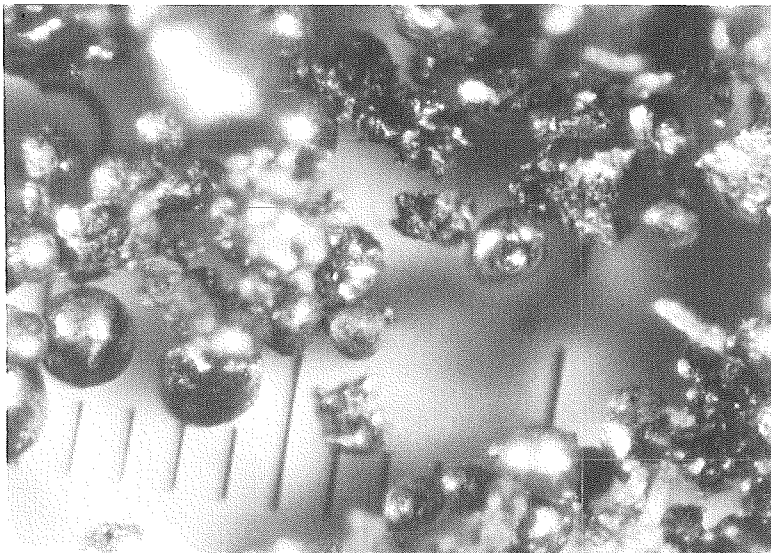
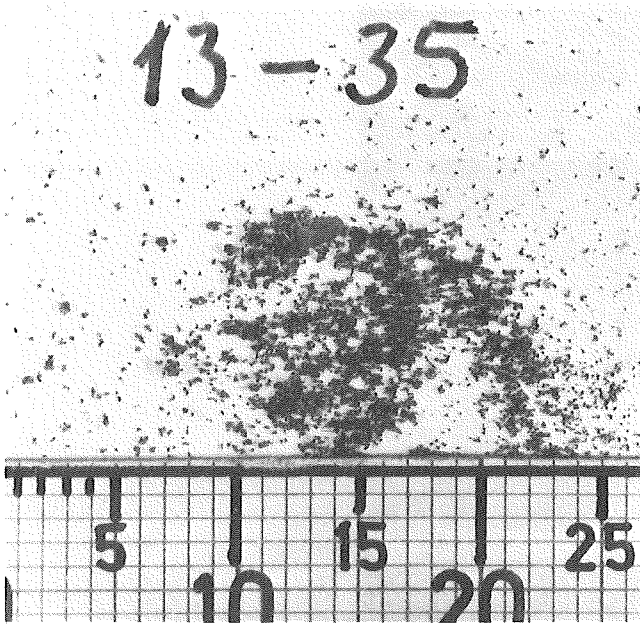
## c) SOLIDIFIED "JETS" FROM THE MAIN COPPER PARTICLE



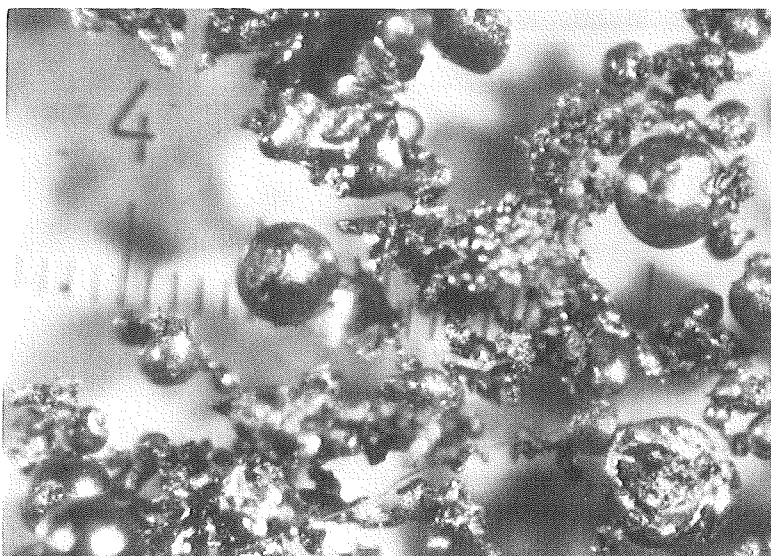
## d) "FUNGUS-FORM" PARTICLE

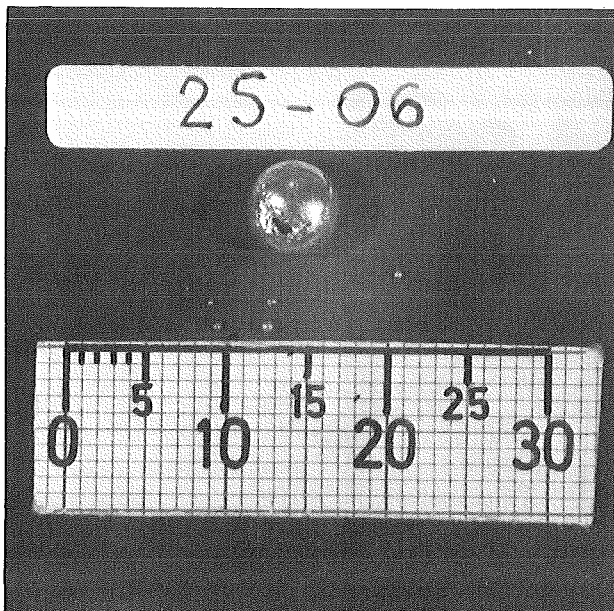
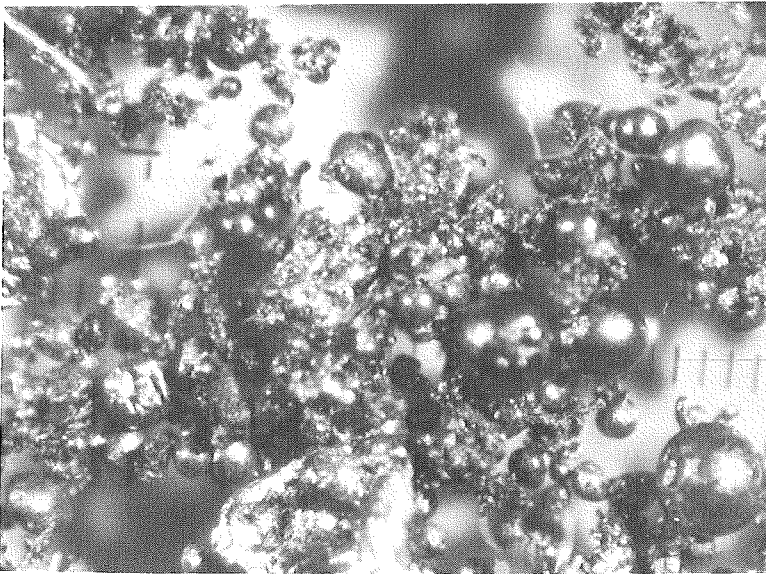
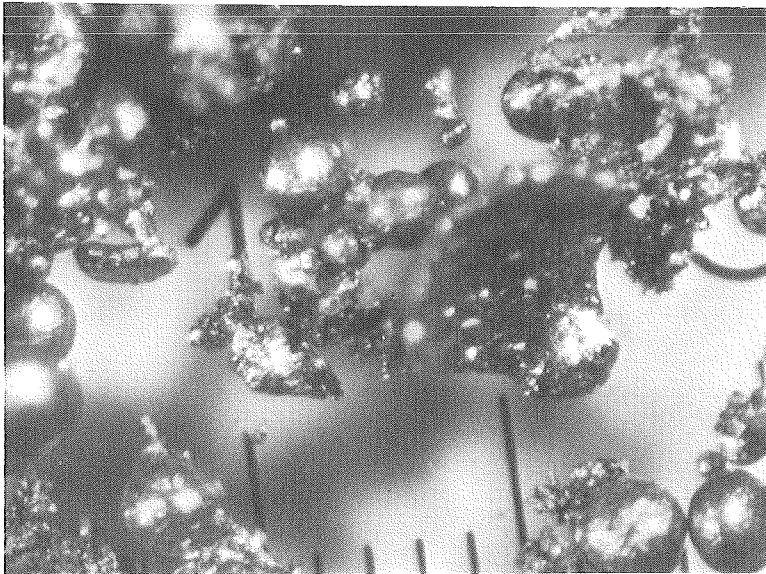


e) DEBRIS OF THERMAL EXPLOSION



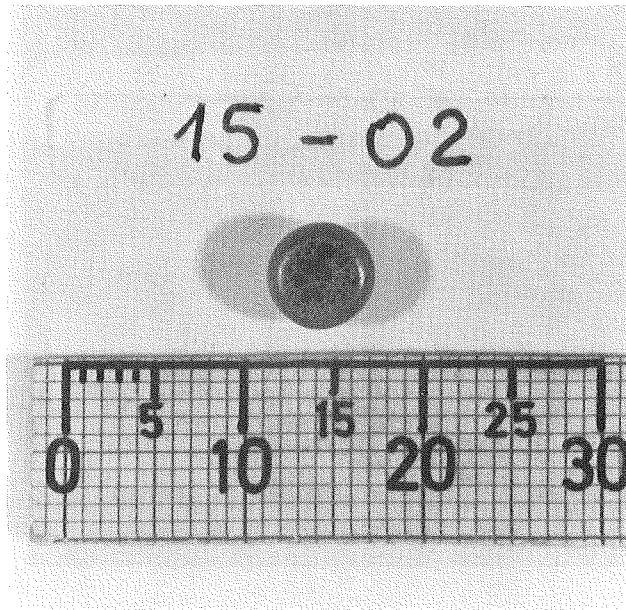
SAMPLE NO.10-14  
AND 13-35.  
SCALE LINES ARE  
0.1 mm APART



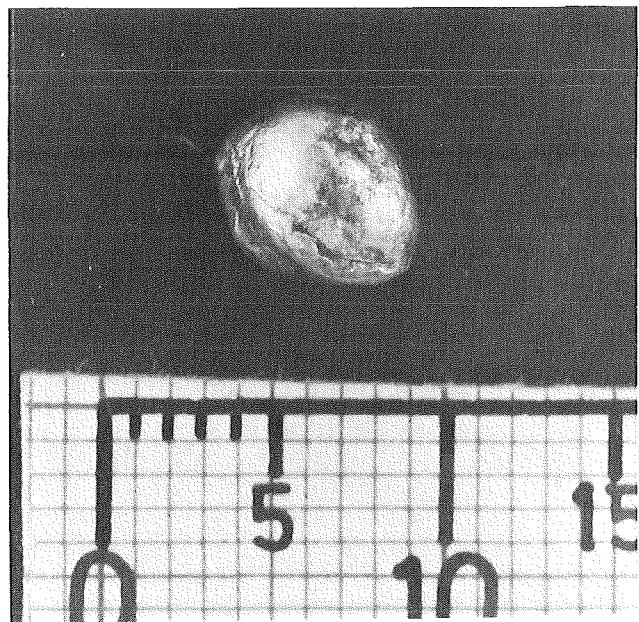
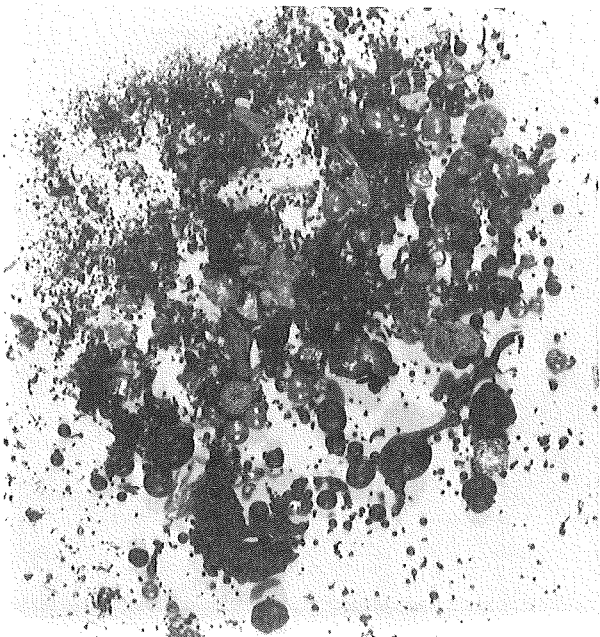


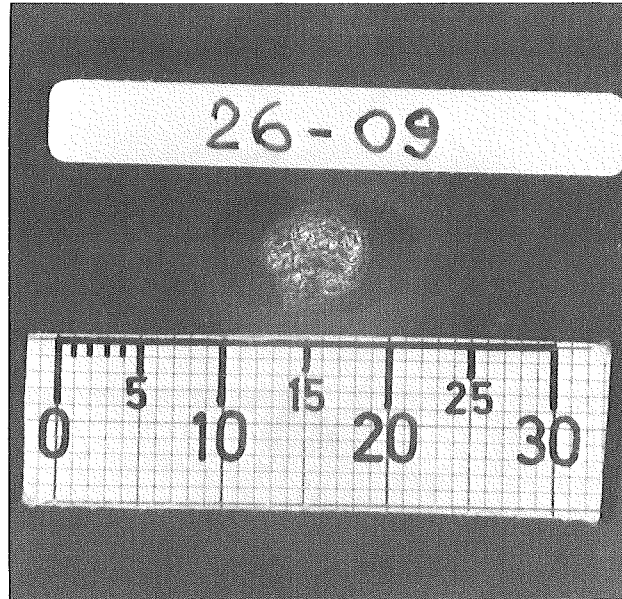
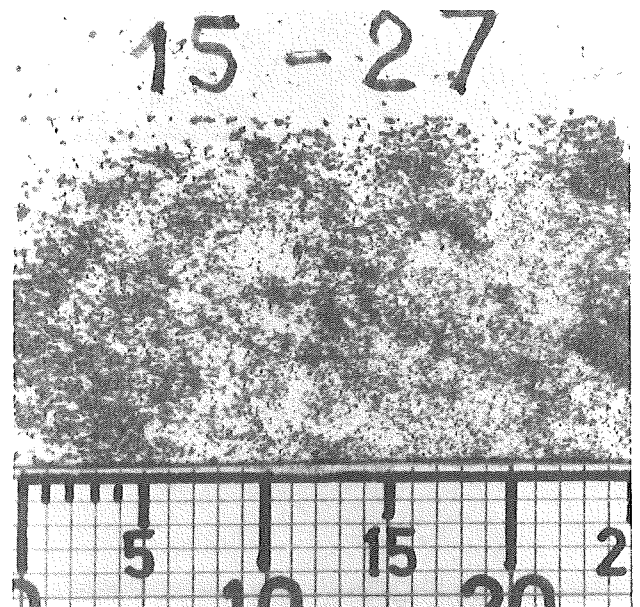
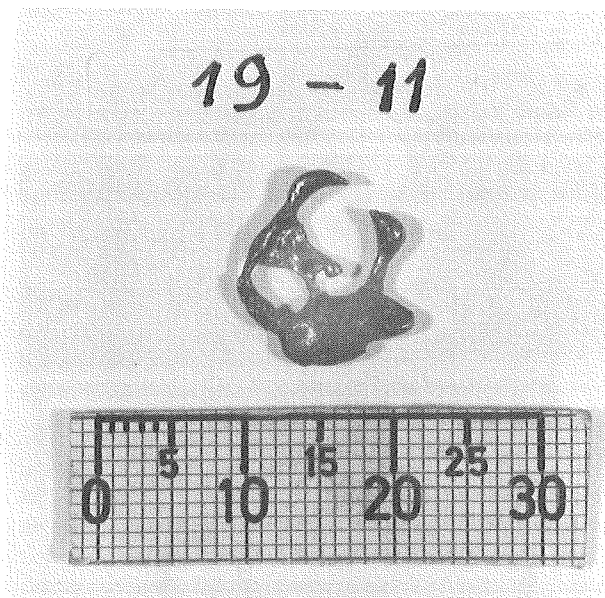
f) "NORMAL" COURSE ;  
COPPER HEATED IN  
NITROGEN

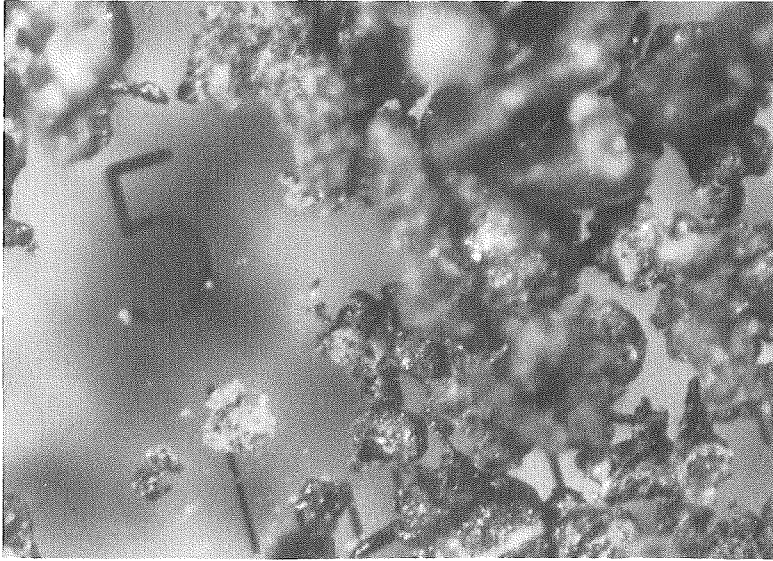
g) BOTTOM SIDE OF THE PARTICLE WHEN COOLED AT THE BOTTOM OF THE VESSEL MADE FROM MICA



V. Cu/Na - THERMAL INTERACTION. DEBRIS AFTER THERMAL EXPLOSION

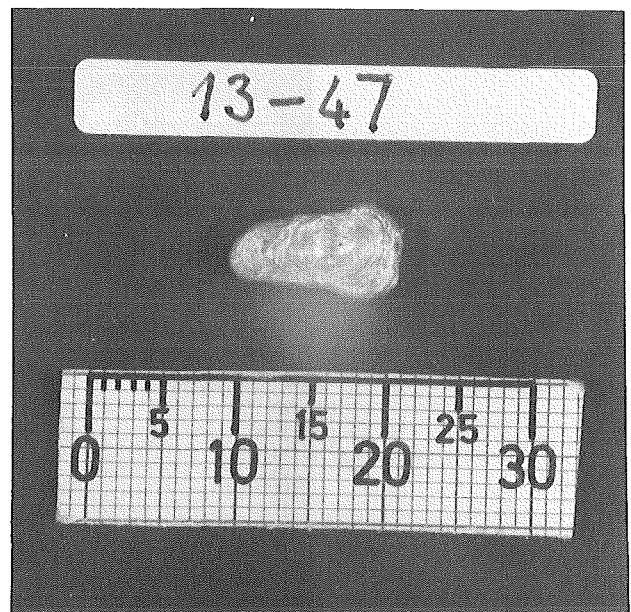
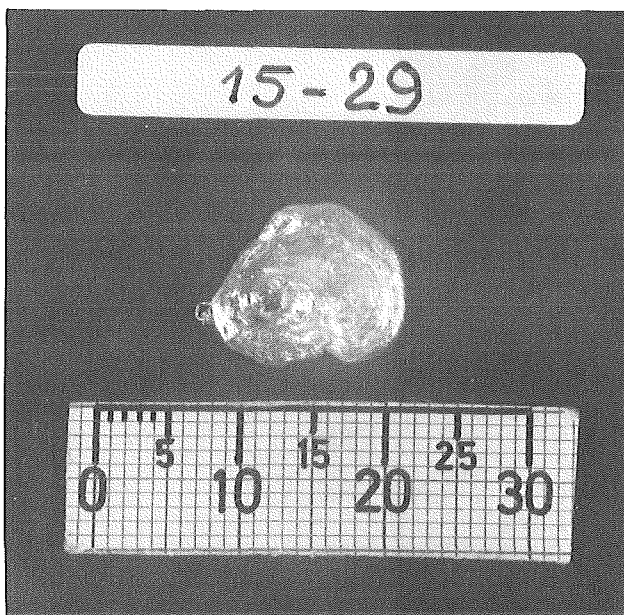


VI. SS/H<sub>2</sub>O - THERMAL INTERACTION. "NORMAL" COURSEVII. Pb/H<sub>2</sub>O - THERMAL INTERACTION. "NORMAL" COURSE AND DEBRIS AFTER THERMAL EXPLOSION, RESPECTIVELY

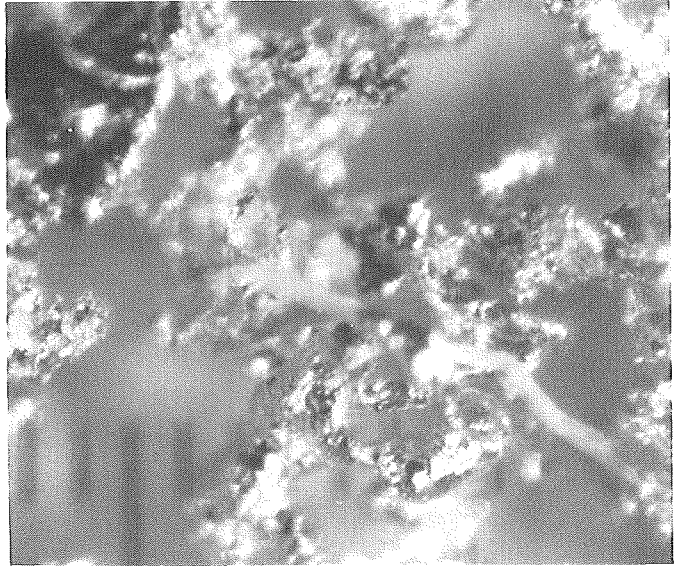
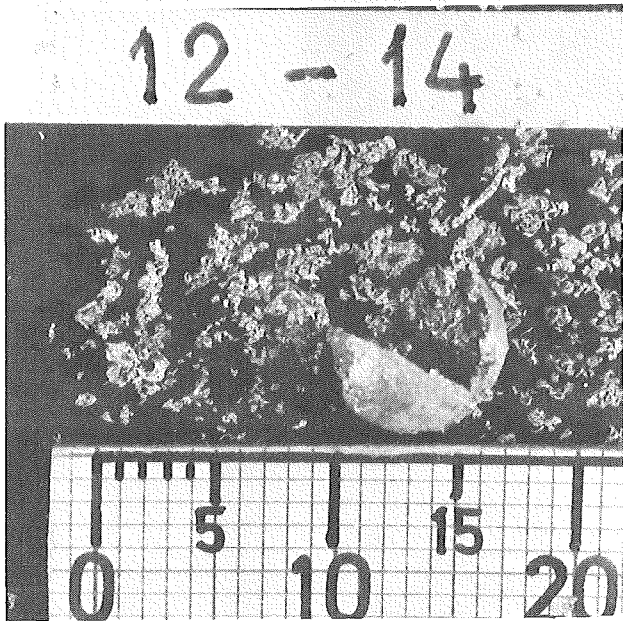
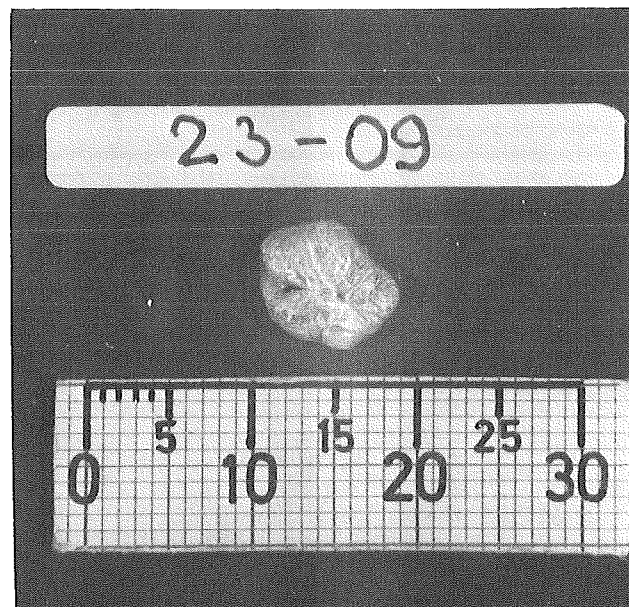


### VIII. Sn/H<sub>2</sub>O - THERMAL INTERACTION

#### a) "NORMAL" COURSE



## b) DEBRIS AFTER THERMAL EXPLOSION

IX. Zn/H<sub>2</sub>O - THERMAL INTERACTION "NORMAL" COURSE

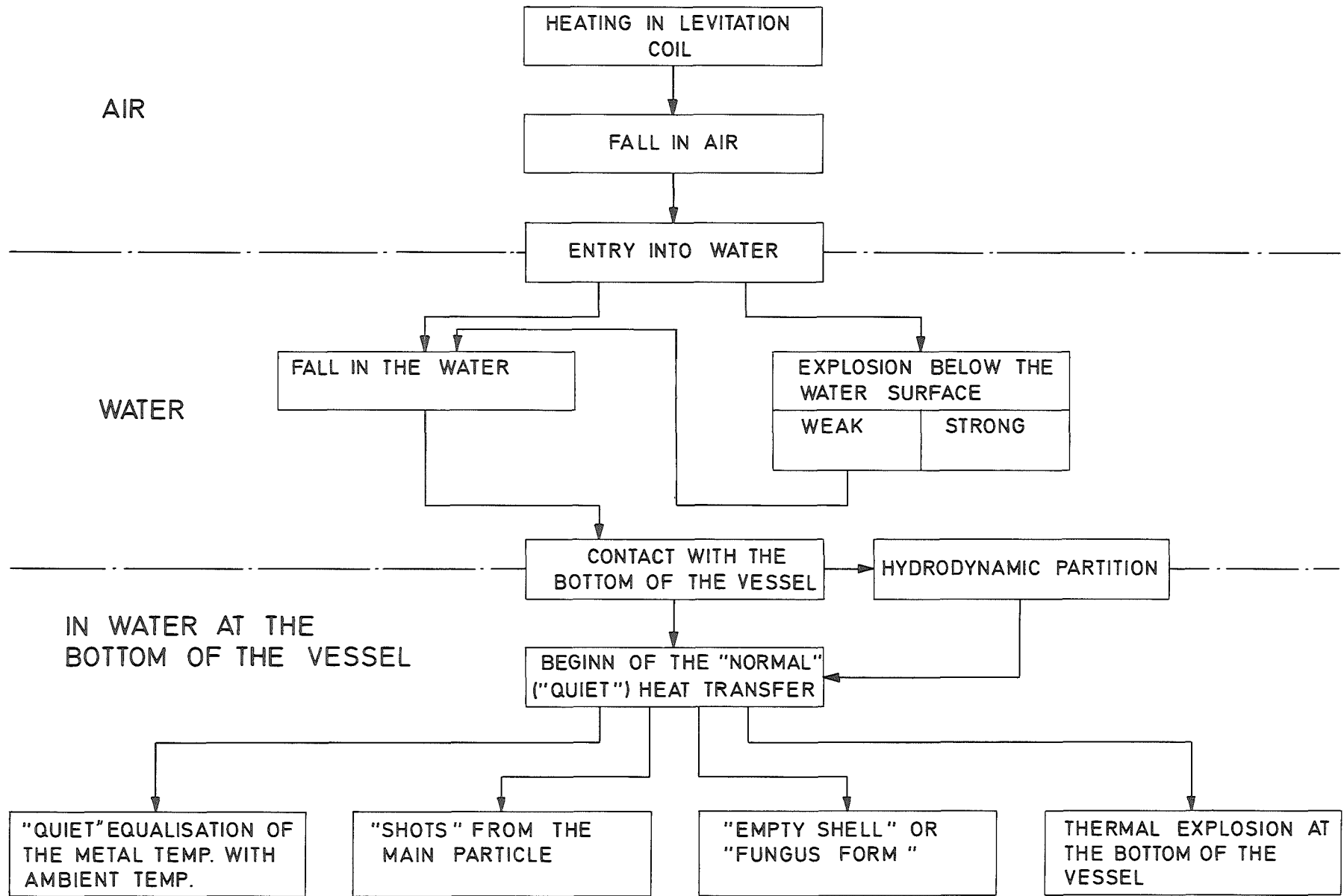
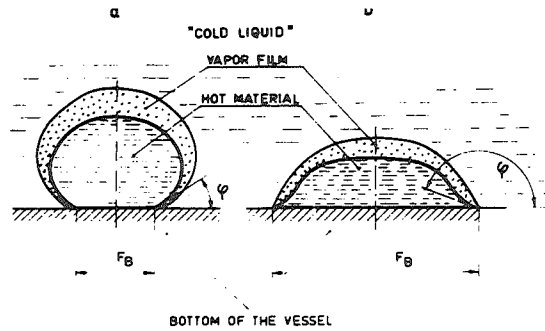
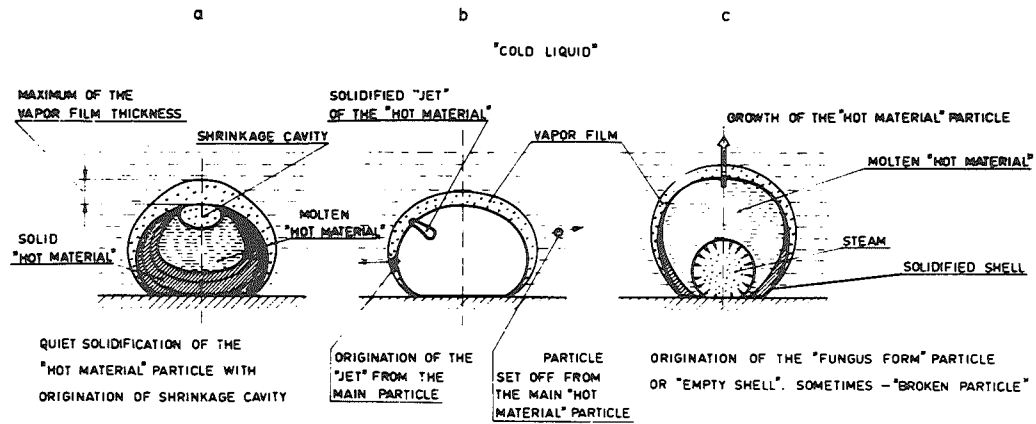


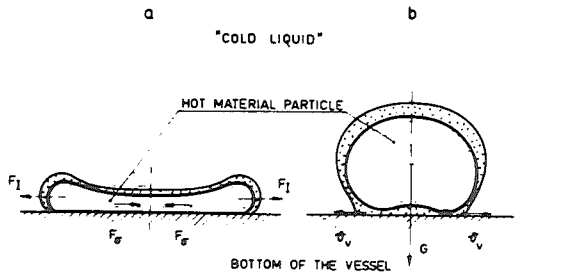
FIG 4 BLOCK DIAGRAM SHOWING THE SEQUENCE OF THE PHENOMENA



I. SHAPE OF THE "HOT MATERIAL" DROPS (PARTICLES) AT THE BOTTOM OF THE VESSEL IN DEPENDENCE ON THE BOTTOM MATERIAL



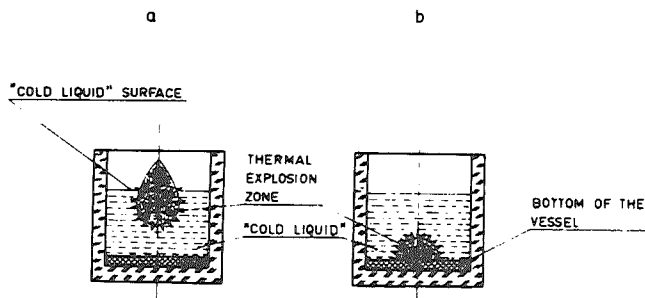
IV. PHENOMENA AT THE BOTTOM OF THE VESSEL



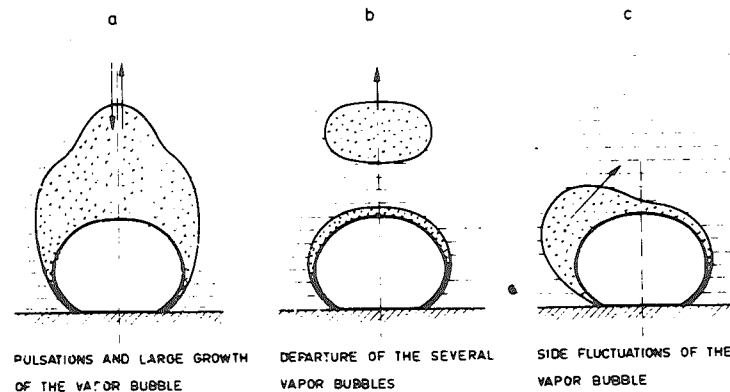
HYDRODYNAMIC PARTITION  
(THE INITIAL STATE)

INVERSE LEIDENFROST PHENOMENON

II. IMPACT PHENOMENA AT THE BOTTOM OF THE VESSEL (OR AT THE "COLD LIQUID" SURFACE)



III. THERMAL EXPLOSION A SHORT DISTANCE BELOW THE "COLD LIQUID" SURFACE AND AT THE BOTTOM OF THE VESSEL



V. TYPES OF THE FILM BOILING REGIME

FIG. 5 THE PHENOMENA WHICH WERE OBSERVED DURING THE THERMAL INTERACTION OF SMALL QUANTITIES OF THE "COLD" AND "HOT" SUBSTANCES

In Figs. 4 and 5, the main phenomena observed and their sequence are presented.

In the experiments with the Cu/water system, the metal particle took a spherical form and during its fall in air (or in the inert gas) it developed a velocity of about 70 cm/sec before it came into contact with the cold liquid surface. This velocity was low enough to prevent hydrodynamic partition, when the hot molten particle submerged in the water. Oxidation of the particle took place during the time it was heated and during its fall in the air which was different from the experiments in the inert gas atmosphere. However, it can not be ruled out, that there was some further oxidation during the cooling phase of the particle in the water.

In the thermal interaction zone, the following main phenomena were observed (Fig. 4):

1. Quiet fall in the cold liquid and then "normal course" of heat transfer at the bottom of the thermal interaction vessel.
2. Thermal explosion:
  - during the fall in the cold liquid or
  - at the bottom of the vessel.
3. Special effects such as hydrodynamic partition, "jets" ("shots"), and the formation of "empty shells" or "fungus form particles".

### 3.1 Normal course of heat transfer

If no thermal explosion occurred during the fall of the particle in water, the particle moved quietly at velocities of 80 to 90 cm/sec. A vapour-air film moved ahead of the copper particle, and a persistent "chimney" was generated behind it. The "chimney" may remain till the copper particle comes to rest at the bottom of the vessel and even afterwards. Later, it pinched out (Fig. 6). The copper particle flattened out at the bottom and subsequently it adopted again the spheroidal shape. For metals such as Ag, Pb, Sn, Zn, the molten metal particle could solidify as a flat "plate" during this phase. Some rings were observed at the surface of such particles (Fig. 3, VIIIa).

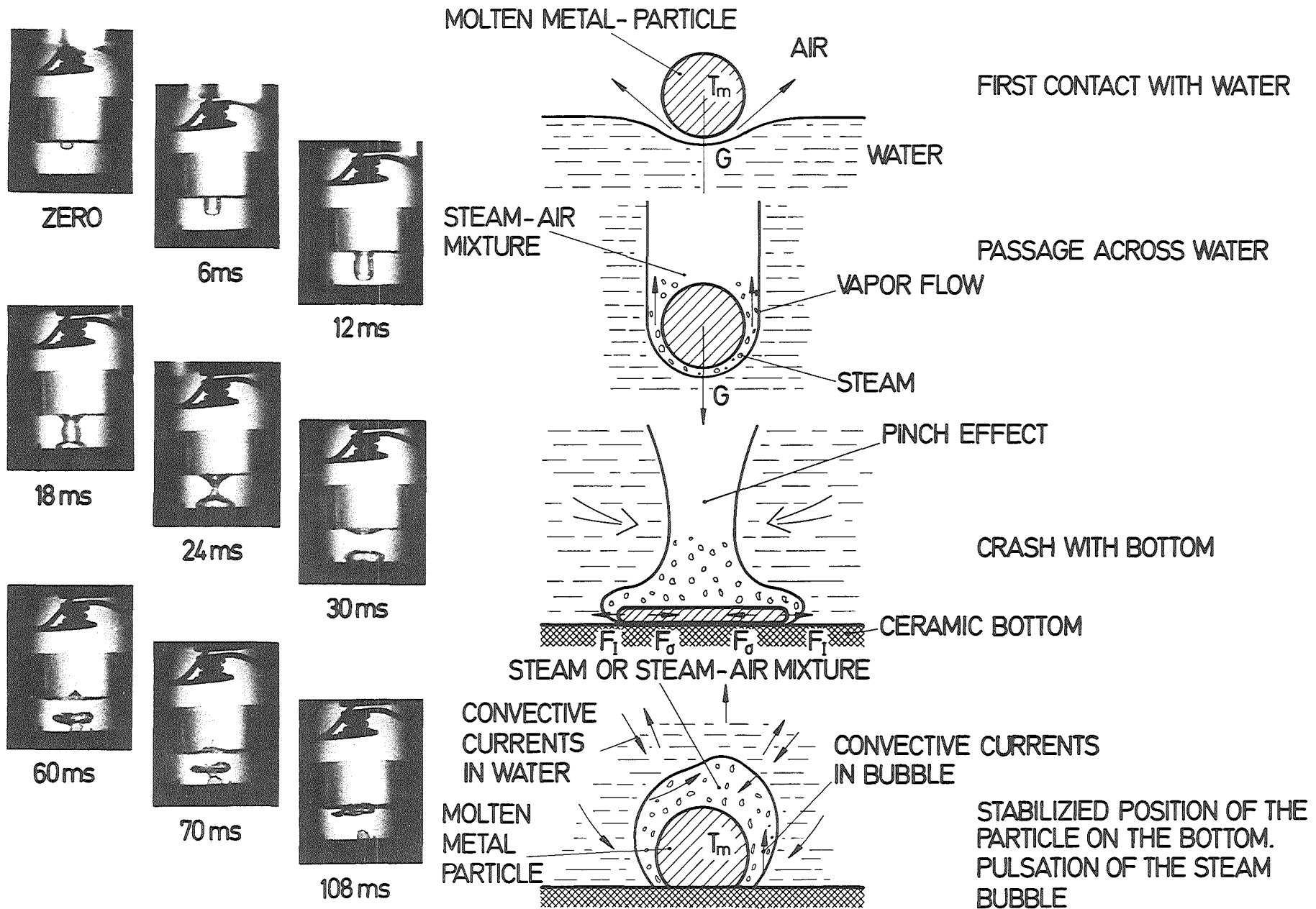


FIG. 6 SCHEMATIC MODEL OF PARTICLE- ENTRY IN WATER

Sometimes, the particle "danced" at the bottom of the vessel and it touched the neighbouring thermocouples before it settled on the thermocouple No. 1. Exceptionally, the "full" inverse Leidenfrost phenomenon was observed at the bottom of the vessel (Fig. 5, IIb). In this case, a vapour film was formed between the hot metal particle and the bottom of the vessel. The particle danced quickly before it finally settled. This phenomenon was only observed for molten zinc in water in these experiments.

The "dance" of the particle and the delay in the thermocouple readings (for the role of the thermometric lag, see Appendix 2) resulted in the temperature of the first particle contact with the bottom of the vessel not being exactly known. However, a maximum temperature  $T_{\max}$  could be obtained. Then, an extrapolated maximum temperature was calculated for the bottom of the vessel (point A in the following Fig.).

The time which elapsed between the shut-off of the current in the levitation coil and the first reading of the thermocouples at the bottom of the vessel was about 40 - 60 msec.

The spheroidal molten metal particle subsequently cooled down at the bottom of the vessel. This period was the longest in the cooling history of the particle; for copper particles it was 2 to 25 sec for various particles tested (Fig. 7).

For the particle No. "i" ( $i=1, 2, 3, \dots$ ), the following phases could be distinguished during its cooling history:

- $(\overline{AL})_i$  - film boiling,
- $(\overline{AC})_i$  - particle was molten,
- $(\overline{CE})_i$  - beginning of solidification (sometimes  $(\overline{BC})_i$ ),
- $(\overline{EF})_i$  - full solidification,
- $(\overline{FL})_i$  - particle was solid,
- $(\overline{LP})_i$  - transition boiling (this phase was often reduced to one point in Fig. 7, i.e.  $L_i = P_i$  because of the short duration of the phenomenon),
- $(\overline{PW})_i$  - violent nucleate boiling,

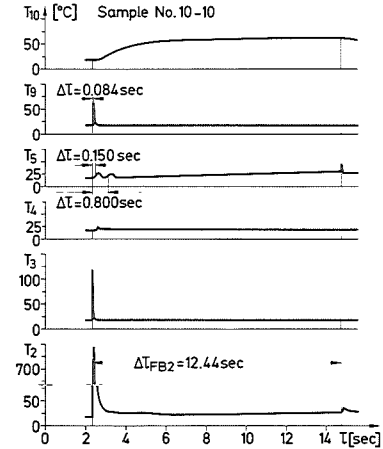
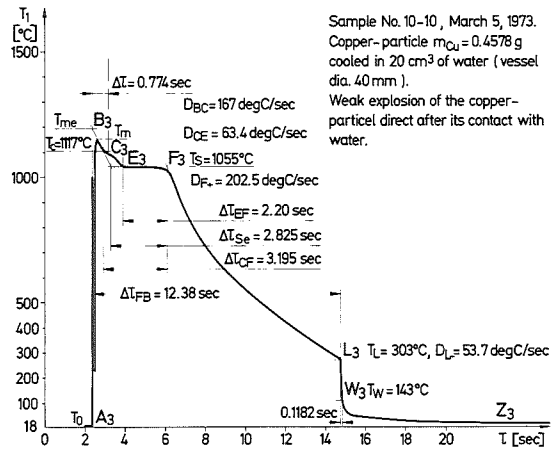
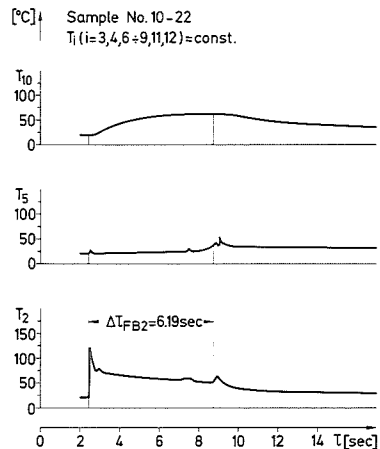
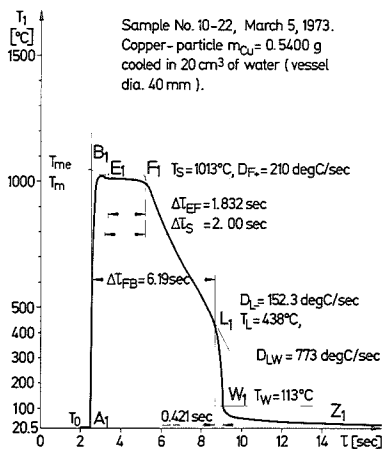
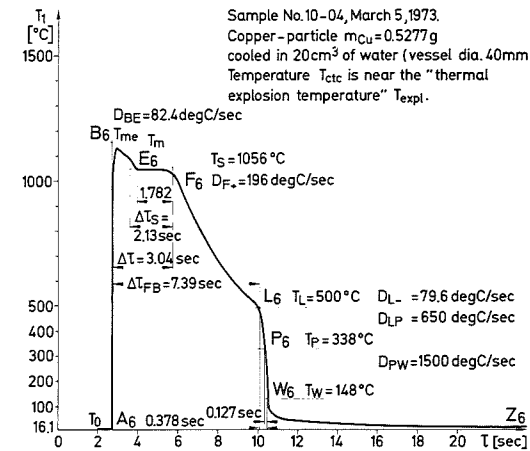
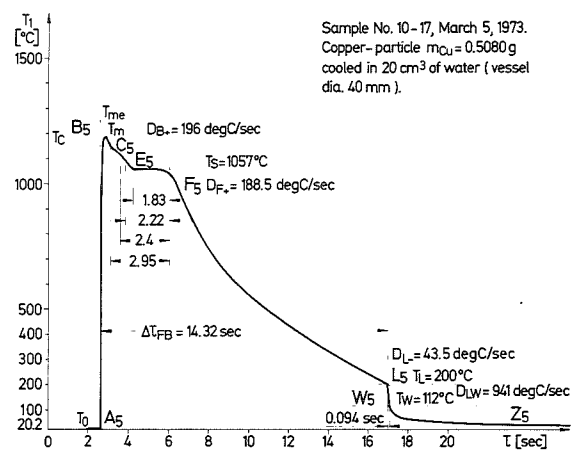
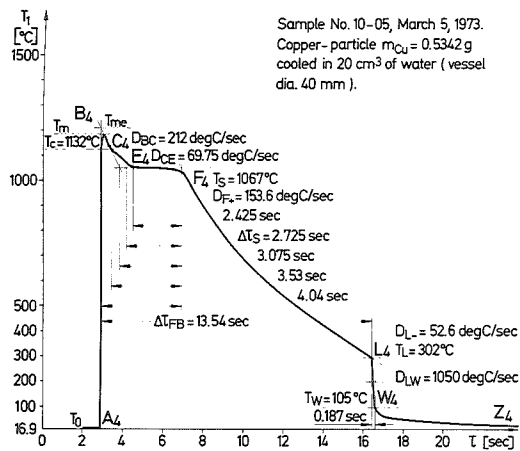


FIG. 7 TEMPERATURE HISTORIES OF THE COOLING OF THE VARIOUS COPPER-PARTICLES IN WATER.

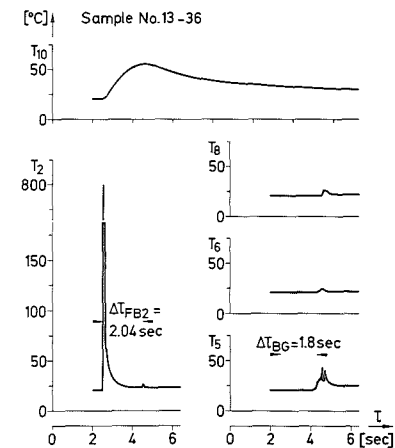
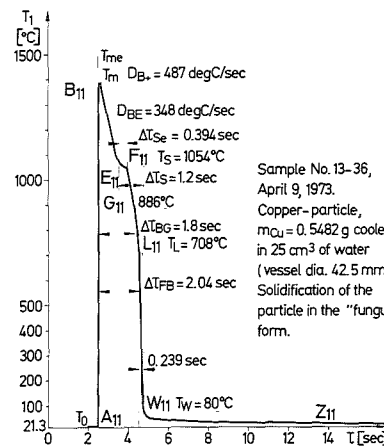
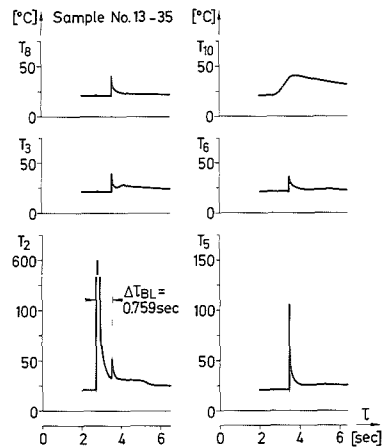
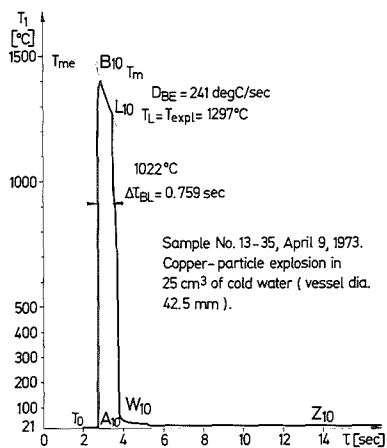
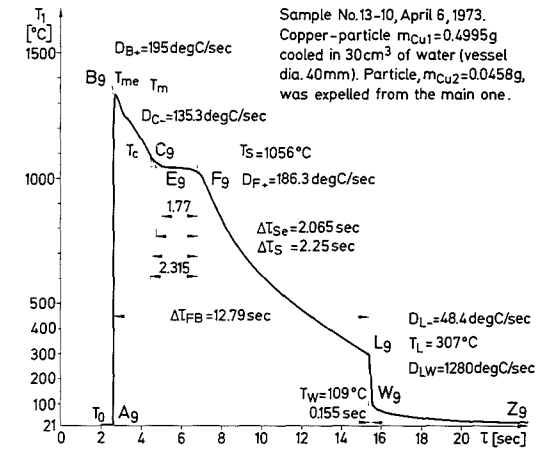
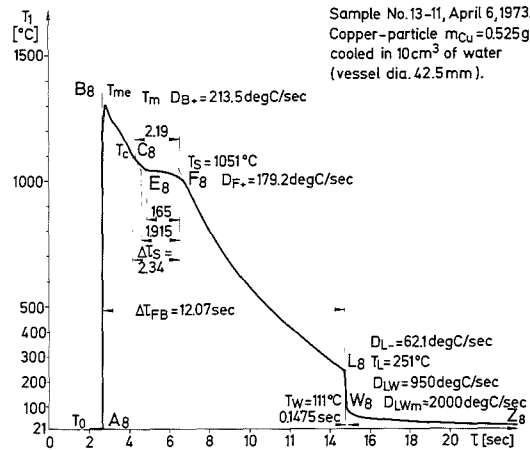
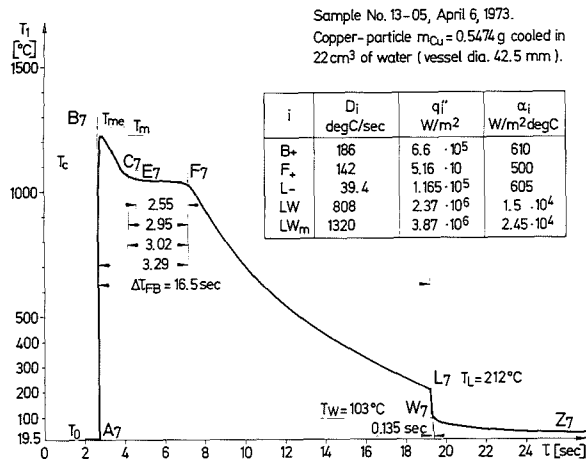


FIG. 8 TEMPERATURE HISTORIES OF THE COOLING OF THE VARIOUS COPPER-PARTICLES IN WATER.

Table 2. Specification of the measurements in this experiment

No	Data of measurements	Sample Nos.:	Interaction zone	Distance: particle in lev. coil - liquid surface	Gas atmosphere	Bottom material	Thermocouples	Hot material/ Cold liquid
1	2	3	4	5	6	7	8	9
0	28.11. - 5.12.1972	00-01 to 00-81	Cylindric, I.Dia.~30	15 + 80	air, p=1 at	Graphit, mica, Thermostix 2000		Ag, Al, Cu, Fe, SS/H <sub>2</sub> O
1	8.12.1972	01-03 to 01-08	Cylindric, I.Dia. 40	30	" "	Thermostix 2000	Chromel-Alumel	Cu/H <sub>2</sub> O
2	12.12.1972	02-01 to 02-14	" "	"	" "	"	"	"
3	15.12.1972	03-02 to 03-17	" "	"	" "	"	"	"
4	19.12.1972	04-01 to 04-14	Half-sphere /top/, R <sub>s</sub> =20	20	" "	"	"	Ag, Cu/H <sub>2</sub> O
5	22.01.1973	05-01 to 05-05	Cylindric, I.Dia. 40	30	" "	"	-	Cu/H <sub>2</sub> O
6	26.01.1973	06-01 to 06-23	" "	"	" "	Thermostix 2000, mica	Chromel-Alumel	"
7	6.02.1973	07-01 to 07-19	" "	"	" "	Thermostix 2000	"	"
8	28.02.1973	08-01 to 08-21	" "	"	" "	"	"	Au, Cu/H <sub>2</sub> O
9	2.03.1973	09-01 to 09-22	" "	"	" "	"	"	Cu/H <sub>2</sub> O
10	5.03.1973	10-01 to 10-23	" "	"	" "	"	"	"
11	6.03.1973	11-01 to 11-10 (27)	" "	"	" "	"	-	Ag, Al, Au, Cu, Nb, Pb, Sn, Zn/H <sub>2</sub> O
12	16.03.1973	12-01 to 12-23	" "	"	" "	"	Chrom.-Al.	Al, Cu, Sn, Zn/H <sub>2</sub> O
13	16.04.1973	13-01 to 13-20	Cylindric, I.Dia. 42,5	"	" "	"	Chrom.-Al./ W 3 Rh-W 25 Rh	Cu, Sn/H <sub>2</sub> O
14	9.04.1973	13-21 to 13-47	" "	"	" "	"	Chrom.-Al.	"
15	16.04.1973	15-01 to 15-31	" "	"	" "	Alumina	-	Ag, Au, Cu, Pb, Sn, Zn/H <sub>2</sub> O
16	17.04.1973	16-01 to 16-05	" "	"	" "	Thermostix 2000	Chrom.-Al.	Cu, Sn/H <sub>2</sub> O
17	28.05.1973	17-01 to 17-11	Cylindric, I.Dia. 30	"	Argon, p=300 tor	"	Chrom.-Al.; W 3 Rh-W 25 Rh	Cu/H <sub>2</sub> O
18	6.06.1973	18-12 to 18-21	" "	"	" "	"	"	"
19	7.06.1973	19-01 to 19-16	" "	"	" "	"	"	Al, Ag, Au, Cu, Pb, Sn, Zn/H <sub>2</sub> O
20	13.06.1973	20-01 to 20-18	" "	"	Ar., p=40, 300 tor; Air, p=1 at /one sample/	"	"	Cu/H <sub>2</sub> O

Table 2./cont./

1	2	3	4	5	6	7	8	9
21	14.06.1973	21-01 to 21-15	Cylindric, I.Dia. 40	30	Argon, p=300 tor	Thermostix 2000	Chrom.-Al. W 3 Rh-W 25 Rh	Ag,Cu/H <sub>2</sub> O
22	28.06.1973	22-01 to 22-08	Cylindric, I.Dia.40; Half-sphere /top/, R <sub>s</sub> =20 /two last samples/	"	Argon, p=40, 300 tor	"	"	Cu/H <sub>2</sub> O
23	29.06.1973	23-01 to 23-10	Half-sphere /top/, R <sub>s</sub> =20, Cylindric, I.Dia.20 /last four samples/	20	"	"	Chrom.-Al.	Au,Cu,Zn/H <sub>2</sub> O
24	16.07.1973	24-01 to 24-12	Cylindric, I.Dia.40	30	Argon, p=760 tor	"	"	Cu,SS/H <sub>2</sub> O
25	7.08.1973	25-01 to 25-12	"	"	Nitrogen, p=500 tor; Air /two samples/	"	"	Cu/H <sub>2</sub> O
26	8.08.1973	26-01 to 26-10	"	"	N <sub>2</sub> , p=300 tor; Air	"	"	Al,Cu,SS/H <sub>2</sub> O
27	13.08.1973	27-01 to 27-08	"	60	N <sub>2</sub> , p=300 tor	"	-	Ag,Al,Au,Cu/ H <sub>2</sub> O
28	14.09.1973	01 to 02	ice	20	"	-	Chrom.-Al.	Cu/H <sub>2</sub> O (ice)
29	17.09.1973	01 to 07	"	"	"	-	"	Cu/CO <sub>2</sub> (ice), N <sub>2</sub> (liq.), CO <sub>2</sub> -H <sub>2</sub> O (ice)
30	18.09.1973	28-01 to 28-03	"	50	"	-	"	Cu/H <sub>2</sub> O (ice)
31	19.09.1973	29-01 to 29-03	"	"	"	-	"	"
32	16.10.1973	30-01	Cylindric, I.Dia.40	30	"	Alumina	"	Cu/Na
33	18.10.1973	31-01	"	"	"	Tungsten	W 3 Rh - W 25 Rh, Chrom.-Al.	"
34	23.10.1973	32-01	Cylindric, I.Dia.30	45	"	"	"	"
35	24.10.1973	33-01	"	"	"	"	"	"
36	30.10.1973	34-01	"	"	"	"	"	Nb/Na
37	31.10.1973	35-01	"	"	"	"	"	"
38	8.11.1973	36-01	"	"	"	"	"	Cu/Na

Table 3. Results of the measurements of copper/cold liquid (mainly water) thermal interaction

No.	Sample No.	Copper				Cold liquid		Type of interaction	Observed phenomena /according to the classification given in Fig. 5 /	Solidifying		Film boiling		Transition boiling		Violent Nucleate Boiling		Debris	Remarks	
		Dimens. $D_p/H_p$	m	$T_m$	$T_{me}$	V	$T_0$			$T_s$	$\Delta t_{se}$	$T_L$	$\Delta t_{WB}$	$T_p$	$\Delta t_{Lp}$	$T_W$	$\Delta t_{pW}$			
		mm	g	$^{\circ}C$	$^{\circ}C$	$cm^3$	$^{\circ}C$			$^{\circ}C$	sec	$^{\circ}C$	sec	$^{\circ}C$	sec	$^{\circ}C$	sec			
1	2	3	4	5	6	7	8	9	10	11	12	13	14	15	16	17	18	19	20	21
1	01-03	5.4/4.0	.5912	1115	1132	~25	19	Normal	Ia, IVa, Vbc	Yes	1032	1.92	307	12.07	~307	-	115	.185	1 particle	
2	01-04	5.36/3.88	.5801	1085	1097	~25	19	"	"	Yes	1028	1.94	422	6.59	~422	-	127	.288	"	
3	01-05	4.79/3.39 3.84/3.08	.3794 .2150	1075	1088	~25	18	"	IIa, IIa/weak/, IVa, Vb	Yes	1033	.921	243	5.77 4.70	~243	-	~100	~.04 ~.0	2 "	
4	02-08	-	~.55	982	996	~25	18	Explosion	IIIa, /weak/	Yes	-	-	927	.537	-	-	104	-	~100 particles	Particles sharp in form from 0.1 to ~4 mm
5	03-04	5.57/3.38	.5850	1074	1108	20	~20	Normal	Ia, IVa	Yes	1050	2.215	527	7.26	392	.351	119	.192	1 particle	
6	03-05	5.52/4.91	.5569	1135	1158	20	~18	"	"	Yes	1051	2.025	341	9.72	243	.092	113	.124		
7	03-06	-	~.5			20	~20	Explosion	IIIa /strong/	Yes	-	-	-	-	-	-	-	-	Many particles	Dia. of the particles ( $D_p$ ) < 0.1 mm; Temp. in levit. coil ~1300 $^{\circ}C$
8	03-07	6.11/5.78	.5770		>1260	20	21	Normal	Ia, IVc/weak/, Va	Yes	1051	1.353	402	6.73	377	.022	120	.158		Shrinkage cavity in the particle
9	03-08	-	~.5		>1260	20	20	Explosion	Ia, IVb, IIIb/strong/	Yes	1065 (?)	.05	1052(?)	.456	894	.112	-	-	Many particles	$D_p$ < .005 mm, $T_{lev}$ ~ 1600 $^{\circ}C$ Bottom of the vessel broken, T.C.-defect. $T_L$ means $T_{HM, expl}$ .
10	03-09	-	~.5		>1260	20	20	"	"	Yes	-	-	1162	.653	-	-	-	-	"	
11	03-13	7.24/	.5422	>1300	>1300	20	20	Normal	Ia, IVb, c	Yes	-	-	990	2.18	-	-	124	~.562	1 particle	Broken particle
12	03-15	5.62/4.23	.5983	1127	1135	~20	"	"	Ia, IVa, Vabc	Yes	1057	2.27	299	11.09	~299	-	118	.185	"	Irregular particle
13	03-16	6.85/5.63	.5810		1333	~20	"	"	Ia	Yes	1055	1.67	522	5.27	397	.422	100	.21	"	Shrinkage cavity in the particle
14	05-01	-	~.6			25	~20	Explosion	IIIa/strong/	Yes	-	-	-	-	-	-	-	-	Many particles	$D_p$ < 0.1 mm /flakes in form/. $T_{lev}$ ~ 1300 $^{\circ}C$
15	06-01	5.40/4.90	.5338	1114	1142	25	17	Normal	Ia, IVa, Vb	Yes	1038	2.045	426	7.12	426	-	100	.296	1 particle	
16	06-04	5.87/4.32	.5609	1180	1220	25	20	"	Ia, IVa, Vb/five bubbles/	Yes	1060	1.8	528	6.65	~528	-	127	.7	"	
17	06-05	5.53/4.03	.5267	1147	1193	25	21	"	Ia, IVa, Vba	Yes	1058	1.8	211	13.6	~210	-	115	.07	"	
18	06-09	5.66/4.03	.5516	1215	1245	25	21	"	Ia, IVa, Vb/three/a	Yes	1054	1.75	588	7.05	433	-	123	.2		$T_{HM, expl}$ ?
19	06-10	-	~.55			25	21	Explosion	IIIa /strong/	Yes	-	-	-	-	-	-	-	-	Many particles	$D_p$ < .01 mm, $T_{lev}$ ~ 1300 $^{\circ}C$ $\Delta p$ ~ 0.1 at
20	06-14	6.49/3.35	.5724	~890	~950	20	20	Normal	Ib, IVb	Yes	-	1.02	307	2.01	307	-	105	.185	1 particle	"Jets" at the bottom; Bottom material - mica
21	07-01	5.54/4.45	.5675	1234	1289	20	21	"	Ia, IVa, Vb	Yes	1064	3.07	248	14.09	~248	-	126	.08	"	
22	07-02	5.88/5.18	.5867		1419	20	20	"	Ia, Vca	Yes	1047	1.85	558	6.72	427	.143	115	.242	"	2 solidified "jets"
23	07-03	-	~.57	1287		20	20	Explosion	IIIb /strong/	Yes	-	-	1287	.246	-	-	-	-	Many particles	$D_p$ < 0.01 mm, $T_L$ means $T_{HM, expl}$
24	07-07	4.16/3.78 2.41/2.05 2.22/1.95	.2023 .0466 .0400	1251	1300	20	20	"	IIIb /weak/	Yes	1054	1.49	311	5.79	~310	-	~100	.121	3 particles + many small	$D_p$ = 4.12; 2.16; 2.03; 1.32; 1.21; 20 particles from (0.5; 1), and ~100 particles from (0.05; 0.5).
25	07-10	5.16/4.46	.5739 .0029 .0021 .3779+	~1300	1350	30	18	Normal	Ia, IVb	Yes	1084	1.468	616	4.36	461	.281	131	.200	1 particle + 2 small one	
26	08-03	-				25	19, 5	Explosion	IIIa /weak/	Yes	-	-	-	-	-	-	-	-	2 particles + ~20 small one	
27	08-05	-	~0.5			25	20	"	IIIa /weak/	Yes	-	-	-	-	-	-	-	-	1+10+many	1 particle $D_p$ = 2.50 mm; 10- $D_p \in (1, 2)$ and ~200 particles $\in (0.05, 1)$
28	08-09	5.51/4.65	.5872	1149	1168	25	21	Normal	Ia, IVab	Yes	1051	1.30	450	4.31	450	-	109	.315	1 particle	
29	09-01	-	~.55	>1300	1424	20	18	Explosion	IIIb /strong/	Yes	1060	1.06	750	3.06	528	.266	130	.165	Many particles	$D_p$ < 0.05 mm, $T_{HM, expl}$ = ?
30	09-02	-	.5867	>1300	1419	20	19	Normal	Ia, IVc	Yes	1047	1.85	558	6.72	427	.143	115	.242	1 particles	
31	09-03	-	.5549	>1300	1435	20	20	Explosion	Ia, IIIb /weak/	Yes	1058	.567	411	5.02	~410	-	~100	0.197	1+5+many	"m" of small particles: .0074; .0070; .0027; .0023; .0018+... Small particles are "empty".

Table 3. /cont./

1	2	3	4	5	6	7	8	9	10	11	12	13	14	15	16	17	18	19	20	21
32	09-04	5.18/5.17	.8878	>1300	1486	20	21	Normal	Ia,IVb /strong/	Yes	1067	2.00	278	13.95	~278	-	104	.15	2+ very small	"jet - particle": $m \sim .0005$ g
33	10-03	-	~.05			20	16	Explosion	IIIa /weak/	Yes									Many particles	$\sim 10 : D_p \in (1,2); \sim 50 : D_p \in (0.1,1)$ and $\sim 1000 : D_p > 0.01$ mm
34	10-04	5.36/4.12	.5277	1139	1160	20	16	Explosion	IIIa /very weak/,Ia	Yes	1056	2.13	500	7.39	338	.251	148	.127	1+~30	$D_p$ of small particles $\in (0.1,2)$
35	10-05	5.60/4.29	.5342	1191	1217	20	17	Normal	Ia,IVa	Yes	1057	3.075	302	13.54	~300	-	105	.187	1 particle	"broken particle"
36	10-10	4.86/3.92	.4578	1146	1206	20	18	Explosion	IIIa /weak/,Ia	Yes	1055	2.825	303	12.38	~300	-	143	.1182	1 + ~30	$D_p$ of small particles $\in (0.1,2)$
37	10-14	-	.0337			20	20	Explosion	IIIa /strong/	Yes									Many particles	$D_p \sim .01$ and smaller, and ~20 "flake-formed" particles
38	10-17	5.40/4.25	.5080	1186	1248	20	20	Normal	Ia,IVa,Vbc	Yes	1057	2.47	200	14.32	200	-	112	.094	1 particle	
39	10-19	4.85/3.95	.4882	1095	1132	20	20	Explosion	IIIa /very weak/,Ia,IVa	Yes	1039	1.549	403	7.99	329	.158	108	.187	1 + ~150	$D_p$ of small particles $\in (.005,1)$
40	10-22	5.50/4.22	.5400	1028	1047	20	20	Normal	Ia,IVa,Vbc	Yes	1013	1.832	438	6.19	438	-	113	.421	1 particle	
41	12-01	5.64/4.48	.5104	1231	1273	25	45	Normal	Ia,Vb	Yes	1046	2.33	272	12.48	260	.059	105	.253	"	
42	12-02	5.33/5.04	.5310	1070	1112	25	50	Normal	"	Yes	1028	1.92	407	7.98	325	.298	108	.318	"	
43	12-03	6.22/4.05	.5500	1320	1389	25	58	Normal	Ia,IVbc /weak/,Vb	Yes	1053	2.43	393	8.92	~393	-	110	.323	1 + 2 small	$D_p$ of small particle = 1.20 and 0.60
44	12-05	5.47/3.97	.5285	1096	1126	25	77	Normal	Ia,IVa,Vb	Yes	1053	2.71	382	10.48	~382	-	119	.788	1 particle	
45	12-06	5.52/4.50	.5465	1184	1219	25	71	Normal	Ia,IVa,Vb	Yes	1051	2.86	340	11.20	211	.522	102	.246	"	
46	12-07	5.60/5.07	.5569	1378	1506	25	~80	Normal	Ia,Vb	Yes	1066	2.42	326	12.48	326	-	120	.386	1 particle	
47	12-08	4.05/3.57	~.4	1436	1482	25	~80	Explosion	Ia,IIIb /weak/,Vcb	Yes	1057	.601	308	5.53	296	.032	112	.234	1 + ~40	Small particles are "empty" and $D_p (0.5,2); T_{expl} \approx 1350^\circ\text{C}$
48	12-09	5.67/4.82	.4940	1380	1454	25	~80	Explosion	Ia,IIIb/very weak/,IVc	Yes	1028	2.04	176	14.92	176	-	126	.079	1 + ~15	$D_p$ of small particles $\sim 0.5$ mm $T_{expl} = 1226^\circ\text{C}$
49	12-10	7.04/7.25	.5206	1438	1488	25	~80	Normal	Ia,IVc,Vba	Yes	1064	1.456	363	7.34	331	.111	114	.320	1 particle	Empty shell; Growth at $\sim 1150^\circ\text{C}$
50	13-01	5.34/4.66	.5501	1134	1197	22	22	Normal	Ia,IVa,Vcb	Yes	1045	2.30	619	6.57	608	.030	~100	.443	"	
51	13-04	-	~.5			22	20	Explosion	IIIa /strong/	Yes									Many particles	$D_p < .01$
52	13-05	5.32/4.40	.5474	1233	1272	22	19	Normal	Ia,IVa,Vb	Yes	1051	3.02	212	16.50	~212	-	103	.135	1 particle	
53	13-09	5.17/4.13	.4685	1195	1296	30	21	Normal	Ia,IVab,Vb	Yes	1035	2.135	203	12.88	~203	-	~100	.224	1 + 2 particles	"Jets" at $T_c \approx 1090^\circ\text{C}$ and in E at $T = 1035^\circ\text{C}$
54	13-10	5.53/3.72	.4995	1346	1368	30	21	Normal	Ia,IIa,IVab,Vb	Yes	1056	2.085	307	12.79	307	-	109	.155	2 particles	"Jet" at $T_c \approx 1090^\circ\text{C}$
55	13-11	6.20/5.54	.5255	1314	1344	10	25	Normal	Ia,IVc,Vcb	Yes	1051	1.915	251	12.07	251	-	111	.148	1 particle	
56	13-32	7.01/7.38	.6126	1380	1408	25	21	Normal	Ia,IVc, /strong/,Vcb	Yes	1046	1.066	654	4.695	654	-	105	.315	"	"Empty shell". Growth at $T_c =$ 1236°C
57	13-35	-	~.55	1408	1454	25	21	Explosion	Ia,IIIb/strong/	Yes	1022	$< 3 \cdot 10^{-5}$	1297	.759	-	-	-	-	Many particles	$D_p < .01$ mm. $T_c$ means $T_{m,expl}$ .
58	13-36	9.00/11.20	.5482	1390	1467	25	21	Normal	Ia,IVc /strong/,Vcb	Yes	1054	.394	1054	1.443	708	.597	100	.239	1 particle	"Fungus form" particle The growth begins at $\sim 1300^\circ\text{C}$
59	13-37	6.85/5.00	.5646	1399	1512	25	22	Normal	Ia,IVb,Vcb	Yes	1037	1.197	573	6.93	573	-	~100	.246	1+~50	$D_p$ of small particles $\sim 0.5$ mm
60	17-01	5.51/4.18	.6249	1100	1185	10	23	Normal	Ia,Vca	No	1037	2.759	347	14.59	347	-	~100	.69	1 particle	Argon-atmosphere (p=300 tor) Cyl. $\phi$ 30
61	17-04	5.70/4.28	.6357			10	25	Normal	Ia,IVb/one jet/,Vcba	No	1059	~3.9	291	21.39	182	.263	~100	.130	1 part. + 1	Argon-atmosph. (p=300 tor), Cyl. $\phi$ 30. Small "jet particle" $D_p = 0.94$ mm
62	18-12	5.63/4.13	.6788	1065	1107	10	19	Normal	Ia,Va	No	1059	3.94	245	22.56	204	.172	~100	.180	1 particle	Ar (p=300 tor), Cyl. $\phi$ 30 mm
63	18-14	5.59/4.33	.6710	1116	1143	10	19	Normal	Ia,Va/very long/	No	1064	3.52	173	25.27	173	-	~100	.138	"	"
64	18-16	5.57/4.17	.6278	1128	1195	10	20	Normal	Ia,Vba	No	1041	3.56	167	22.52	167	-	~100	.111	"	"
65	19-03	6.12/4.23	.6079	1000	1000	15	21	Normal	Ia,Vb/many bubbles/	No	1000	(498) 218	7.45+2.84	~218	-	-	100	.335	1 particle	Ar. p=300 tor. Particle irre- gular /partially solidifica- tion in air/. Twice $T_c$ !
66	19-04	5.90/4.17	.6544	1042	1043	15	20	Normal	Ia,Vb	No	1043		345	10.20	196	.502	~100	.123	"	Ar (p=300 tor), Cyl. $\phi$ 30 mm
67	19-08	5.68/4.25	.6838	1056	1056	15	20	Normal	Ia,Vb	No	1056	~3.4	251	21.04	186	.204	~100	.130	"	"
68	20-13	5.50/3.91		1110	1128	15	18	Normal	Ia,Vb /many bubbles/	No	1065	3.12	318	15.00	188	.808	~100	.448	"	Vacuum (p=40 tor), Cyl. $\phi$ 30
69	20-14	5.63/4.59		1379	1406	15	14	Normal	"	No	1069	2.73	467	9.69	178	.735	~100	.092	"	Ar. (p=300 tor), Cyl. $\phi$ 30
70	22-01	5.50/4.03		1116	1130	25	20	Normal	Ia,Va	No	1077	3.402	193	21.97	193	-	~100	.121	"	Ar. (p=300 tor), Cyl. $\phi$ 40
71	24-11	5.63/6.50		1234	1260	25	20	Normal	Ia,IVc,Vb	No	1072	2.278	310	11.39	230	.345	104	.202	"	Ar. (p=760 tor), shrinkage cavity in the particle
72	25-02	4.91/4.89		1123	1140	30	0	Normal	Ia,IVa,Va	Yes	1075	3.89	201	34.4	201	-	-	-	"	Air
73	29-03	5.45/3.92		993	1025	30	0	Normal	Ia,IVb,Va	Yes	946	3.173	235	13.15	235	-	119	.094	1 part.+3"jets"	Air: Two "jets" solidified Cu/Na, N <sub>2</sub> (p=300 tor),
74	30-01					30	200	Normal	Ia,IIa/solidified/,IVc	No									"	"
75	31-01		~.6			30	200	Explosion	IIIa /mild/	No									"	"
76	32-01					40	400	Normal	Ia,IVc	No									"	"
77	33-01		~.6			40	400	Explosion	Fragmentation only	No									"	"
78	35-01		~.6			30	400	Explosion	Fragmentation only	No									"	"

Table 4. Characteristic of measurements of hot material /cold liquid thermal interaction

No	Sample No	Hot material					Cold water		Type of interaction	Observed phenomena /according to the classification given in Fig. 5/	Solidifying			Film boiling		Transition boiling		Violent Nucleate Boiling		Debris	Remarks
		Kind	m	T <sub>m</sub>	T <sub>me</sub>	V	T <sub>o</sub>	Oxide layer obser.			T <sub>s</sub>	t <sub>se</sub>	T <sub>L</sub>	t <sub>WB</sub>	T <sub>p</sub>	t <sub>LP</sub>	T <sub>w</sub>	t <sub>PW</sub>			
																			g		
0	1	2	3	4	5	6	7	8	9	10	11	12	13	14	15	16	17	18	19	20	
1	0-01	Al	.4078	~850		25	18	Intensive	IVc	No									1 "empty shell"	Particle moved as a rocket	
2	12-22	Al	~.4		~720	25	21	Normal	Ia,IIa	Yes	500		1.57				~100		1 "flat plate"	Solidification during IIa.	
3	04-08	Ag	.6379	~934			21	"	Ia, IIa /begin/	No	934	.712	715	2.17	420	.44	~100	.243	1 "flat plate"		
4	04-09	Ag	.6084	~955			20	"	"	No	948	.738	678	2.175	273	.685	~100	.065	2 particles		
5	04-10	Ag	.6751	1019			19	"	Ia,IVa,Vb	No	929	.795	307	7.41	240	.198	~100	.121	1 particle		
6	04-11	Ag	.6607	1151	1174		20	"	Ia,IVa,Vb	No	936	.837	274	3.08	274	-	100	.080	"		
7	04-12	Ag	.5501	1137	1181		20	"	Ia,IIa,IVa,Vb	No	934	.643	248	2.72	200	-	100	.075	2 particles		
			.0663																		
8	04-13	Ag	.6685	1267	1355		17	"	Ia,IVa,Vbc	No	960	.944	370	4.21	285	0.05	~100	.105	1 particle	large shrinkage	
9	04-14	Ag	.6028	1166	1320		18	"	"	No	936	1.40	348	4.92	223	.145	~100	.070	1 particle		
10	15-19	Ag	~.6	1100		20	18	"	"	No									1 particle	Photos in Fig. 3	
11	15-20	Ag	~.6	1100		20	18	"	"	No									1 particle		
12	21-04	Ag	1.1369	1311	1331	25	19	"	Ia,IVa,Vb	No	948	2.571	312	13.812	312	-	~100	.441	1 particle	Argon - 300 tor.	
13	21-05	Ag	1.3040	1031	1086	25	19	"	"	No	940	2.939	223	17.831	223	-	~100	.441	1 particle	" "	
14	21-13	Ag	1.26	1000		19.5	20	"	"	No									1 particle	Argon - atmosphere	
15	08-10	Au	1.2711/4	981	1054	20	21	"	Ia,IIa,Vb	No	894	.406	276	2.29	276	-	110	.082	4 large particles + many small one		
16	19-14	Au	~.6	1012	1012	15	20	"	Ia,IVab	No	1012	1.224					100	.15	1 large + 2	1 "jet" observed	
17	26-09	SS	~.6	1500		25	21	"	Ia,IVa	Yes									1 particle	N <sub>2</sub> atmosphere, p~ 300 tor.	
	15-27	Pb	~1.0	~500				"	IIIa /strong/	Yes									Many particles	D <sub>p</sub> ≤ 0.1 mm	
18	19-11	Pb	~1.0	~500		15	18	"	IIa	Yes	registered peak of short duration							1 irregular	Ar - atmos.		
19	12-14	Sn	~.8	~600		15	19.5	Explosion	IIb,IIIb	Yes									part of shell + many ~ 10 <sup>-4</sup> m		
20	12-15	Sn	.8247			25	22	Normal	Ia,IVa,Vb	Yes	141	283	575	1.625	316	.350	141	.087	1 particle		
21	13-16	Sn	~.8	192	>250	16	21.	"	IIa,Va	Yes			250		250		107	~.3	1 particle		
22	13-47	Sn				20	23	"	IIa,Va	Yes	registered peak of short duration							1 particle	rings at the surface		
23	15-29	Sn	~.8			20	20	"	IIa,Va	Yes	"	"	"	"	"	"	"	"	1 flat plate		
24	23-09	Zn				20	25	"	IIa,Va	Yes	"	"	"	"	"	"	"	"		rings at the surface	
25	12-17	Zn	~.47	>383	383	25	19	"	Ia,IIa	Yes	383	<.411	383	.411	383	-	157	.162	1 particle	irregular	
26	12-20	Zn	~.47	666	710	25	19	"	Ia,IIa	Yes	392	.115	392	.588	392	-	129	.132	1 particle	irregular	

$(\overline{WZ})_i$  - end of violent nucleate boiling and beginning of pure convection.

The heat transfer history according to the classification above and thermal interaction of hot and cold substances can be regarded as "normal or quiet" in this case. It usually took place for particles with a higher solidification temperature than the Leidenfrost temperature of the cooling liquid in these experiments, as e.g. Ag, Au, Cu, Fe. Deviations from such "normal course" are however possible, and various courses of the phenomena were observed.

The "normal" or "quiet" heat transfer was the most probable interaction observed in these experiments with hot and cold substances. For the "normal course" of heat transfer during Cu/water - thermal interaction, a vapour film existed around the particle during and for some time after the end of solidification of the particle. The solidified particle had the form of a spheroid with a small shrinkage cavity (Fig. 3, IVa,f). The cavity could be hidden in the centre of the particle (Fig. 3, IVb).

Pictures of the particles of various metals after "normal course" of thermal interaction are presented in Fig. 3, Ia, b, VI, VII, VIIIa, IX. The shape of the particle depended on the wettability characteristic at the bottom of the vessel and on the surface tension forces of the hot molten material (Fig. 5, I a, b), and in case of e.g. Pb, on Thermostix 2000- bottom it resulted in an irregular shape of the particle. An analogous effect was observed for cooling of Cu on mica or on  $Al_2O_3$ .

In Figs. 7, 8, 9, temperature readings of the "normal course" of thermal interaction are presented for the Cu/water system. The duration of the plateau of the temperature reading  $T_1$  for the "normal course" of cooling of the pure metal particle is proportional to the time of solidification. Such temperature readings are also characteristic for Ag, Au particles and copper if it is heated in an inert gas atmosphere (Table 4).

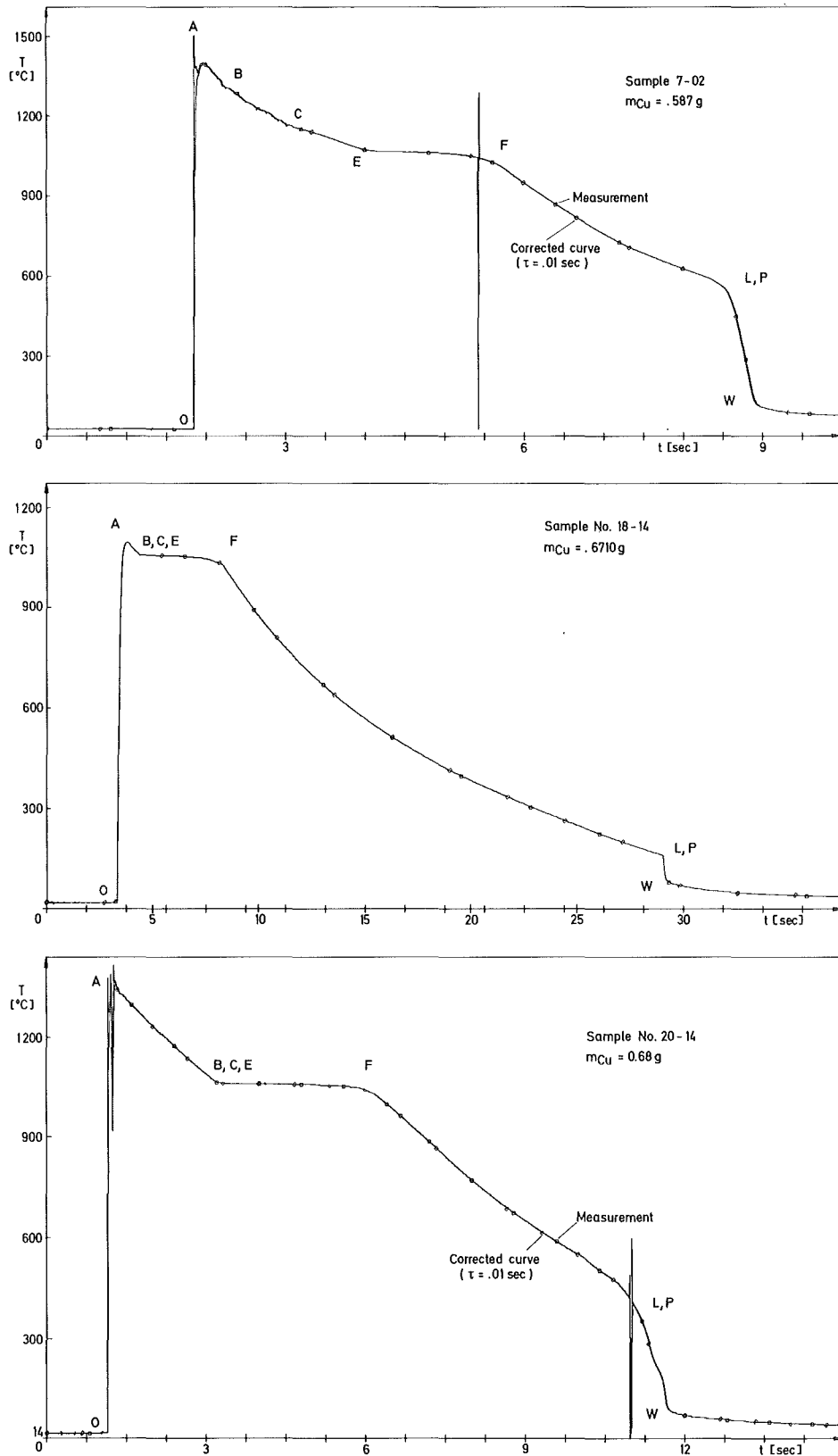


Fig. 9 Temperature histories of cooling of the copper particles in water. The particles molten in: air (Sample 7-02), argon (Sample 18-14) and nitrogen (Sample 20-14) gas atmosphere, respectively.

On the other hand, if copper was heated in air, the solidification process began, however, at a higher temperature than the solidification point of copper (point C in Figs. 7, 8). This was due to the existence of oxide in the particle. Metal oxide was formed in the levitation coil during heating and fall in air.

For the "normal course" of thermal interaction the following mean times of solidification are distinguished:  $\Delta\tau_{Se}$ , the extrapolated value of the solidification time obtained from the "idealized" temperature measurement, and  $\Delta\tau_S$ , the calculated value obtained on the assumption of continuity of the heat transfer rate before and after solidification of the particle:

$$\Delta\tau_S = \frac{L_{HM} \cdot m_{HM}}{F_1 \cdot \alpha (T_S - T_{CL}) + F_2 \cdot \frac{\lambda}{\Delta l} (T_S - T_a)} \quad (1)$$

where  $F_1$ ,  $F_2$  are surfaces of the particle in contact with the fluid and with the bottom of the vessel, respectively (Fig. 2). It is assumed that the whole surface of the particle is  $F = F_1 + F_2$ . The surfaces  $F_1$  and  $F_2$  were derived by measurement in several directions of the particle after thermal interaction and by geometrical considerations.

The foregoing values  $\Delta\tau_{Se}$  and  $\Delta\tau_S$  are compared with the result of the simplified calculations according to the following formula (for  $1/Bi \gg \gamma$ ) [10]:

$$\Delta\tau_{S\ cl} = \frac{\rho \cdot r^2 \cdot L_{HM}}{\lambda \cdot (T_S - T_{CL})} \cdot \frac{1 + 2/Bi}{Bi} \quad (2)$$

where  $Bi = \frac{\alpha r}{\lambda}$  Biot number;  $\gamma = C_p (T_S - T_{CL})/L_{HM}$ ;  
 $\lambda$ ,  $C_p$ ,  $L_{HM}$ ,  $r$  are the thermal conductivity, heat capacity,  
 heat of fusion, and radius of the metal particle, respec-  
 tively; and  $\alpha$  is the heat transfer coefficient.  
 Results will be presented in [19].

### 3.1.1 Film boiling

Heat transfer film boiling takes place when the bulk of the "cold liquid" is separated from the heating surface by a continuous vapour layer. The phenomenon was studied by several authors and its mechanism has been satisfactorily described [e.g. 7].

This, however, concerns mostly "hot solid - cold liquid" systems. In this study, results are given for the "hot molten material - cold liquid" system when the hot material solidifies during the film boiling regime. In addition comparison of the results with the data available allows to check up in some way the measurement technique which was used in these experiments.

If film boiling occurs the heat is transferred mainly by conduction and radiation through the vapour film which covers the hot material surface. Film boiling of the surrounding "cold liquid" in the "hot material/cold liquid system" is promoted when the "hot material" temperature exceeds the Leidenfrost temperature for this system. In the majority of tests this condition was fulfilled and the "normal" heat transfer began with the film boiling regime. The following observations were made:

1. The initial phase of film boiling was unstable.
2. Several types of vapour spaces (film) were observed around the particle (Fig. 5:V).

3. The value of the Leidenfrost temperature had a random character and was measured within a broad range of temperatures.

The initial instability of the vapour film was due to the strong initial turbulence of the cold liquid after the impact of the particle at the bottom of the vessel (Fig. 5:IIa).

At first, the vapour film pulsed irregularly around the particle surface and a local "direct contact" of the molten metal with water is conceivable. The vapour film grew over a portion of the particle while it decreased in thickness at another point (Fig. 5:Vc). This period was short (order of magnitude 0.1 - 1 sec) in comparison with the total time of the film boiling regime, which e.g. for Cu/H<sub>2</sub>O thermal interaction usually took from 2 to 20 sec (Table 3).

Then, film boiling became stable in character, but one could, however, distinguish between the following three types of courses:

- one vapour bubble of almost constant size surrounded the metal particle;
- one vapour bubble existed which strongly increased in size or pulsed (Fig. 5:Va);
- several vapour bubbles occurred which left the metal particle one after the other (Fig. 5:Vb).

Considering the particle as a lumped parameter system, the heat transfer rate can be computed from the temperature measurements as follows:

$$q'' = \dot{Q}/F \quad (3)$$

where:

$$\dot{Q} = \begin{cases} m_{HM} L_{HM} / \Delta\tau_S & \text{for the solidification process} \\ & \text{(EF-range).} \\ m_{HM} C_p D_K & \text{for pure cooling at the particle} \end{cases}$$

and

$$\alpha = \frac{\dot{Q}}{F_1 \cdot (T_{HM} - T_{CL})} - \frac{F_2 (T_{HM} - T_\alpha) \cdot \lambda}{F_1 (T_{HM} - T_{CL}) \cdot \Delta l} \quad (4)$$

where  $D_K = \partial T / \partial \tau$  is the tangent to the temperature curve.

The heat flux  $q''$  as a function of the difference  $\Delta T$ , i.e. the temperature between the copper particle and the water temperature, is shown in Fig. 10. This graph is the summary of about 100 measurements. In these experiments the heat flux decreased continuously during the film boiling regime from its initial value  $q_B'' \sim 10^6 \text{ W/m}^2$  and it can approach the value  $q_L'' \sim 10^5 \text{ W/m}^2$  (the range  $\overline{BL}$  in Figs. 7, 8, 9). Afterwards, stable film boiling ceased abruptly (transplosion [9]) and after a very short transition (order of magnitude 0.2 msec), violent nucleate boiling began. In the space between the double line of the  $\overline{BL}$  region the measurement results of film boiling of water on the copper particle are shown, the size of which is  $\sim 0.5$  gramme. The boiling ranges mentioned before are all listed in Fig. 10. The results are in quite good agreement with the existing literature data on the heat flux characteristic [4]. However, it should be noted that these measurements were made under transient conditions where the heat flux can be appreciably higher than in steady-state boiling due to the rapid formation and evaporation of a thin liquid film.

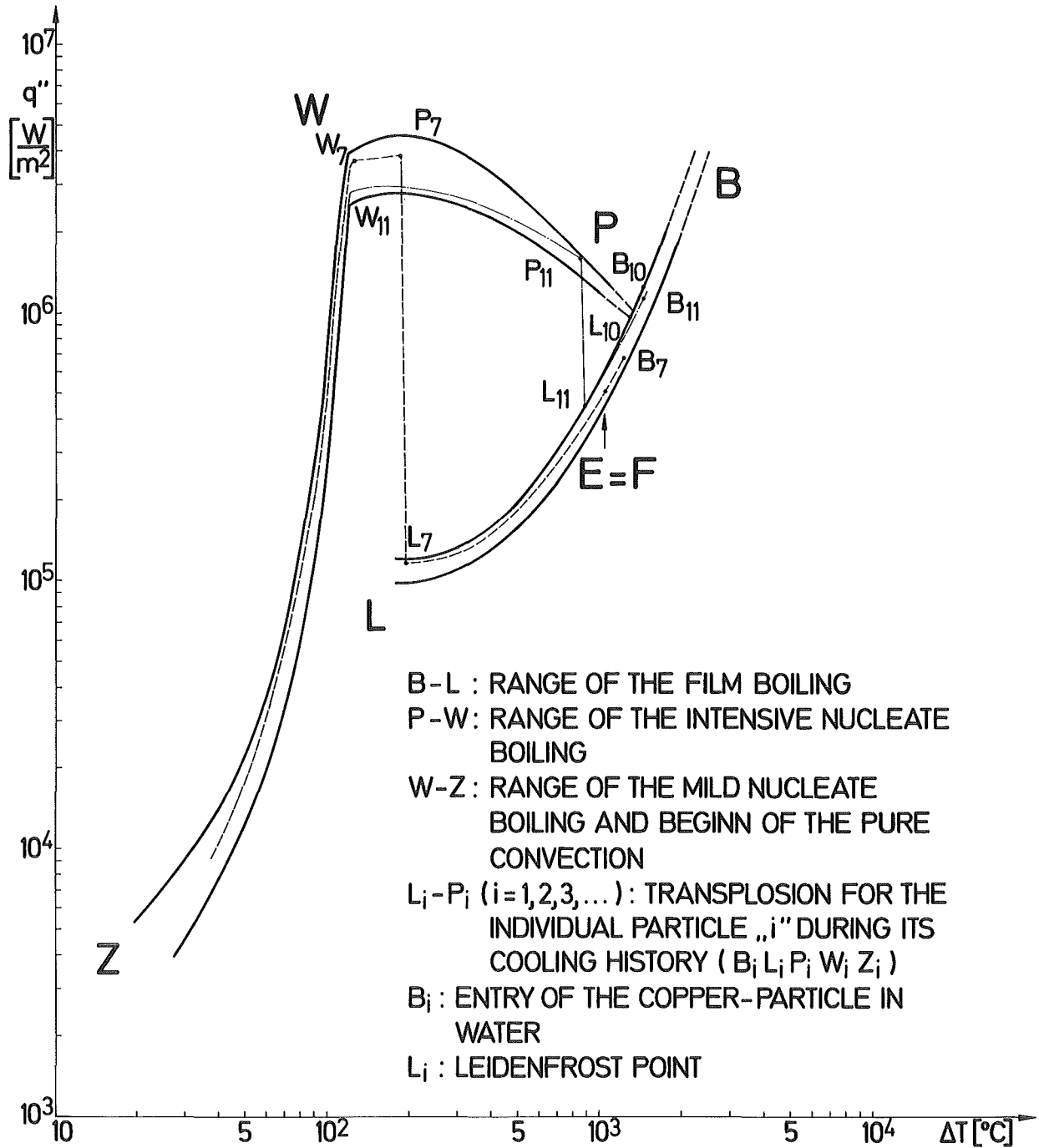


FIG.10 HEAT FLUX CHARACTERISTIC OF THE QUENCHING OF THE MOLTEN COPPER-PARTICLES IN COLD WATER. ( $T_0 \approx 20^\circ C$ )

### 3.1.2 Transplosion and the following phenomena

The film boiling regime stops at transplosion (point L in Figs. 7-10), i.e. when the vapour film collapses. Transplosion has a random character and for "normal" heat transfer it can happen in a wide range of temperatures, as e.g. for the Cu/H<sub>2</sub>O thermal interaction in the range from 165°C to about 750°C [18\_7].

Transplosion depends on many factors as the hot surface characteristic, the hydrodynamic conditions and the external disturbances during the boiling phase.

After transplosion, the nucleate boiling regime ( $\overline{PW}$  or usually  $\overline{LW}$  segment, Figs. 7-9) or sometimes also the transition boiling regime ( $\overline{LP}$  segment, Fig. 7-9) occurs.

The heat flux jumps from its value at the end of the film boiling regime to the value of the violent nucleate boiling regime ( $q_{LW}'' \sim 1 - 5 \cdot 10^6 \text{ W/m}^2$ , the range PW in Fig. 10). This value stays almost constant for some short period of time ( $\sim (0.05) 0.1 - 0.5 (0.8) \text{ sec}$ ).

Violent nucleate boiling is followed by quiet nucleate boiling, if the temperature for water decreases to about 120°C, and then by pure natural convection of the non-boiling liquid. The heat flux vanishes quietly and becomes zero.

The measurements with water up to about 80°C demonstrate the similar character of the phenomena (see table 3). The theoretical interpretation of the Leidenfrost point measurements for this experiment is given in [18\_7].

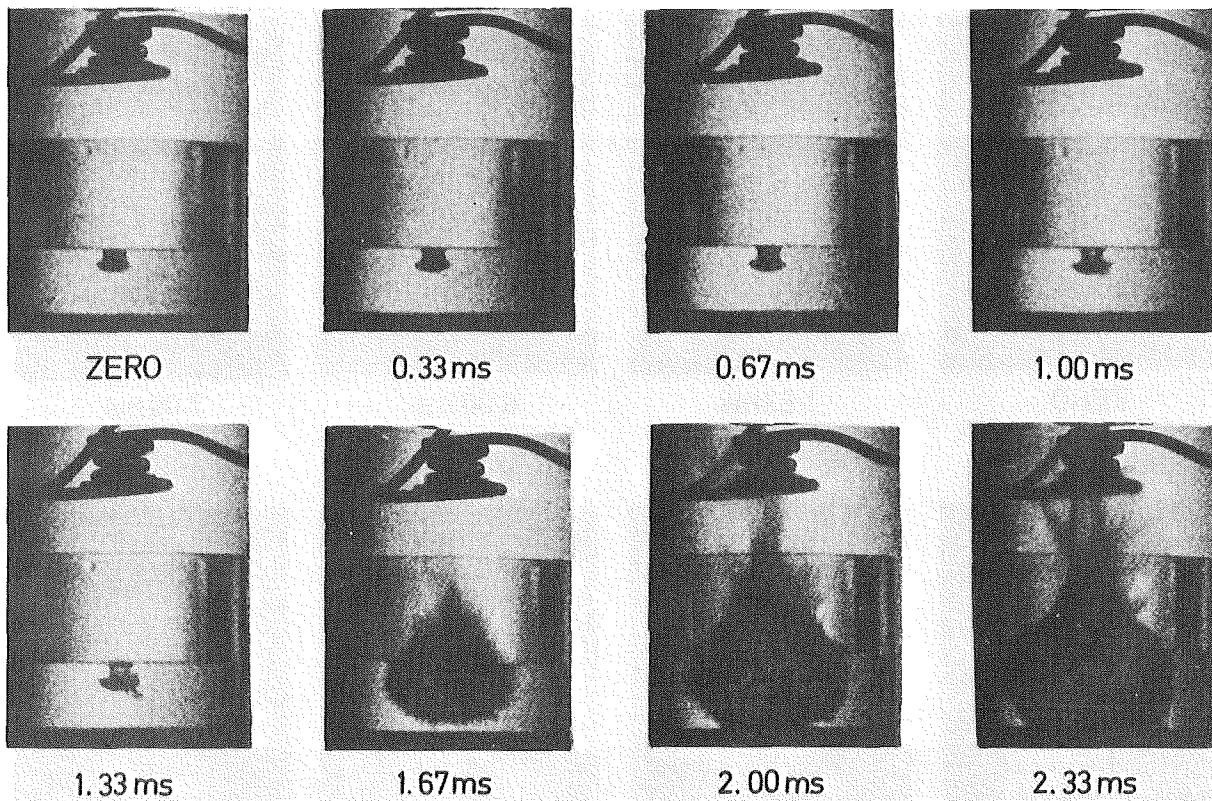


FIG.11 SEQUENCE FROM A FILM SHOWING DEVELOPMENT OF A THERMAL EXPLOSION. COPPER IN WATER.  $T_{CTC} \sim 1300$  deg C,  $T_W = 19.5$  deg C,  $m_{Cu} \approx 0.5$  g. SAMPLE NO. 13-04.

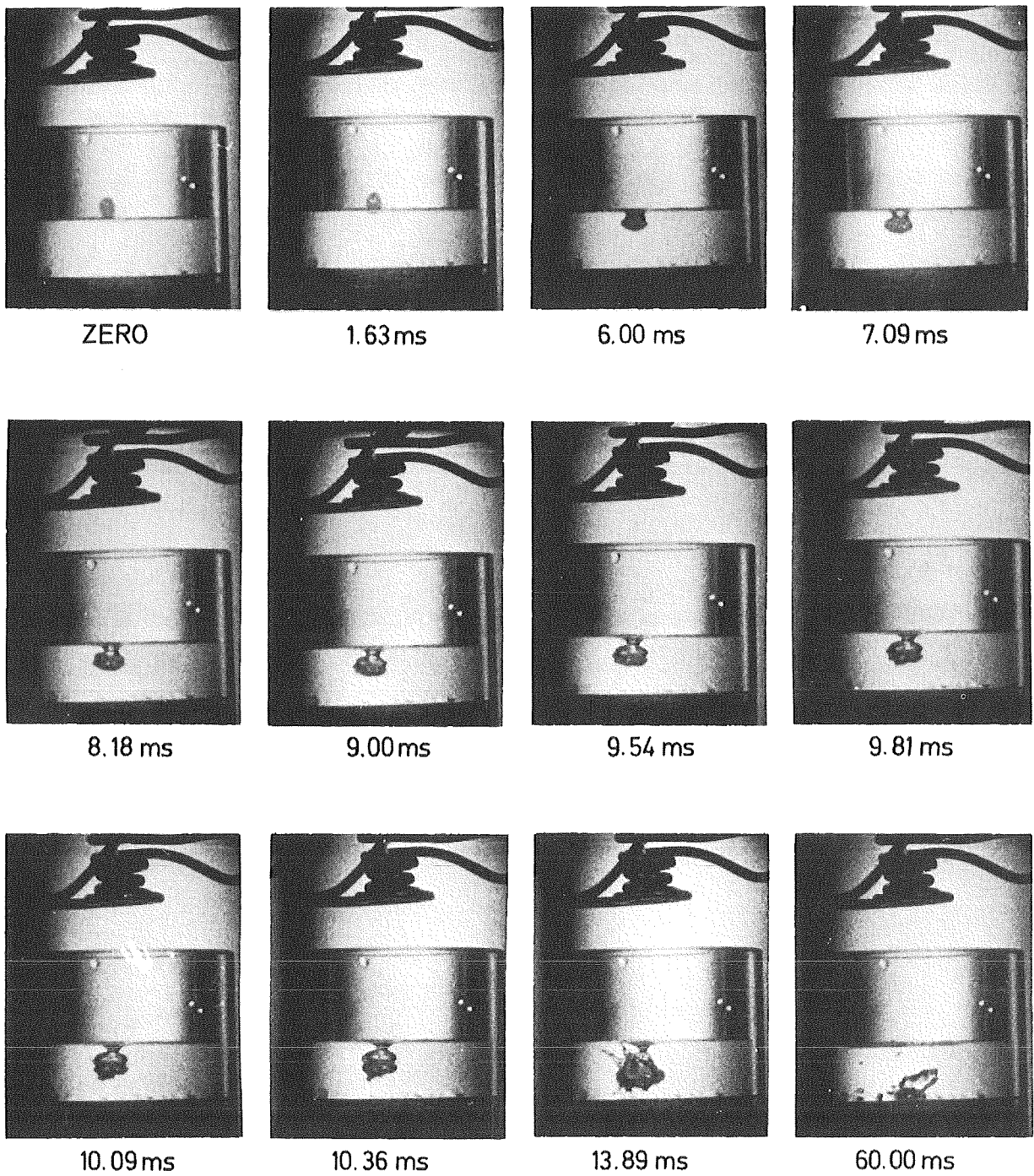


FIG. 12 SEQUENCE FROM A FILM SHOWING DEVELOPMENT OF A WEAK THERMAL EXPLOSION. COPPER IN WATER.  
 $T_{ctc} \sim 1300$  deg C,  $T_0 \sim 20$  deg C,  $m_{Cu} \approx 0.5$  g.

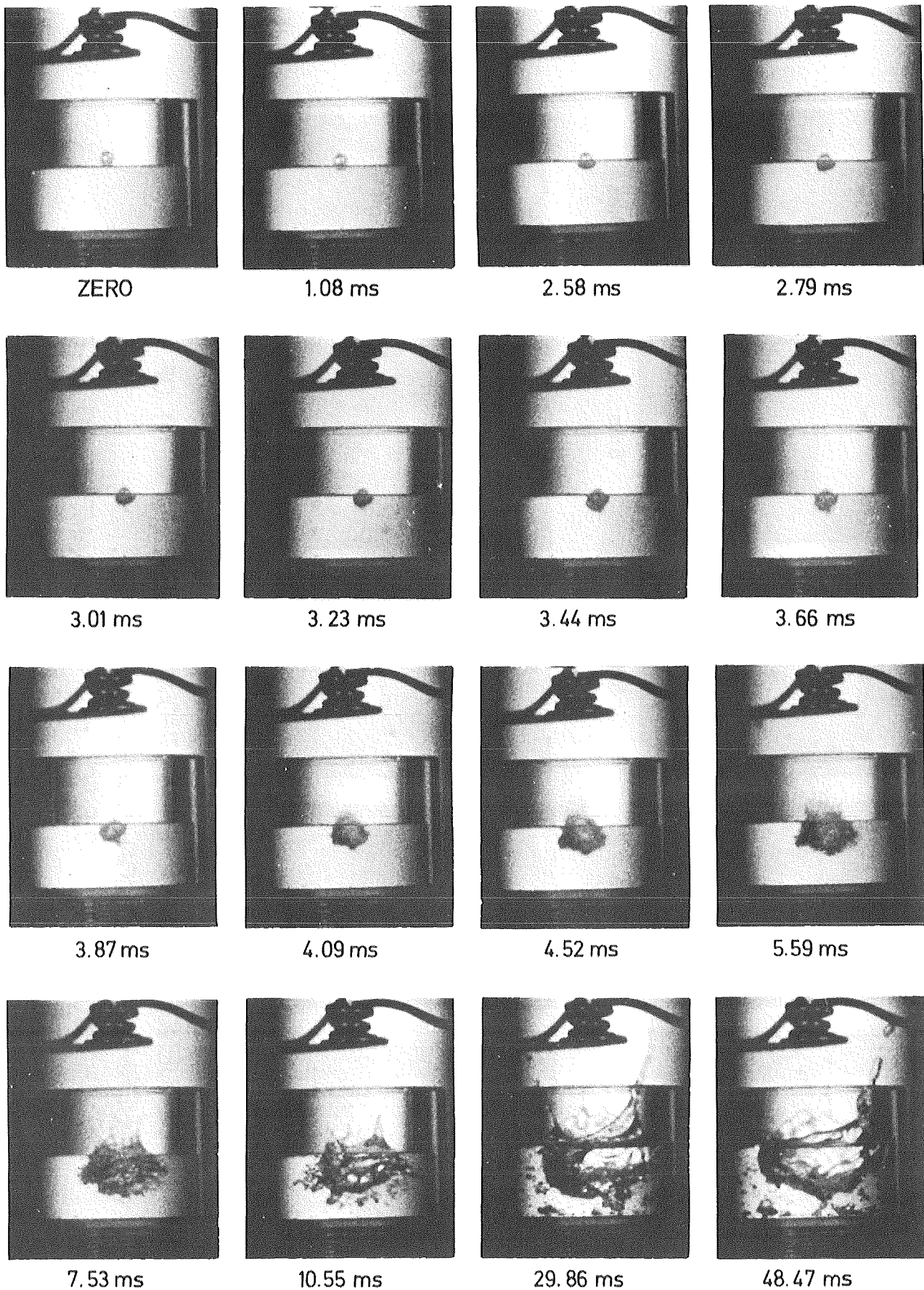


FIG.13 SEQUENCE FROM A FILM SHOWING DEVELOPMENT OF A WEAK THERMAL EXPLOSION. COPPER IN WATER. SAMPLE NO. 8-05.  $T_{ctc} \sim 1300^\circ\text{C}$ ,  $T_0 = 20^\circ\text{C}$ ,  $m_{\text{Cu}} = 0.55 \text{ g}$ ,  $V_{\text{H}_2\text{O}} = 25 \text{ cm}^3$ .

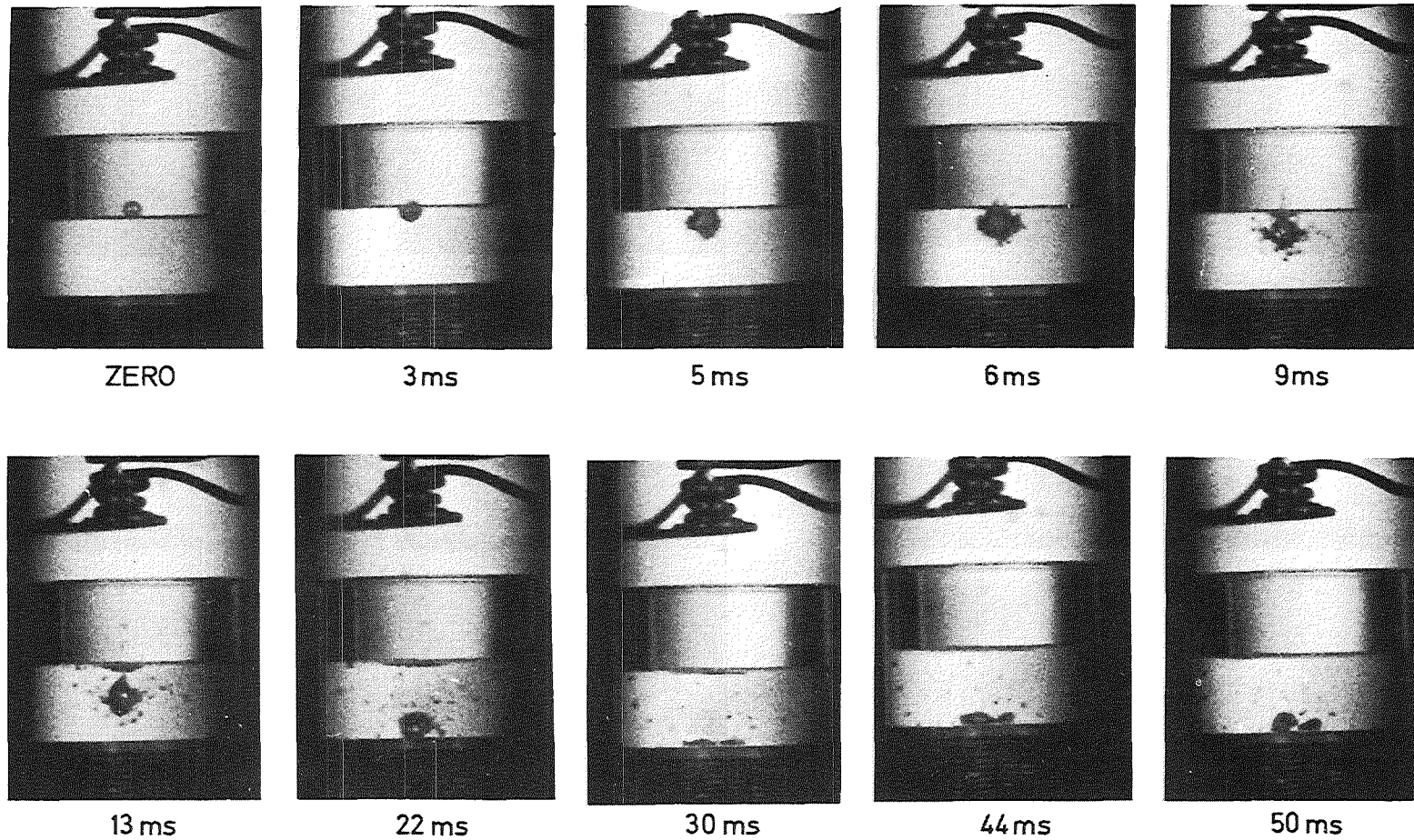


FIG.14 SEQUENCE FROM A FILM SHOWING DEVELOPMENT OF A WEAK THERMAL EXPLOSION. COPPER IN WATER.

$T_{bott} \sim 1300 \text{ }^\circ\text{C}$  ,  $T_0 = 19.5 \text{ }^\circ\text{C}$  ,  $m_{Cu} = 0.5\text{g}$ . SAMPLE NO. 8 - 03.

## 3.2 Thermal Explosion

The quiet thermal interaction of hot molten material with relatively cold liquid ("normal course") was sometimes interrupted by fragmentation of the hot material, fast vaporization of the cold liquid, and rapid expulsion of interacting substances from the thermal interaction zone (Fig. 4). The phenomenon was often characterized by a high pressure peak and a loud acoustic effect.

The phenomenon (thermal explosion phenomenon) was observed in the following two locations:

- at a small distance below the cold liquid surface, or
- at the bottom of the vessel.

### 3.2.1 Thermal explosion a short distance below the cold liquid surface

At a short distance below the water surface, a sudden thermal explosion of the copper particle can occur. It was observed several times, when the levitation time of the copper in the levitation coil was about 6.4 sec (i.e. corresponding to about 1400°C. Other parameters were the diameter of the vessel, 40 mm, the distance between the water surface and the levitation coil, 30 mm, and the water volume, 20 to 30 ml, the temperature being about 20°C).

No temperature readings could be made for copper during thermal explosion because it took place before the thermocouple at the bottom of the vessel was touched. Only limited conclusions can be drawn, but strong (Fig. 11) and weak (Figs. 12, 13, 14) thermal explosions can be distinguished. On the high-speed films, a "jet" from the main particle into water can be observed about 1 to 5 msec before thermal explosion. It seems also that the vapour film disappears and a kind of "directed contact" can be supposed. The nature

of this contact cannot be stated precisely because of the limited possibilities of high-speed cinematography used in the first stage of the experiments. Only the time of the "jet"-expulsion can be determined (Figs. 11-14). For example in Fig. 11, the "jet" appears in the interval between 0.67 msec and 1 msec after the first contact of the particle with the water surface, and the thermal explosion takes place between the 1.33 msec and the 1.67 msec picture.

The spherical front of the strong thermal explosion expands at a velocity  $> 35-50$  m/sec (or  $> .2$  m<sup>3</sup>/sec) for the Cu/H<sub>2</sub>O thermal interaction. The pictures taken "before" and "after" the event allows one to approximate such a value for the lower limit of the expansion velocity of the thermal explosion front.

For the weak thermal explosion below the water surface, the copper particle can break up later at the bottom of the vessel (hydrodynamic partition) (Fig. 5IIa). If, however, the particle splits into comparatively large particles during a weak thermal explosion, these particles can again come together as they move further to the bottom.

The study of debris of thermal explosion yields two kinds of particles, "shattered" and spherical particles, both of the same order of magnitude regarding strong thermal explosion (Fig. 3, IVe). For weak thermal explosion, the spherical particles are larger in diameter, and sometimes "empty". Debris of Cu/Na fragmentation have a similar shape (Fig. 3:V). The foregoing finding suggests that the hot material was partially molten and partially solid during the fragmentation process. This will be discussed in more detail in the next section.

### 3.2.2 Thermal explosion at the bottom of the vessel

A thermal explosion can also occur at the bottom of the vessel. Such a thermal explosion of copper particles was only observed in these experiments when the temperature of the copper before the interaction was about  $1650^{\circ}\text{C}$  (levitation time about 10 sec, 7 - 25 ml of water of  $10 - 25^{\circ}\text{C}$ , plexiglass vessel of 30 - 40 mm I.D., distance between levitating particle and the bottom of the vessel 65 - 70 mm).

In the first stage of experiments, the bottom of the vessel was flat. The copper particle dropped and covered thermocouple No. 1 (Fig. 2). The beginning of the "normal course" was usually unstable and the vapour dome above the particle pulsed irregularly. Subsequently, "jets" ("shots") of small particles go off from the main metal mass. Then, thermal explosion occurred abruptly and the substances were expelled from the thermal explosion zone into surroundings.

In the second stage of the experiments, the experimental apparatus was modified: A short copper pin, 1 - 1.35 mm O.D., was installed in the bottom of the vessel (Fig. 2), which built a thermal bridge between the copper particle and the water. In addition, the bottom of the vessel was made in the form of a  $160^{\circ}$  cone, which forced the particle to go to the center. In this way, the frequency of thermal explosion occurrence was increased as compared to the first stage of experiments (Tables 3, 4, 5).

In the Table 5 a specification is presented of the measurements of thermal explosion performed in the second stage of the experiments. The temperature at which thermal explosion occurred ( $T_{\text{expl}}$ ) is determined from the temperature readings (Figs. 15 - 17) and reconciled with the pressure peak and with the sequence of pictures from high-speed films (Figs. 18-21). The maximum temperature recorded by thermocouple No. 1 is usually below  $1500^{\circ}\text{C}$ , but the corresponding extrapolated maximum temperature is between  $1400 - 1650^{\circ}\text{C}$  (Table 5). The particle does not settle at once at the thermocouple, at the beginning it "dances" on the bottom of the vessel.

Table 5 Measurement results for the strong thermal explosion

Sample No.	Hot material		Air temperature	Cold liquid: water			"Artificial jet" O.D. mm	T <sub>max</sub> in water (approx.) °C	Explosion temperature (approx.) °C	Oxygen content %wt	Total surface m <sup>2</sup>	Pressure		Remarks
	Kind	Mass g		Vessel diam. mm	Volume ml	Temp. °C						Maximum Value bar	Duration msec	
7-03	Cu	~.57	~20	40	20	20	-	1300	1290					Results of the experiments of the first stage
13-35	Cu	~.55	~20	42.5	25	21	-	1450	1300					
37-04	Cu	1.10	16	40	15	16	1.0	1500	1120					Strong explosion. Thermocouple broken.
37-09	Ag+Cu	1.03 (Ag. 54)	16	30	10	16	-							
37-10	Ag+Cu	.98 (Ag. 50)	16	40	15	16	-							"
37-15	Cu	1.10	16	40	15	18	1.0			1.41-1.46				
38-04	Ag+Cu	.91 (Ag. 52)	20	30	10	18	-		1370					"
39-05	Cu	1.11	22	30	10	15	1.0	>1500						
39-07	Cu	1.07	20	40	15	22	1.0	1500	1228					Strong explosion. Thermocouple broken.
40-04	Cu	.82	21	30	7	14	1.0	1660	1300					
41-06	Cu	1.42	18	30	7	12	1.1			2.27-2.39				"
41-09	Cu	1.26	18	30	7	14	1.1	>1650	1400					
42-07	Cu	1.23	18	30	7	14	1.2	>1500	1310			-10	~.5	Strong explosion a small distance below the water surface
43-01	Cu	1.34	18	30	7	18	1.35			1.15-4.57				
43-04	Cu	1.35	18	30	7	14	1.35	1460	1310			-7	~.3	Strong explosion a small distance below the water surface
43-05	Cu	1.35	18	30	7	12	1.35			1.89-2.37				
43-08	Cu	1.35	18	30	7	14	1.35							"
44-01	Cu	1.22	17	30	7	10	1.35			1.58-1.71				
44-04	Cu	1.58	18	30	7	16	1.35	1390	1160			>15	~1.0	"
44-05	Cu	1.56	20	30	7	14	1.35	1470	1230			-12	.4	
44-09	Cu	1.57	20	30	7	17	1.35	1540	1173			.51		"
44-12	Cu	1.59	20	30	7	17	1.35					.57		

Empty positions in the above table show that no measurement exists

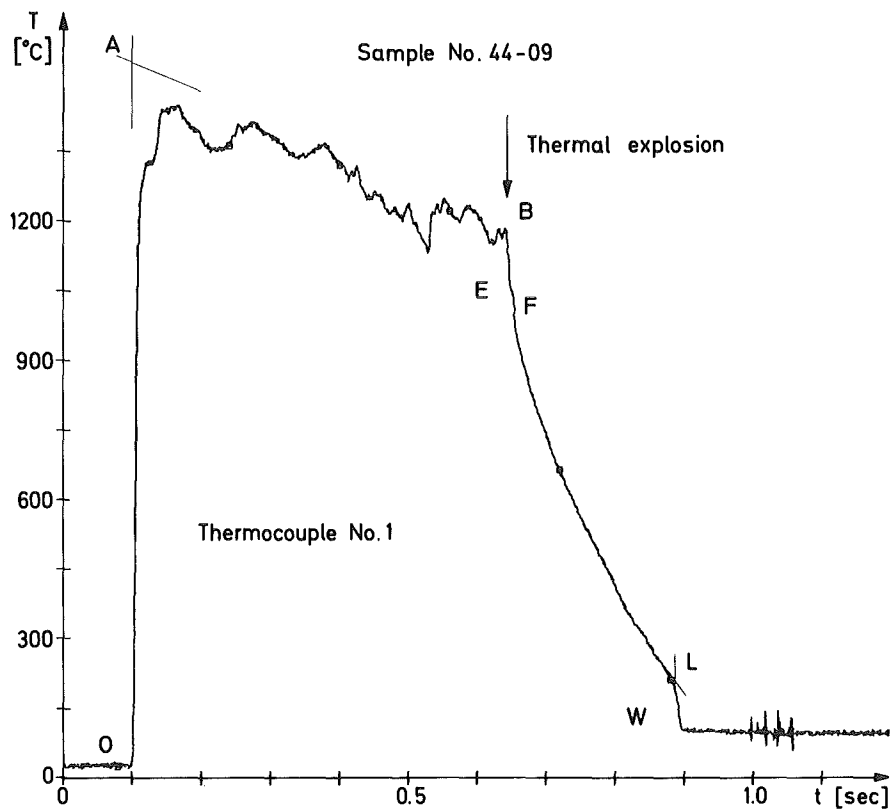
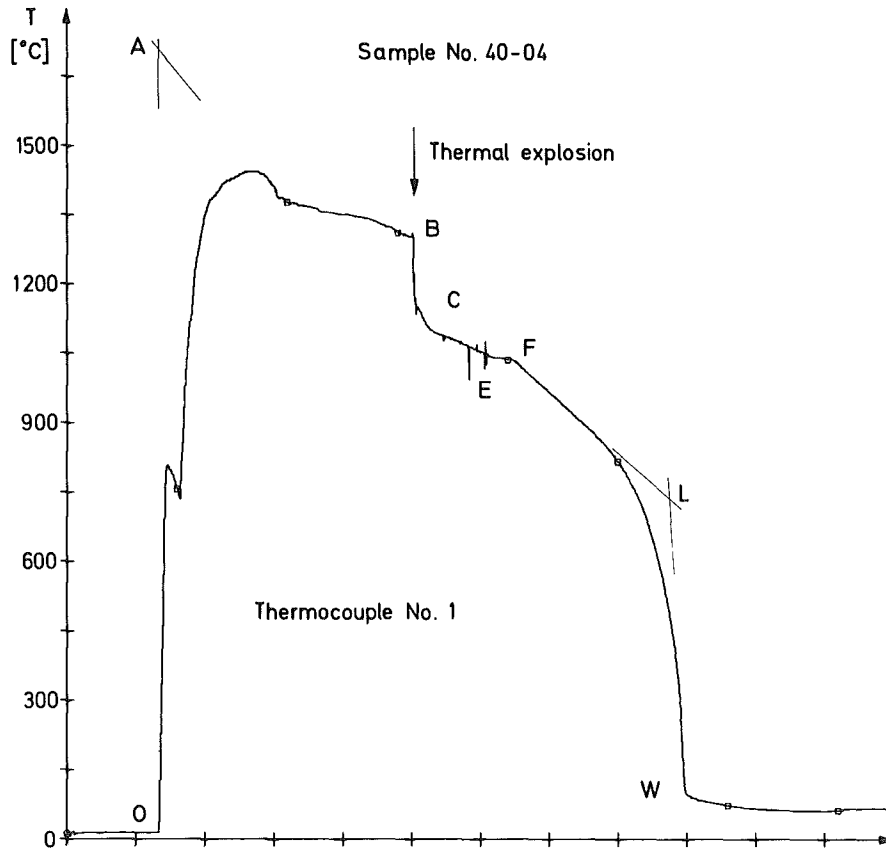


Fig. 15 Temperature histories of thermal explosion for Cu/water system (Samples 40-04 and 44-09).

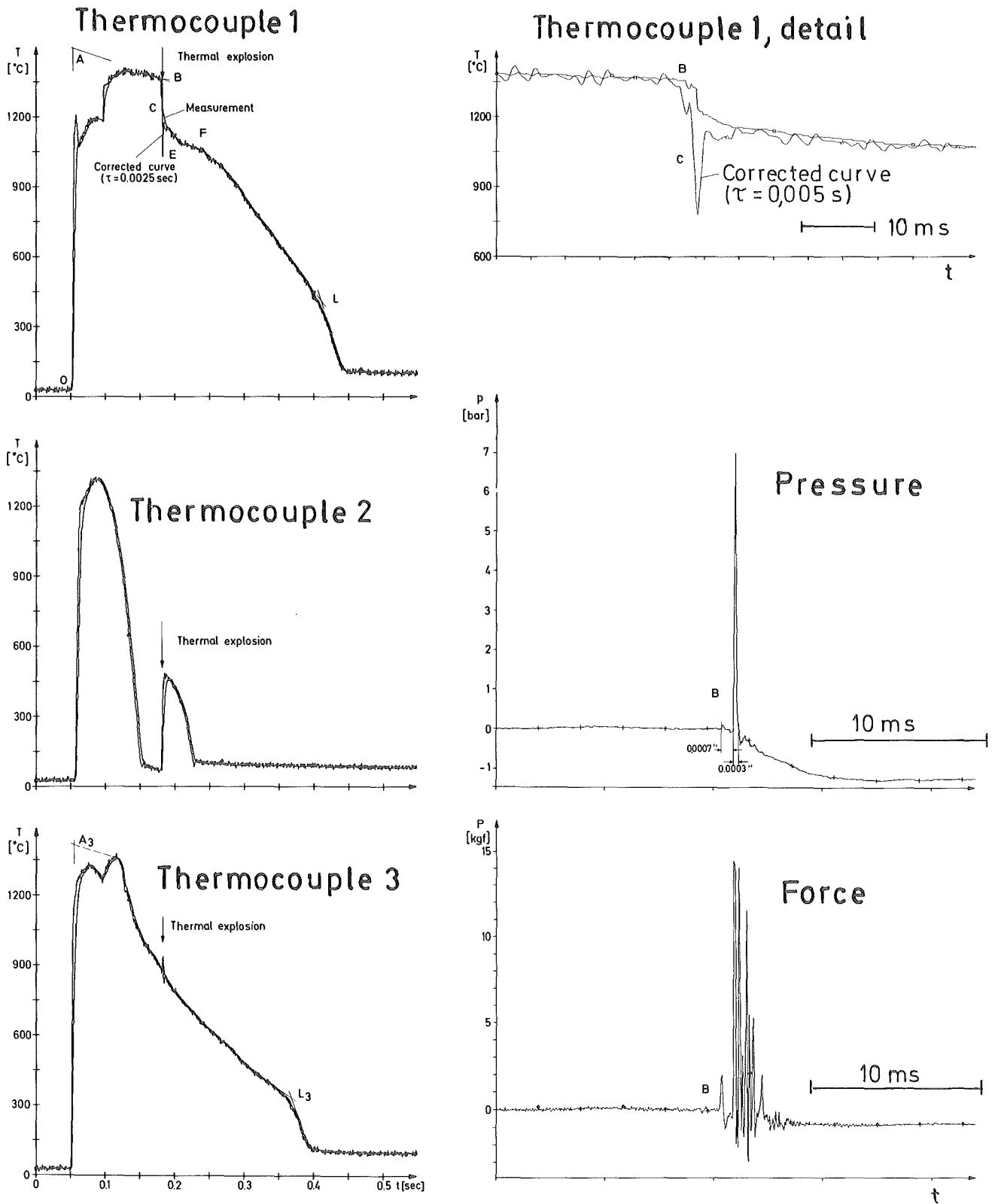


Fig. 16: Temperature, pressure and reactive force recording of thermal explosion for the Cu/water system (Sample 43-04). For position of thermocouples see Fig. 2 .

## Thermocouple

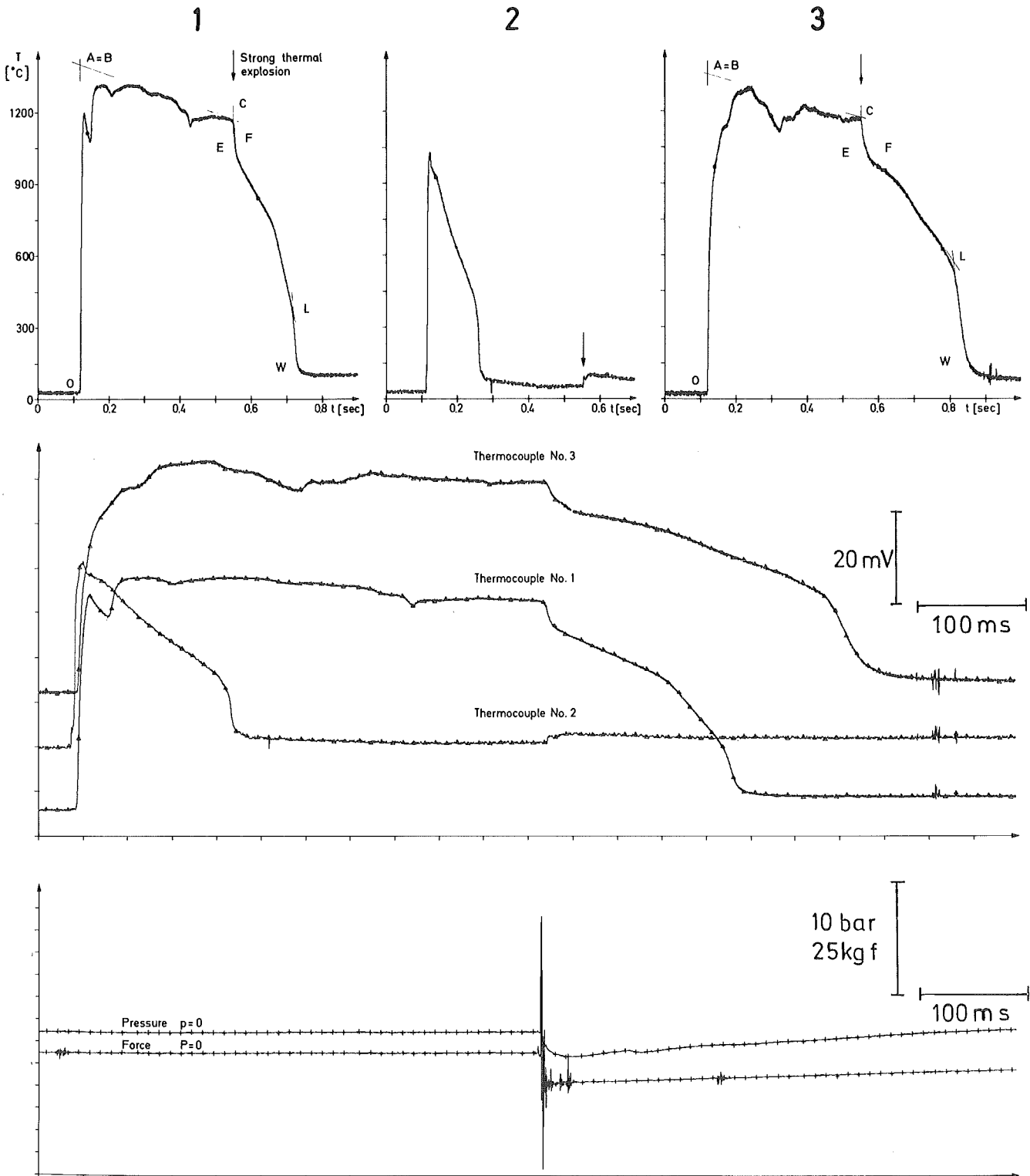


Fig. 17: Temperature, pressure and reactive force recording of thermal explosion for the Cu/water system (Sample 44-04).

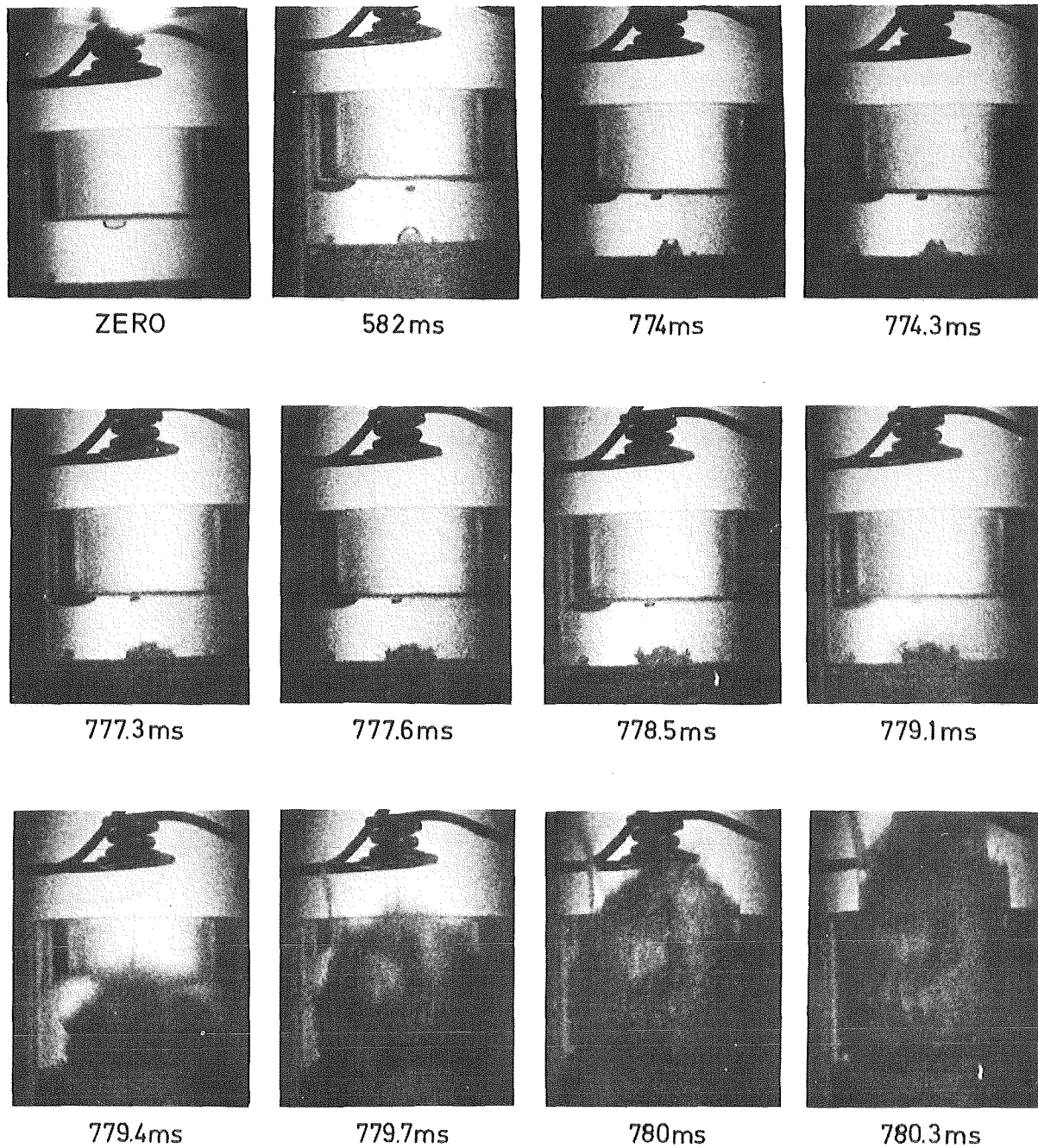


FIG. 18 SEQUENCE FROM A FILM SHOWING DEVELOPMENT OF A THERMAL EXPLOSION ON THE BOTTOM. COPPER IN WATER.  $T_{\text{bott}} = 1454 \text{ deg C}$ ,  $T_0 = 21 \text{ deg C}$ ,  $m_{\text{Cu}} \approx 0.5 \text{ g}$ . SAMPLE NO. 13-35.

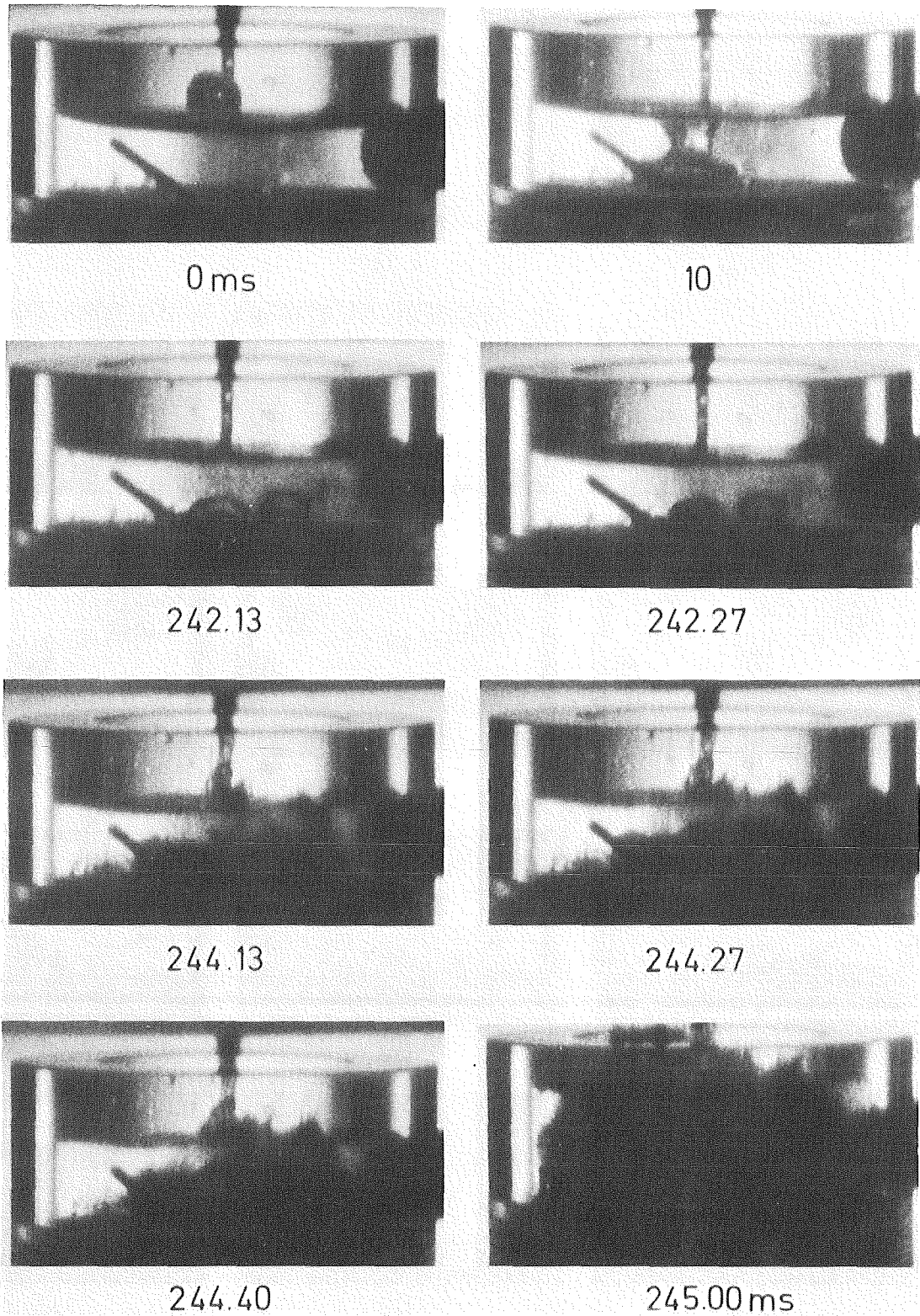


Fig. 19 Development of thermal explosion at the bottom of the vessel (Sample 44-01).

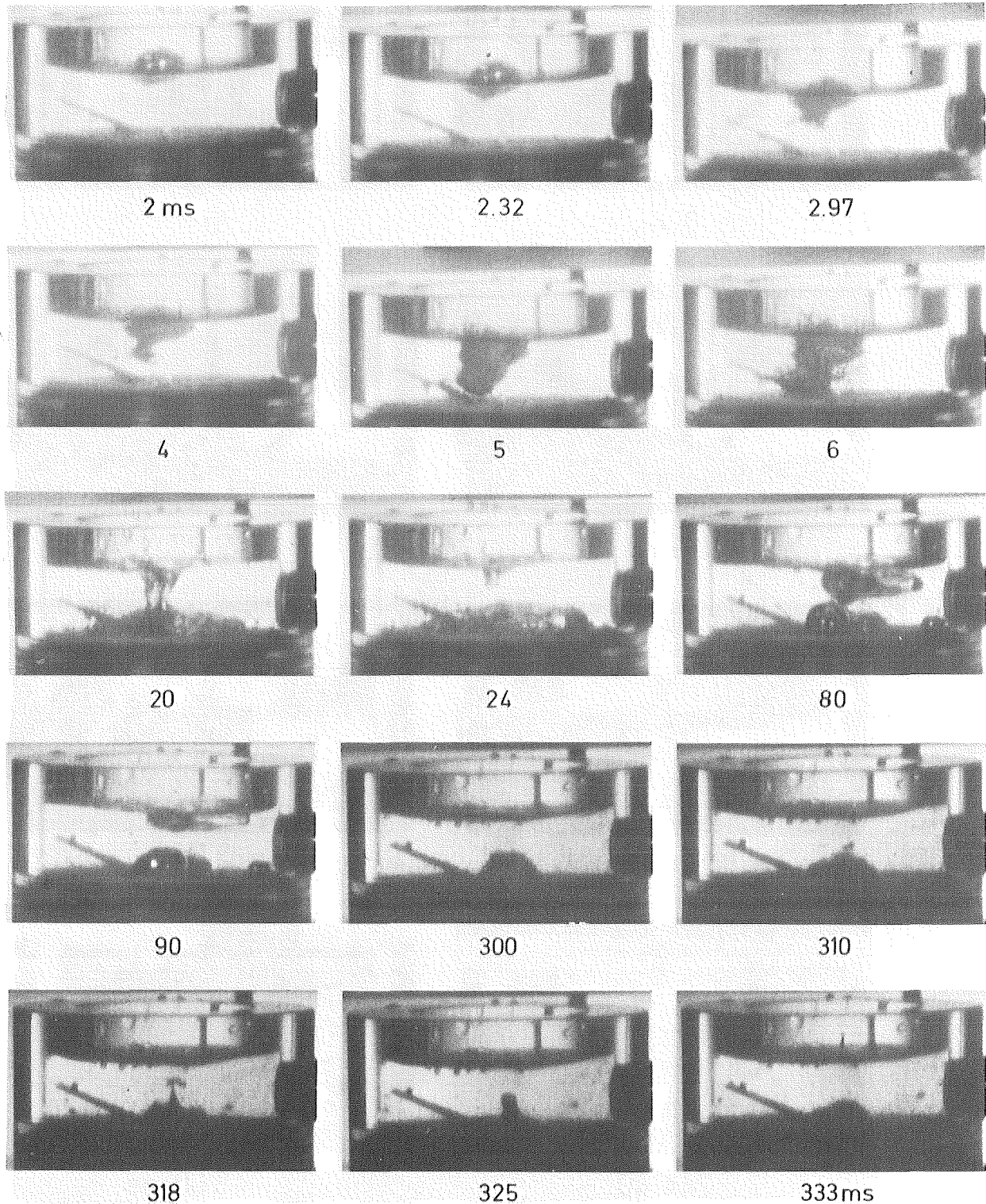


Fig. 20 Development of thermal interaction (Sample 44-04) characterized by double thermal explosion: a small distance below the water surface and at the bottom of the vessel.

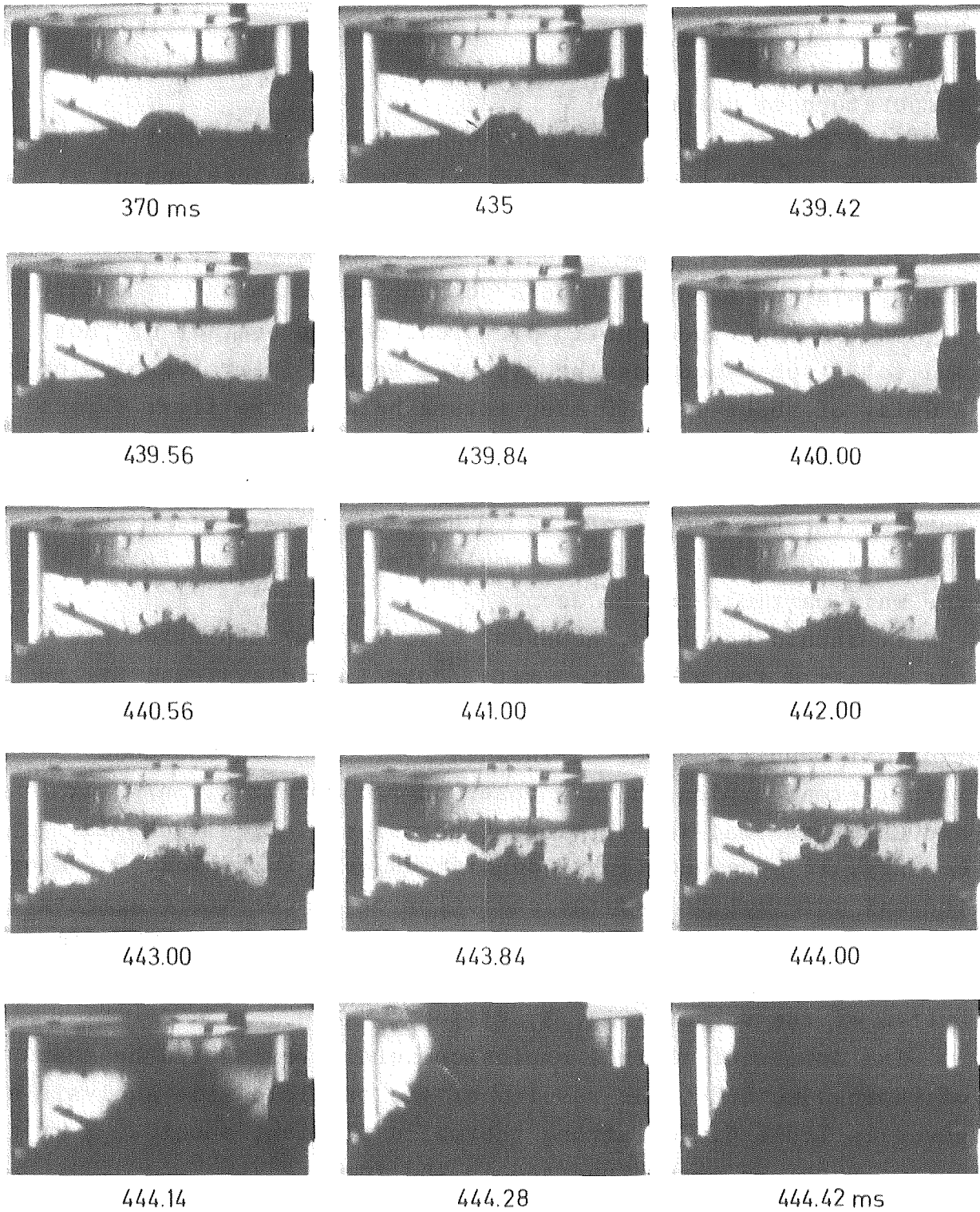


Fig. 21 Continuation of the thermal interaction development for Sample 44-04.

The particle is surrounded by the vapour film. After the time period of about 0.1 to 0.8 sec of the film boiling mode, thermal explosion occurs. One can observe that the temperature slope changes abruptly at a temperature in the range of 1115 to 1400°C, mostly however at a temperature ~1300°C (Table 5). Then, the temperature reading drops almost vertically to a temperature which is close to the solidification temperature of copper.

In Figs. 18 - 21, the corresponding sequences from the high speed movies can be seen of thermal explosion development at the bottom of the vessel. Some period of time after the first contact of the particle with the water surface, the vapour film disappears and the first "jets" of the molten metal is observed.

On the high-speed movie pictures, direct contact of "hot and cold" substances can be expected before thermal explosion. A delay of about 1 to 10 msec exists between the first direct contact and thermal explosion similar to the delay observed before thermal explosion at a small distance below the water surface. At the moment of the "direct contact" between the "hot and cold" substances, a small "initiating jet" from the main particle can be seen.

It should be noted, however, that thermal explosion was not observed for all molten metal/cold liquid systems. Strong thermal explosion was observed for Cu/water thermal interaction, if copper was heated in air. Fragmentation and moderate thermal explosion were observed for Pb/water, Sn/water and Cu/Na thermal interactions. Thermal explosion took place only, if some additional conditions were fulfilled. Sn/water thermal interaction had the character of a moderate fragmentation for the determined range of the initial molten tin temperatures. In such a case, the tin particles grew into a "coral-form" at the bottom of the vessel (Fig. 3, VIII b).

The debris of thermal explosion were investigated by means of various methods. The results of the particle size analysis are given in Table 6. For strong thermal explosion, about 50 % of the copper particle were dispersed in the form

Mesh diameter [ $\mu\text{m}$ ]	Percentage of particles of diameter smaller respectively larger than the noted mesh diameter [ $\% \text{ wt.}$ ]													
	Sample No.													
	37-04	37-10	37-15	38-04	39-05	39-07	40-04	41-09	42-07	43-01	43-04	43-05	43-08	
800	5,5	1,9	21,0	17,8	5,6	17,8	0,1	-	4,9	13,0	3,2	2,1	3,3	
800 500	9,2	2,7	19,4	12,6	1,8	14,2	1,0	0,8	7,3	12,4	7,9	7,5	7,4	
500 200	38,1	39,6	26,3	39,3	22,5	32,8	16,0	23,7	29,8	35,8	37,1	37,7	36,7	
200 100	28,5	8,1	19,3	21,0	37,9	14,2	25,0	30,9	24,2	18,9	27,2	25,3	28,7	
100 80	5,7	8,0	6,3	2,8	9,6	2,4	7,6	9,2	6,6	4,4	0,8	5,7	6,2	
80 50	7,6	2,9	6,6	3,5	12,0	4,0	14,9	14,7	10,1	7,1	12,6	11,2	8,6	
50 30	3,8	1,4	0,7	1,9	9,2	2,1	13,3	13,6	8,8	5,0	7,5	6,6	5,8	
30 10	1,0	33,8	0,4	0,7	1,4	0,9	4,4	6,5	7,0	2,4	2,1	2,8	2,5	
10 0	0,6	1,6	-	0,4	-	11,6	17,7	0,6	1,3	1,0	1,6	1,1	0,8	
$\frac{m_{\text{analysed}}}{m_{\text{total}}}$	0,66	0,55	0,57	0,65	0,67	0,94	0,65	0,67	0,79	0,89	0,76	0,86	0,93	

The measurements were performed at the Institut für Mechanische Verfahrenstechnik of the Universität Karlsruhe (TH).

Table 6: Results of the mesh sieved measurements for various samples after thermal explosion.

of particles less than 100 - 150  $\mu\text{m}$  in size (e.g. samples 37-10, 39-05, 40-04, 41-09, 42-07). Portion of the small particles of less than 10  $\mu\text{m}$  is variable from almost zero (sample 37-15) to about 18% (sample 40-04). It should be noted that the small particles below 10  $\mu\text{m}$  are difficult to collect after the test. (The samples from 39-05 to 43-08 are more representative because of the improved method of debris collecting).

After strong thermal explosion of Cu in water a part of the debris have a spherical form, and part of them have "shattered" form (Fig. 3, IVe). After thermal explosion of Pb the debris have a very similar form (Fig. 3, VII). The debris of Sn/water thermal explosion have the form of shattered pieces usually solidified in a "coral-form" "tree". The fine structure of the "tree" easily breaks down into separate small particles having the form shown in Fig. 3, VIIIb.

Figs. 22 - 29 demonstrate the study by means of scanning microscope. Spherical and "shattered" particles can be found both for debris produced by weak and strong thermal explosions.

In Figs. 30 - 34 the results of the metallographic study are presented. Particles were investigated after weak thermal explosions. An inhomogeneous structure can be observed. Copper oxide dendrites with a coarse and fine structure can be found dispersed in the copper matrix.

The results of chemical analysis of the oxygen content are given in Table 5. They are in agreement with the presence of the copper oxide dendrites, which was shown by the metallographic study.

The results of the total surface measurements (Table 5) are about 200 times larger than the surface one can calculate from the measured particle size distribution if spherical form is assumed. This indicates the porous structure of the debris.

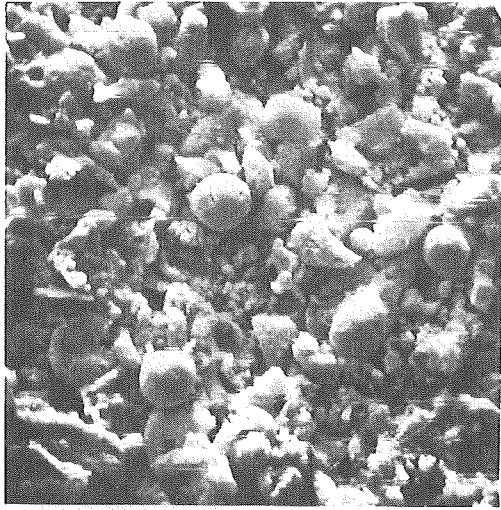
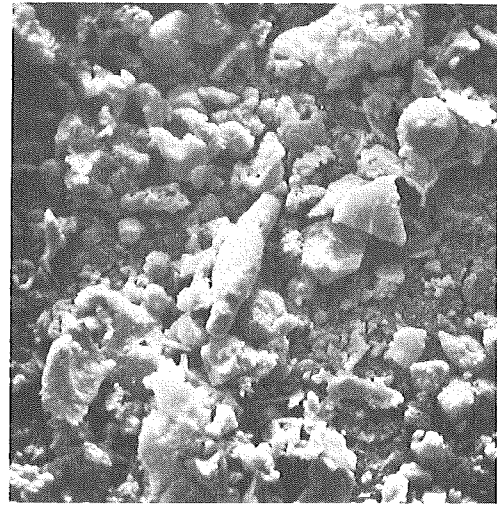
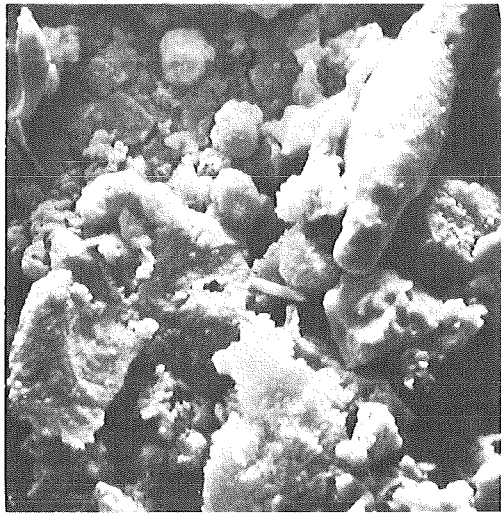
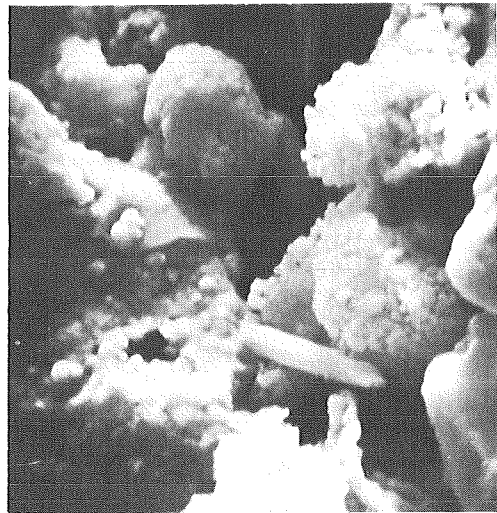
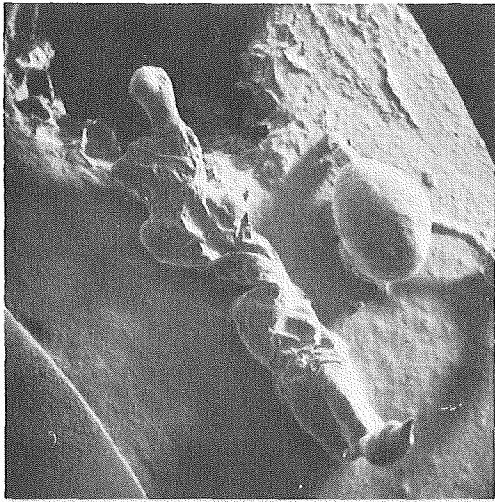
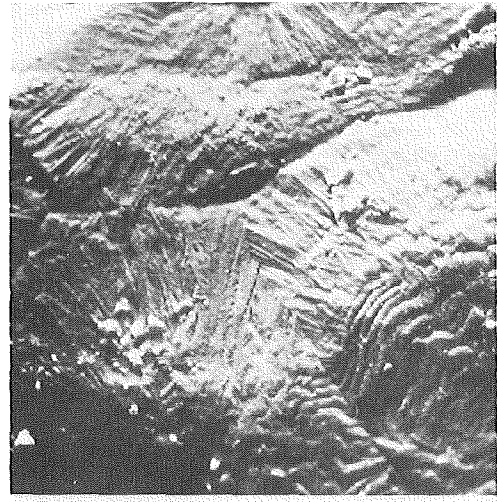
a.  $\longleftarrow$   $\longrightarrow$  25  $\mu\text{m}$ b.  $\longleftarrow$   $\longrightarrow$  25  $\mu\text{m}$ c.  $\longleftarrow$   $\longrightarrow$  10  $\mu\text{m}$ d.  $\longleftarrow$   $\longrightarrow$  5  $\mu\text{m}$ 

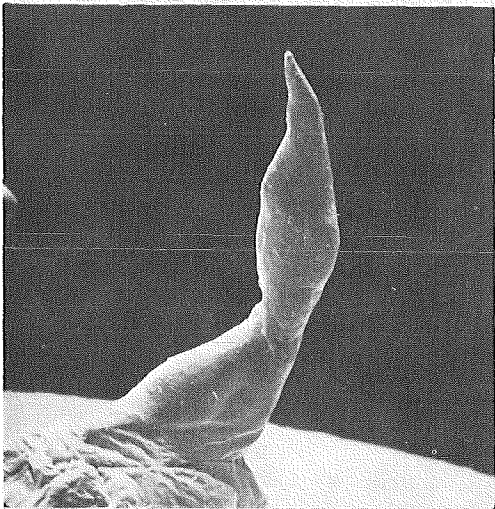
Fig. 22 Microscopic study of thermal explosion debris of particles below 10  $\mu\text{m}$  mesh size (Sample 42-07).



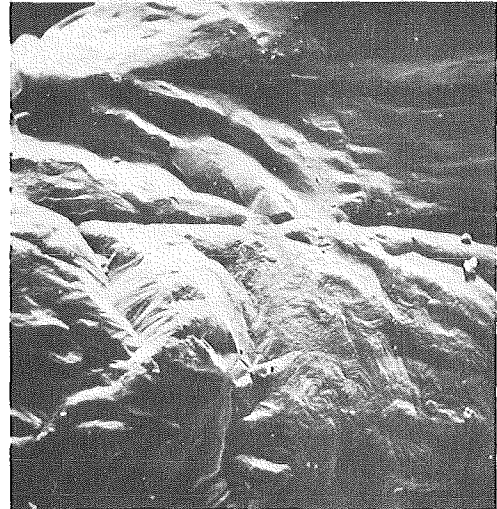
a. |————| 2 mm



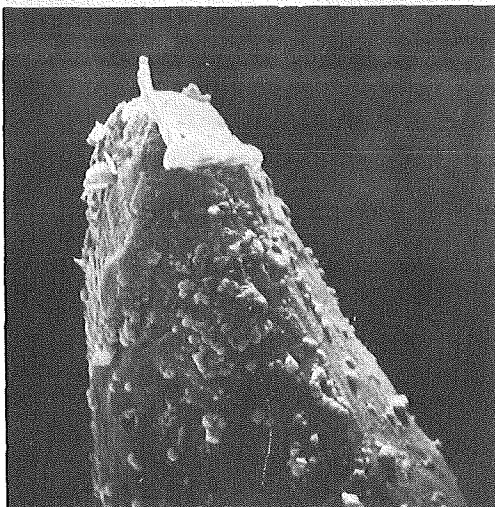
b. |————| 25 μm



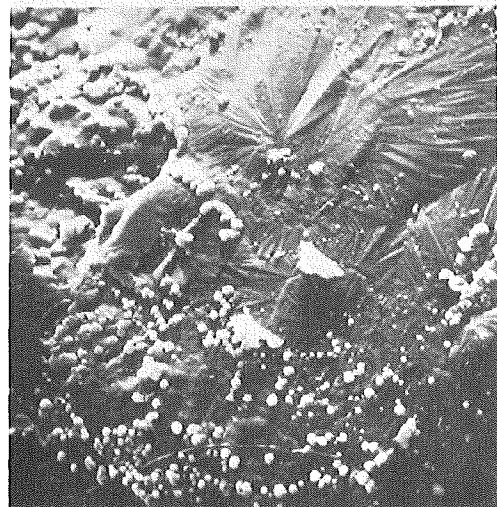
c. |————| 1 mm



d. |————| 250 μm



e. |————| 25 μm



f. |————| 25 μm

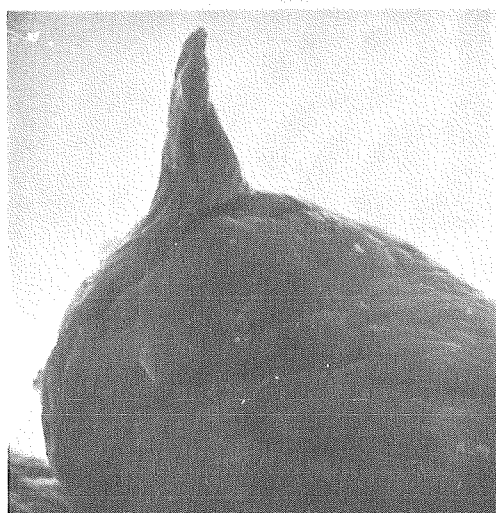
Fig. 23 Microscopic study of weak thermal explosion products (Sample 43-14).



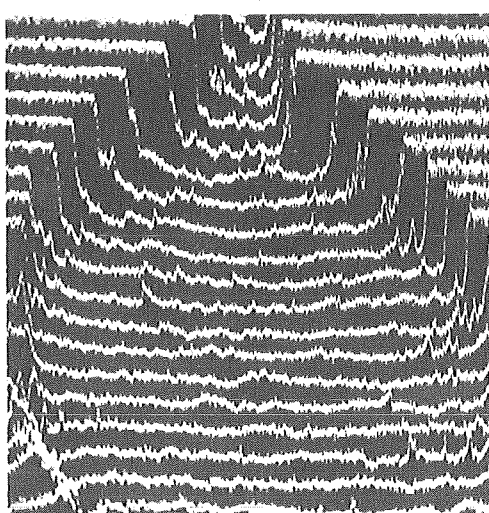
a. |-----| 500 μm



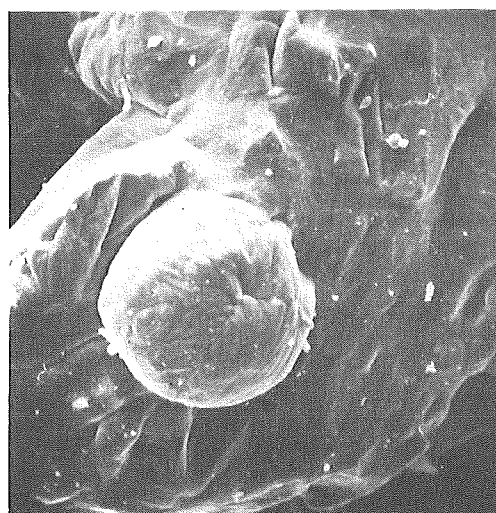
b. |-----| 100 μm



c. |-----| 10 μm



d. |-----| 10 μm

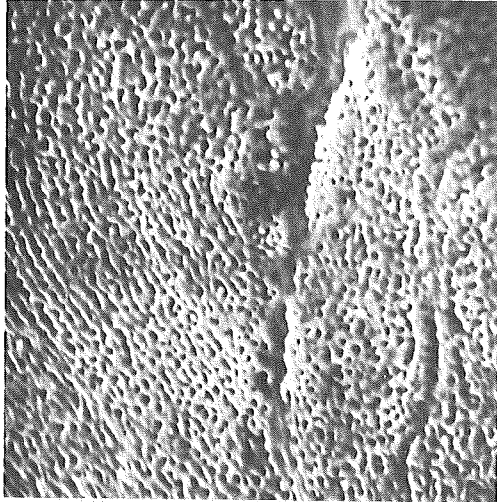


e. |-----| 50 μm

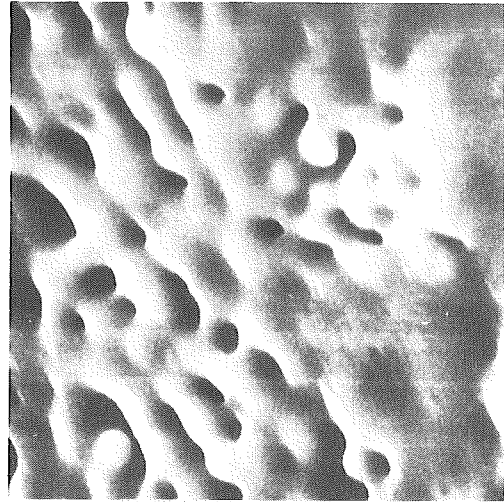


f. |-----| 200 μm

Fig. 24 Microscopic study at the "micro-jet"-origination. Debris of strong thermal explosion (Sample 39-09). d.) gives an intensity profile of the sample shown in c.).

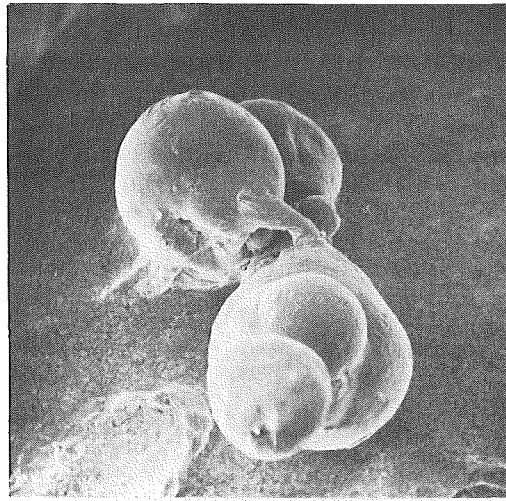


a. ——— 10  $\mu\text{m}$

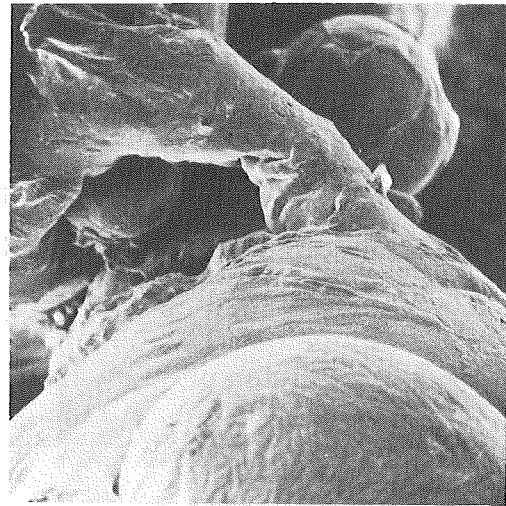


b. ——— 2  $\mu\text{m}$

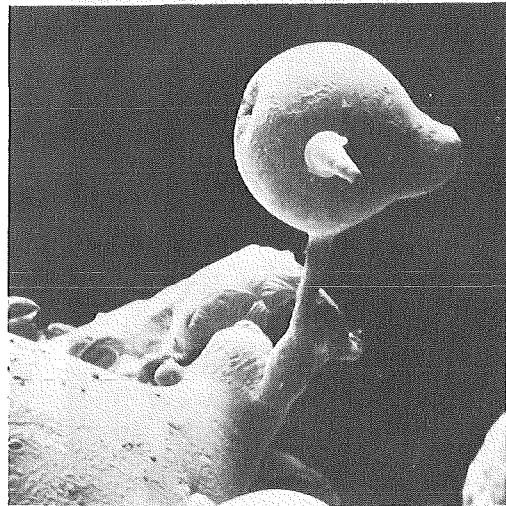
Fig. 25 Microscopic study at the copper particle surface (Sample 43-14).



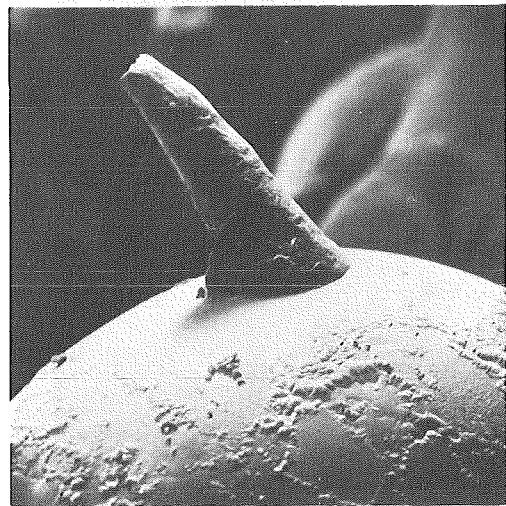
a. |————| 500 μm



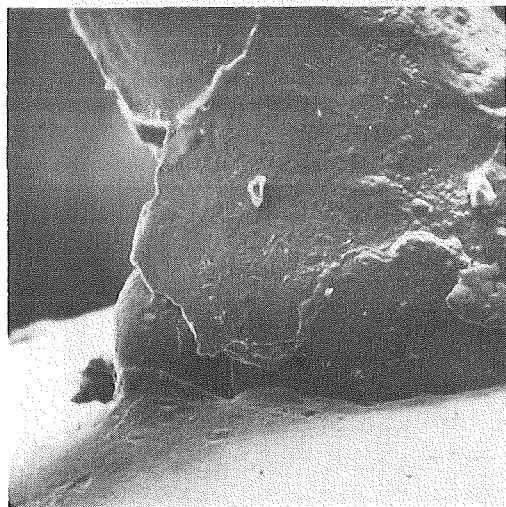
b. |————| 100 μm



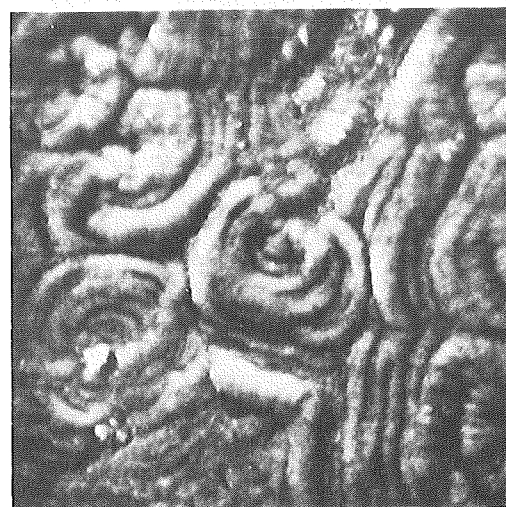
c. |————| 2 mm



d. |————| 500 μm

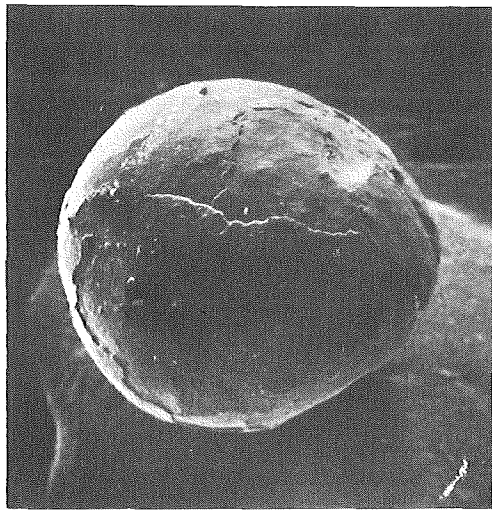


e. |————| 100 μm

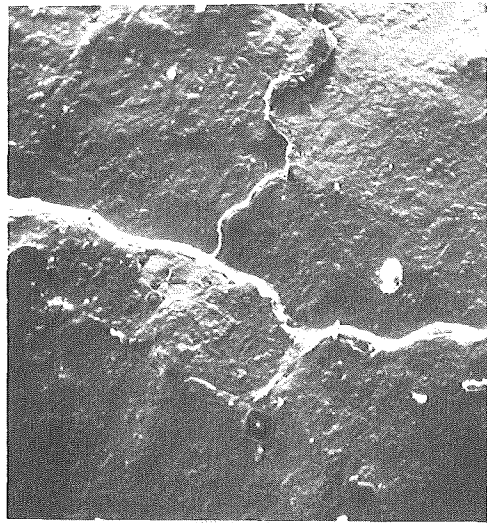


f. |————| 10 μm

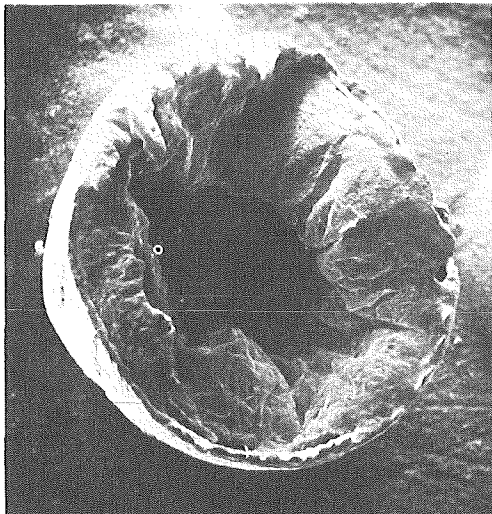
Fig. 26 Microscopic study of a "jet" (Sample 43-14).



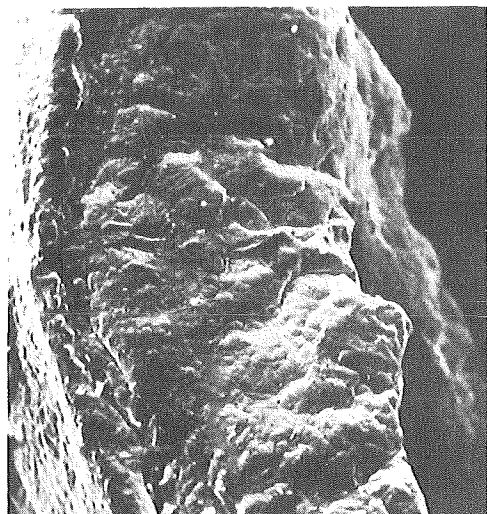
a. |————| 1mm



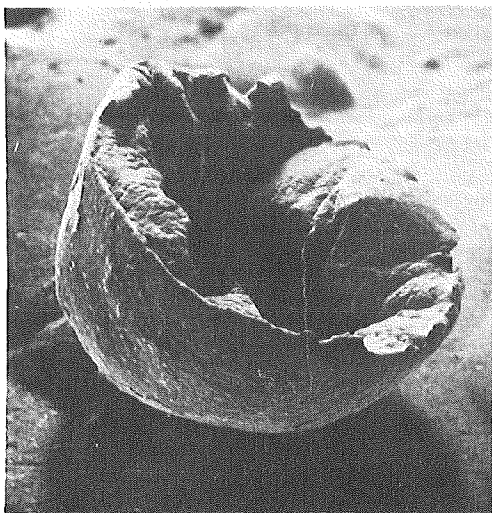
b. |————| 100 μm



c. |————| 1mm



d. |————| 100 μm



e. |————| 1mm



f. |————| 100 μm

Fig. 27 Microscopic study of spherical particle and the surface layer structure (Sample 41-03)

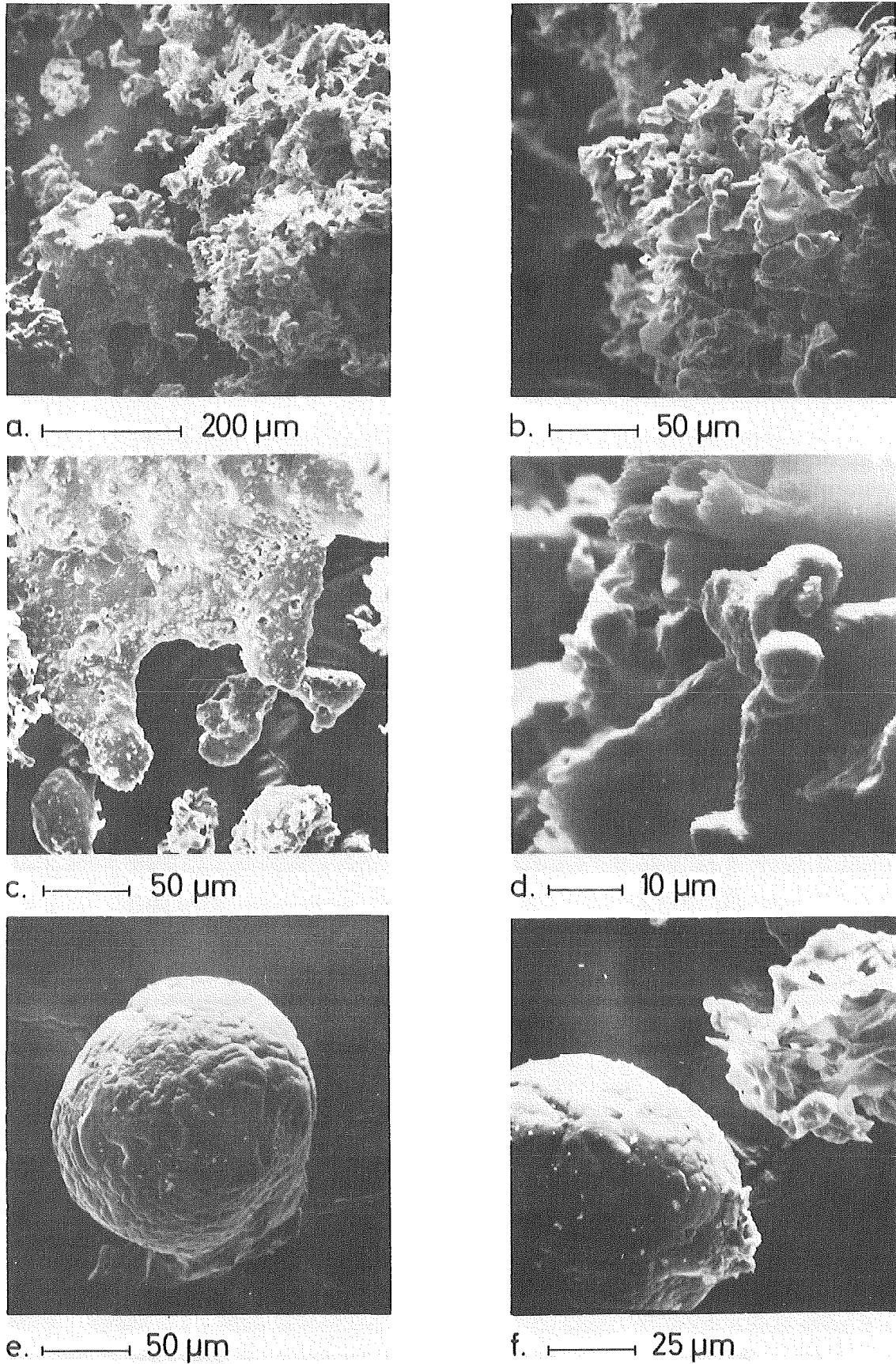
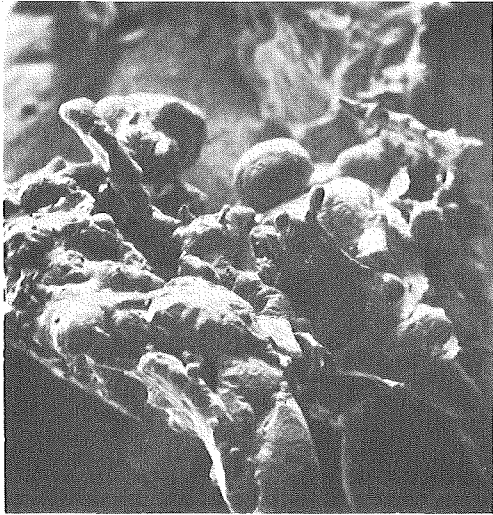
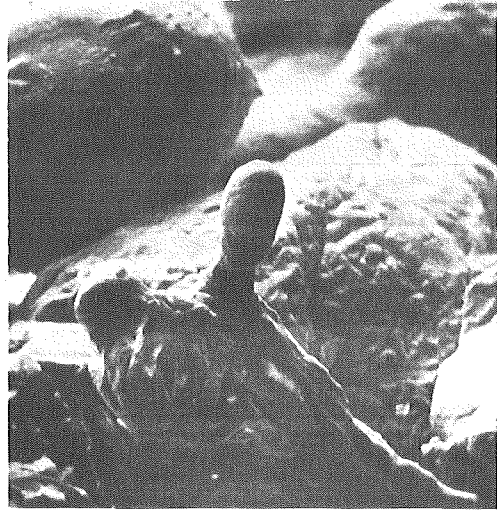


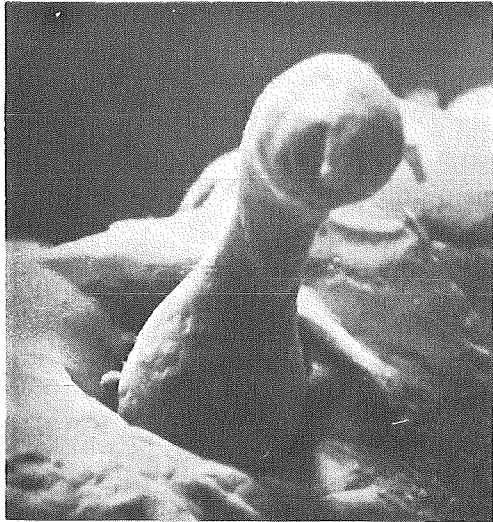
Fig. 28 Microscopic study of thermal explosion debris (Sample 39-07).



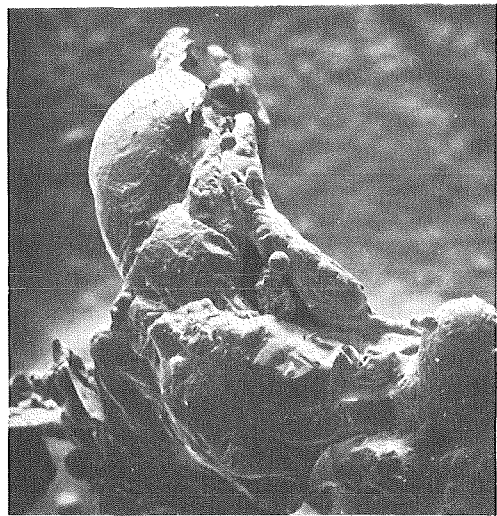
a. |————| 500 μm



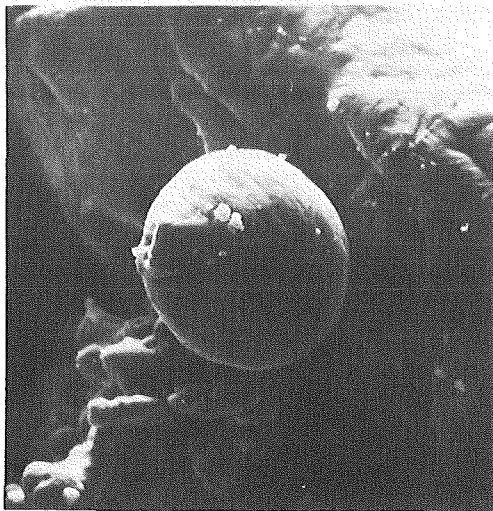
b. |————| 100 μm



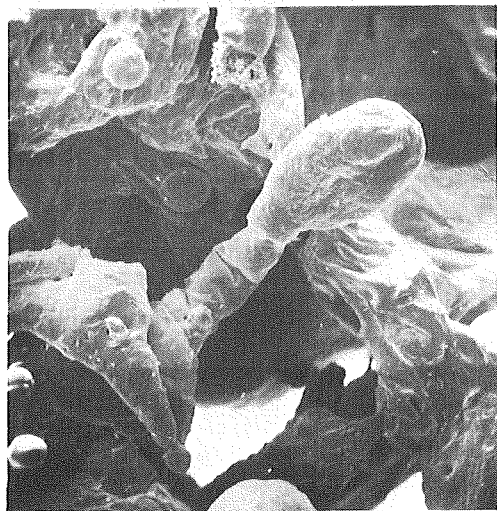
c. |————| 20 μm



d. |————| 250 μm

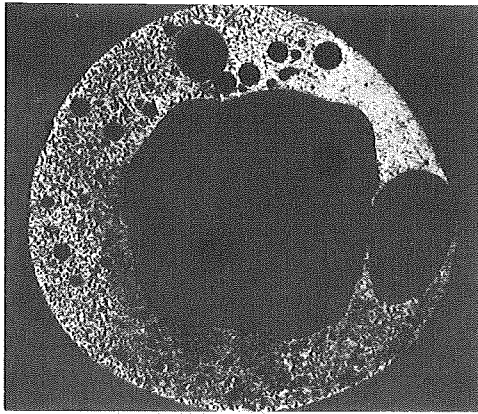


e. |————| 20 μm

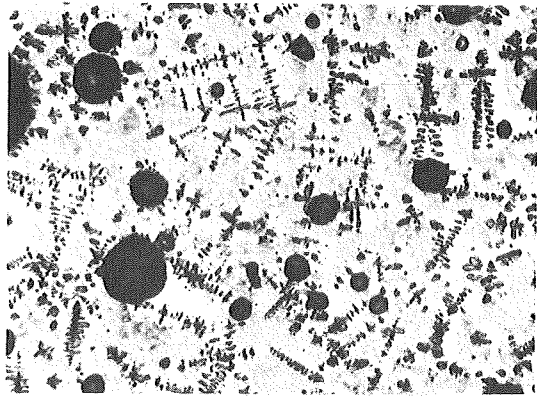


f. |————| 250 μm

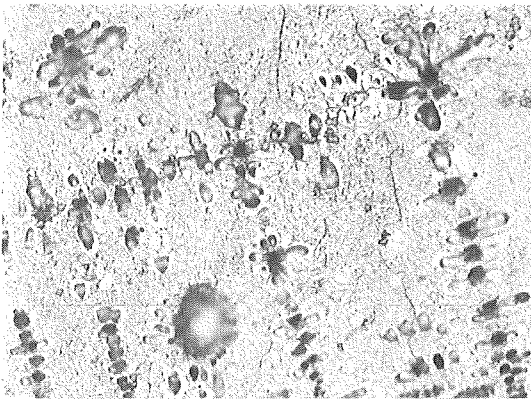
Fig. 29 Microscopic study of thermal explosion debris (Sample 39-07).



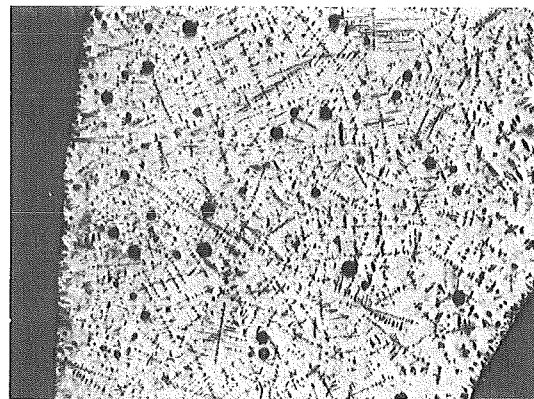
— 1mm



— 100  $\mu$ m



— 20  $\mu$ m



— 100  $\mu$ m



— 20  $\mu$ m

Fig. 30 Metallography of thermal explosion debris (Sample 41-03).

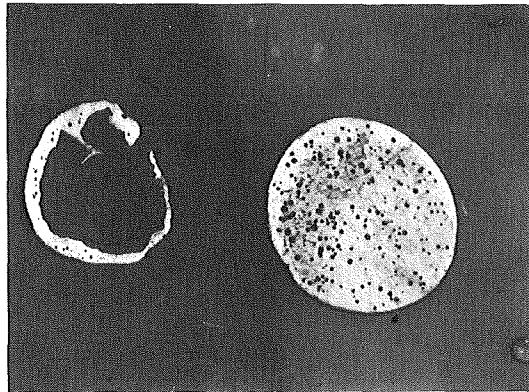
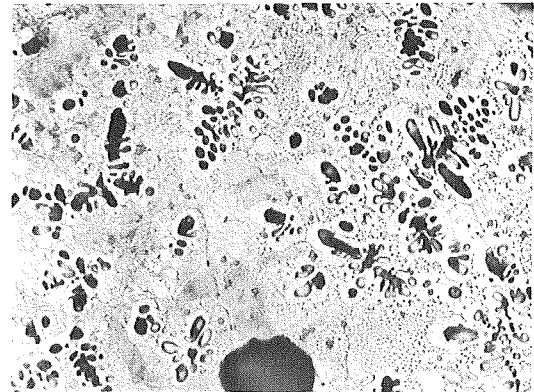
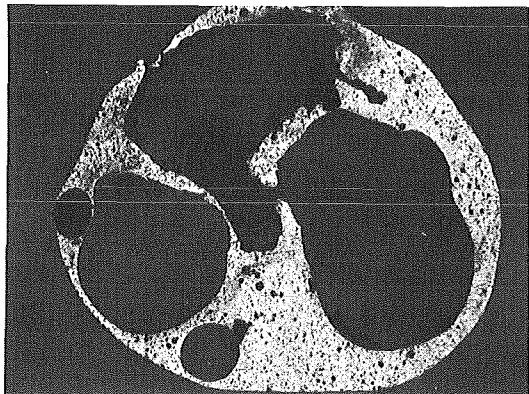
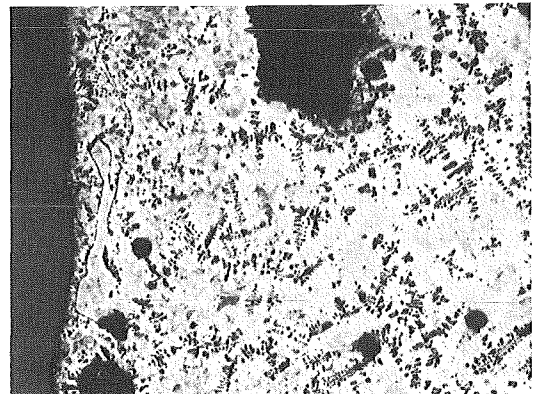
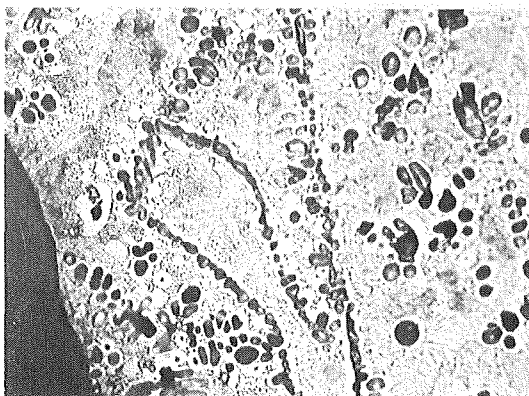
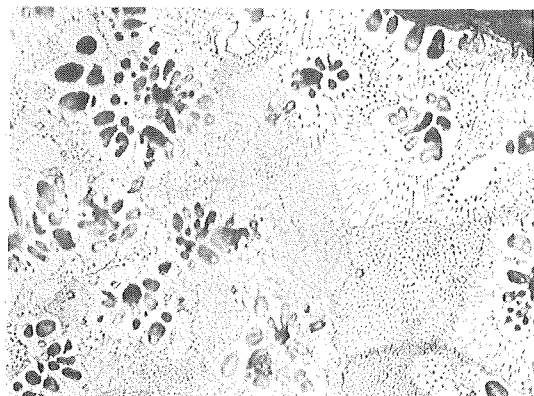
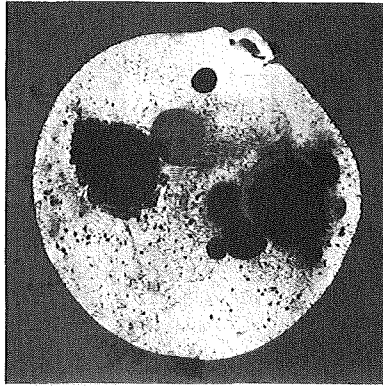
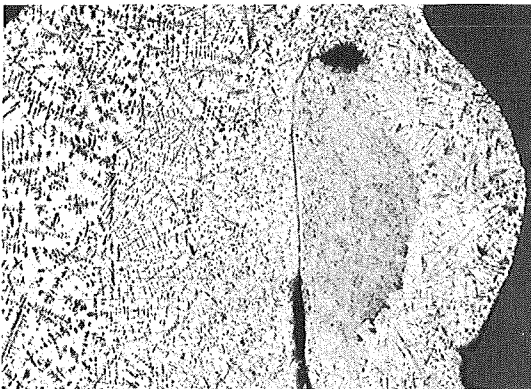
a.  $\longleftarrow$  1mm $\longleftarrow$  20  $\mu$ mb.  $\longleftarrow$  1mm $\longleftarrow$  100  $\mu$ m $\longleftarrow$  20  $\mu$ m $\longleftarrow$  20  $\mu$ m

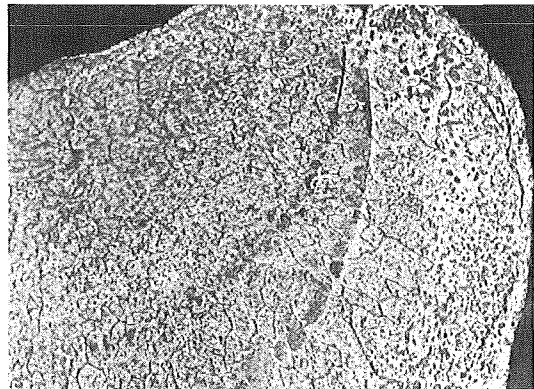
Fig. 31 Metallography of thermal explosion debris (a - Sample 43-11, b - Sample 42-08).



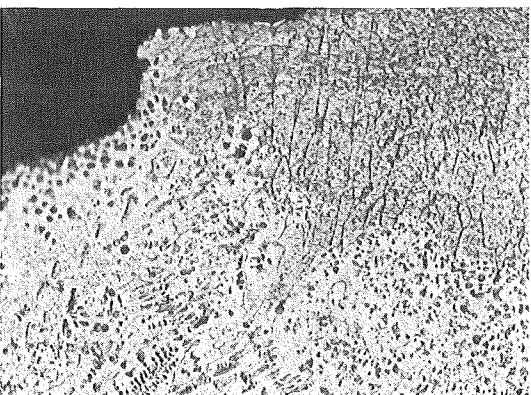
┆ 1mm



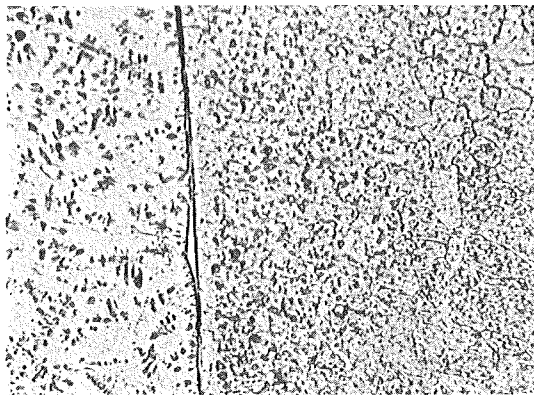
┆ 100μm



┆ 20μm

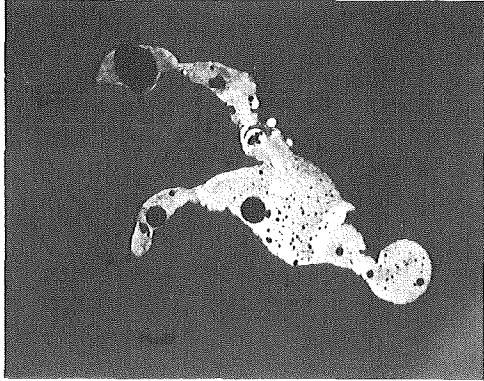


┆ 20μm

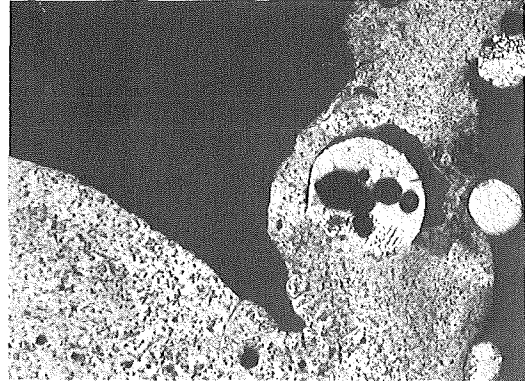


┆ 20μm

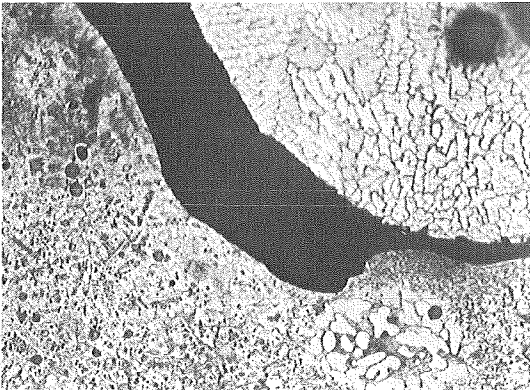
Fig. 32 Metallography of thermal explosion debris (Sample 40-08).



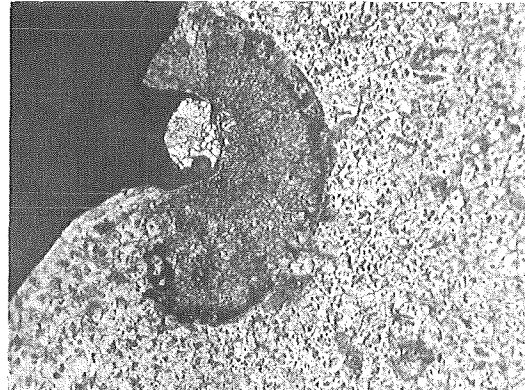
1 mm



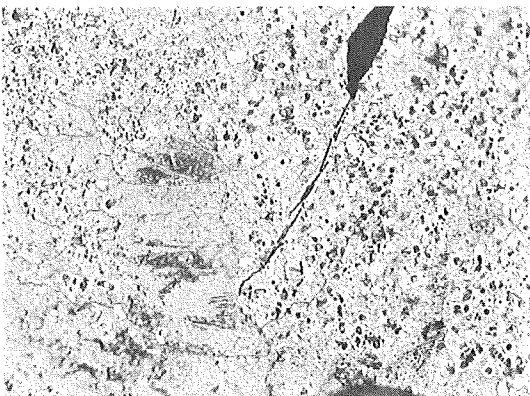
100 μm



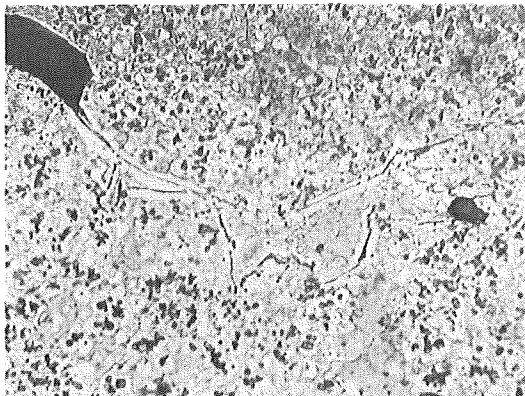
20 μm



20 μm

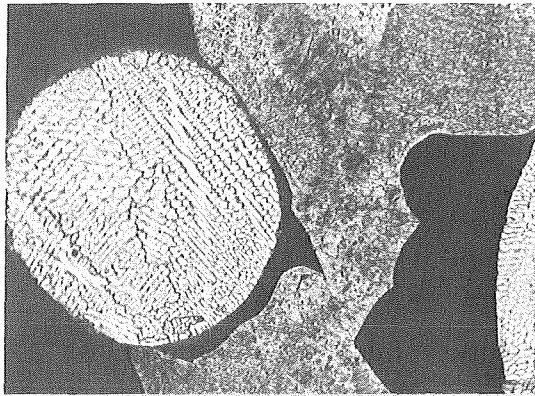


20 μm

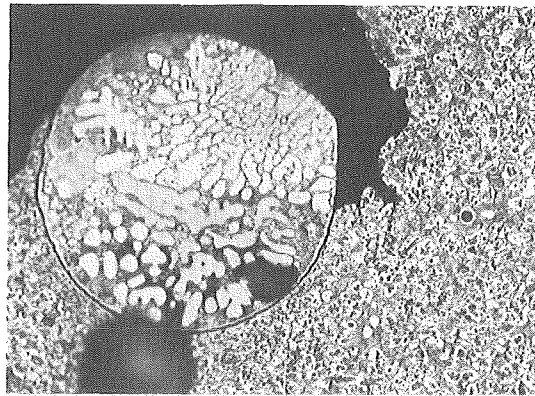


20 μm

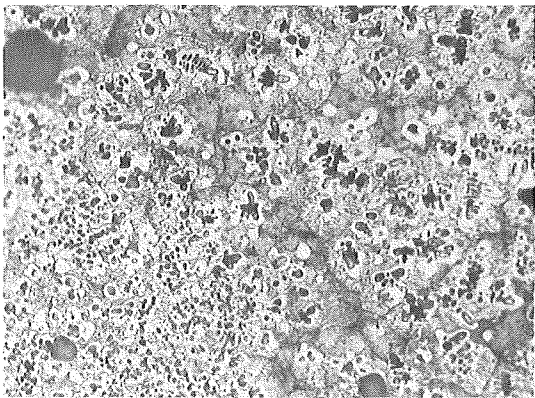
Fig. 33 Metallography of the thermal explosion debris (Sample 43-12).



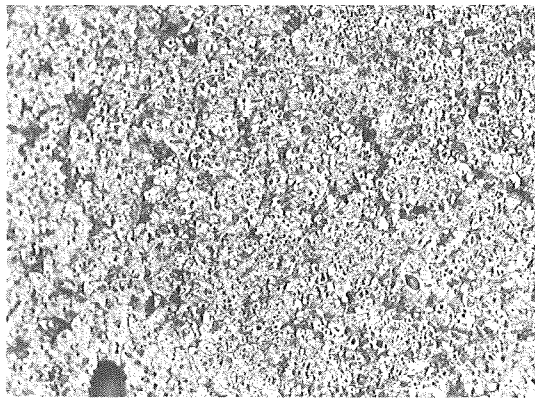
20  $\mu\text{m}$



20  $\mu\text{m}$



20  $\mu\text{m}$



20  $\mu\text{m}$

Fig. 34 Metallography of the thermal explosion debris (Sample 43-12) - continuation.

### 3.3 Special effects

The main special effects observed in these experiments are:

1. hydrodynamic partition;
2. "jets" ("shots") of small particles from the main particle;
3. growth in form of an "empty shell" or "fungus form" particle.

#### 3.3.1 Hydrodynamic partition

Hydrodynamic partition was sometimes observed at the contact with the surface or at the bottom of the vessel. The breakup of the hot particle is due to inertia forces, if they are sufficiently high to overcome the cohesive forces of the particle surface tension. The effect is described by the Weber number. Hydrodynamic partition seems to have no particular influence on other phenomena appearing in these experiments, as e.g. on thermal explosion. Thermal explosion took place already during the fall of the hot particle in the cold liquid, and the event was independent of the partition at the surface of the cold liquid. Similarly, thermal explosion at the bottom of the vessel was observed some time after the contact of the particle with the bottom. Additionally, gold particles broke up easily at the contact with the water surface, but thermal explosion was never observed.

#### 3.3.2 "Jets"

The generation of "jets" ("shots") of small particles expelled from the main particle was often observed in these experiments with respect to Cu/water thermal interaction. The study of fast movie pictures and temperature readings shows that

these "jets" appear only in the course of cooling in some ranges of temperatures, and for Cu/water thermal interaction, if the actual particle temperature lies between  $\sim 1300$  and  $1100^{\circ}\text{C}$ . Usually, these "jets" have the form of small spherical particles,  $\sim 0.1 - 1.0$  mm in diameter and are expelled with  $\sim 25\text{m/sec}$ . Sometimes, however, a "jet" solidifies during the expulsion phase. The picture of the "solidified jet" (Fig. 35) suggests that the heat transfer rate was high during the expulsion of the "jet" from the mass of the hot material, which resulted in its solidification, which means that the local "liquid-liquid contact" is conceivable. The "jet" shown in Fig. 35 has a more complex shape and suggests the existence of a "sequence of sub-jets". The split at the basis of the jet indicates an empty form of the particle and of the "jet".

### 3.3.3 "Empty shell"-particles

Close to the temperature range in which thermal explosion occurs at the bottom of the vessel particles can be observed in the form of an "empty shell" or "fungus form". The cooling temperature history of the "fungus form" particle resembles to a certain degree that of the thermal explosion at the bottom of the vessel. The solidification time is shorter compared to the solidification time of the "normal course" because of the larger surface of the particle. In the temperature range of  $1100$  to  $1400^{\circ}\text{C}$ , some disturbance of the temperature recording can be observed (Fig. 36). The sequence from the film (Fig. 37) shows the growth of the particle at the bottom of the vessel. It seems that a vapour film exists partly at the surface of the particle for some time after the start of particle solidification.

FIG. 35 PICTURES OF THE "JET" FROM THE COPPER PARTICLE ( ENLARGEMENT  $\sim 80$  TIMES )



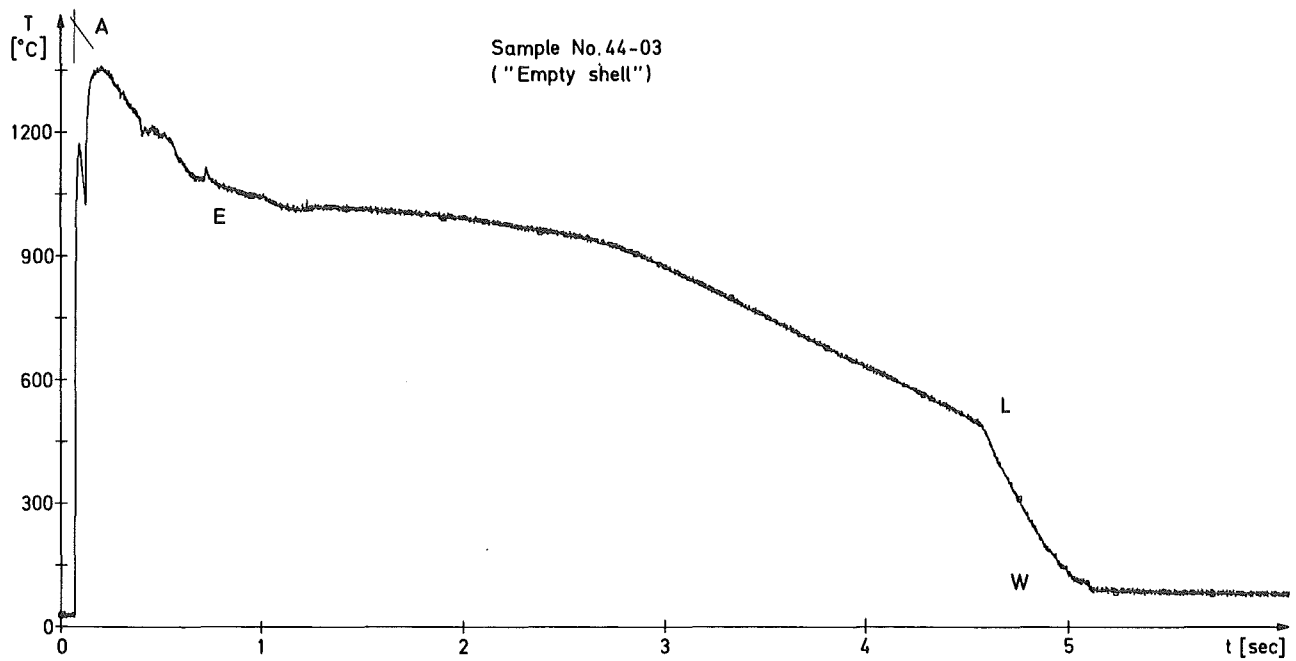
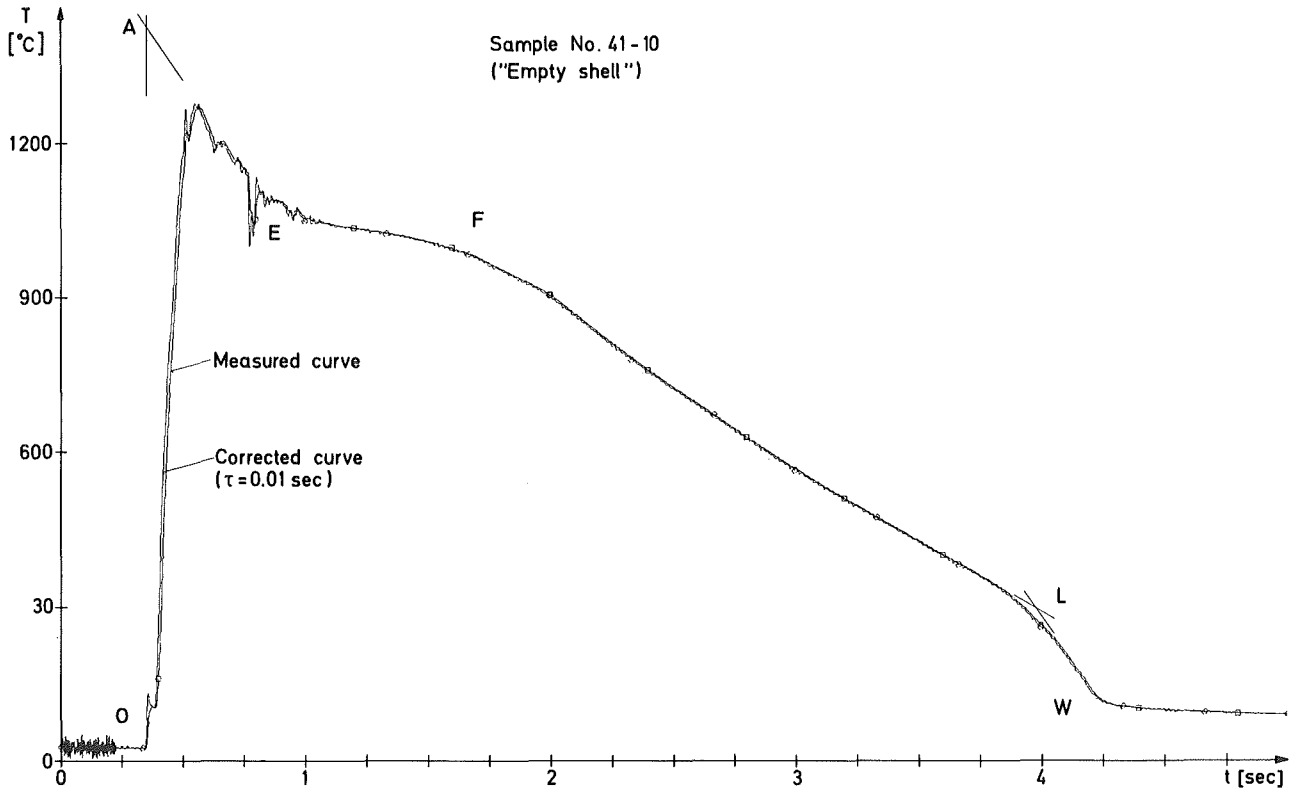


Fig. 36 Temperature histories taken during "empty shell"-origination (Samples 41-10 and 44-03).

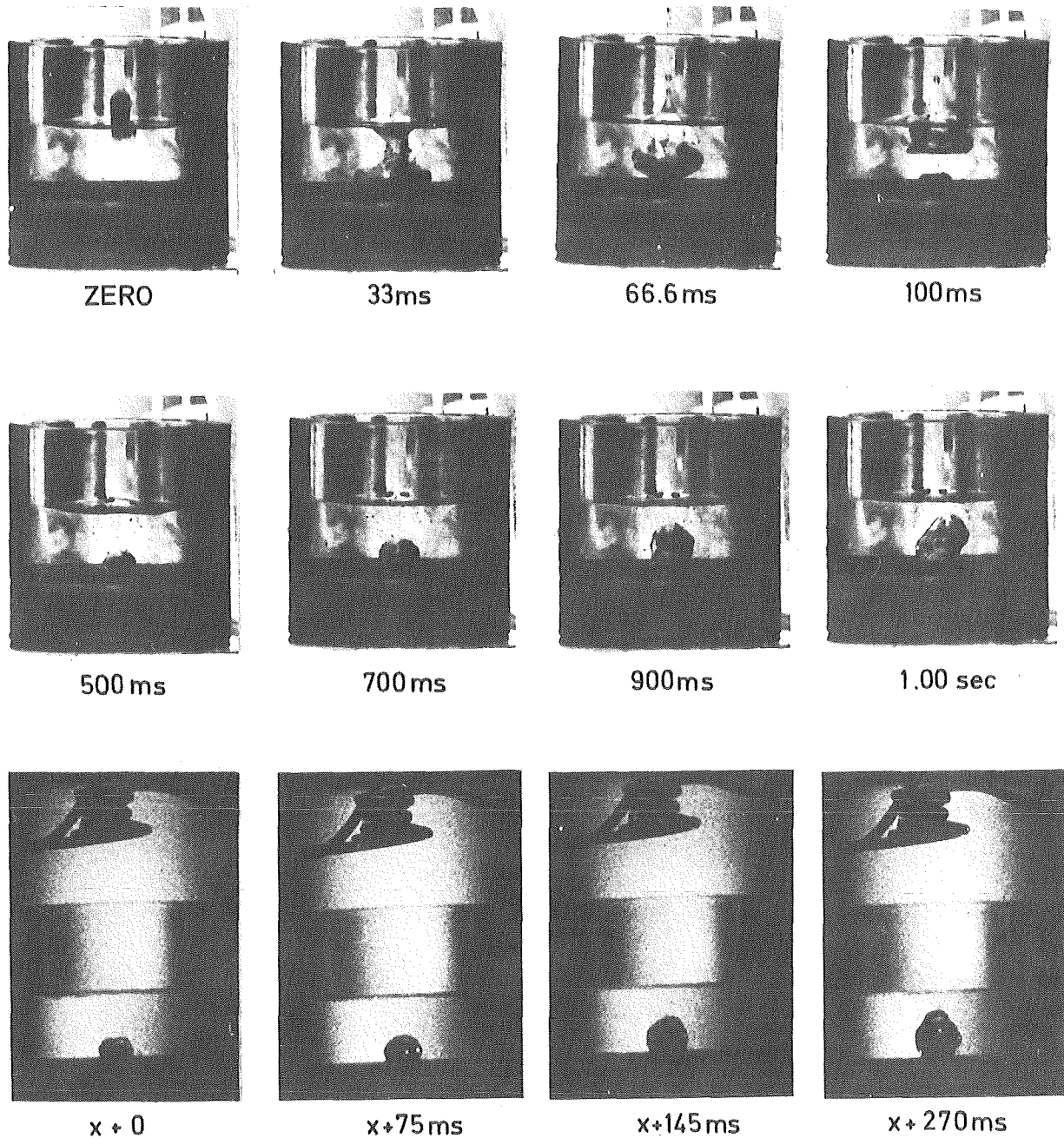


FIG.37 SEQUENCE FROM THE FRAME CAMERA FILM AND HIGH SPEED FILM SHOWING GROWTH OF THE "EMPTY SHELL" PARTICLE. COPPER IN WATER.

$T_{\text{bott}} = 1467\text{ }^{\circ}\text{C}$ ,  $T_0 = 21.3\text{ }^{\circ}\text{C}$ ,  $m_{\text{Cu}} = 0.5482\text{g}$ . SAMPLE NO.13-36.

#### 4. Conclusions

Extensive experimental material has been obtained from these experiments which relates to the main phenomena occurring during thermal interaction of molten metals with a relatively cold liquid (water). The theoretical interpretation of the experiments is presented elsewhere [15 - 19]. Measurements of the "normal course" of heat transfer allowed to study the heat transfer intensity (heat flux and heat transfer coefficient [14, 17]) and to determine the Leidenfrost temperature [18] for the copper/water system.

Results concerning thermal explosion allow the description of the thermal explosion stages and the determination of its triggering mechanism [17, 19]. The most significant observation is that small "jets" from the main particle mass occurring 1 to 10 msec before, precede thermal explosion. It seems that the processes occurring in the hot particle trigger the phenomenon.

## 5. References

- [1] L. Caldarola - Current Status of Knowledge of Molten Fuel/Sodium Thermal Interactions, KFK 1944 (EUR 4973e), Febr. 1974
- [2] J. van Audenhove - Vacuum Evaporation of Metals by High Frequency Levitation Heating, the Review of Scientific Instruments, Vol. 36, No. 3 (1965), pp. 383-385.
- [3] J. van Audenhove, J. Joyeux - The Preparation by Levitation Melting in Argon of Homogeneous Aluminium Alloys FDR Neutron Measurements, Journal of Nuclear Materials, Vol. 19, (1966), pp. 97-102
- [4] E. Burck, W. Hufschmidt, E. de Clercq - Instationäre Wärmeübertragung beim Sieden von Wasser an der senkrechten Wand eines Reaktordruckbehälters, Atomkernenergie, Vol. U, (1973), pp. 127-135
- [5] E. Fromm, H. Jehn - Das Schwebeschmelzverfahren, Z. Metallkde, Vd. 58, No. 6, (1967), pp. 366
- [6] G. Gomentz, J.W. Salatka - Ten - Gram Levitation - Melted Ignots, J. of Electrochem. Soc., Vol. 105, (1958), pp. 673-676.
- [7] S.S. Kutateladze, V.M. Borishanskii - A Concise Encyclopedia of Heat Transfer, Pergamon Press, Oxford, 1966, pp. 1-489.
- [8] G. Rittirsch - Kriterien zur Wahl der Meßfilter und Abtastfrequenz sowie Methoden zur Meßfehlerkorrektur, angewandt bei Temperaturmessungen in Natrium, GfK Karlsruhe, Externer Bericht 8/71-3, (1971), pp. 1-24.
- [9] J.W. Stevens, L.C. Witte - Transient Film and Transition Boiling from a Sphere, Int. J. Heat Mass Transfer, Vol.14, (1971), pp. 443-450.

- [<sup>-</sup>10\_] L.C. Tao - Generalized Numerical Solution of Freezing a Saturated Liquid in Cylinders and Spheres, Aiche Journal, Vol. 13, (Jan. 1967), pp. 165-169.
- [<sup>-</sup>11\_] H. Will, W. Żyszkowski - Untersuchungen zur thermischen Wechselwirkung zwischen geschmolzenen Metallen und Flüssigkeit, KFK 1273/4 (EUR 4974 d), pp. 123-29 to 123-33, (1974).
- [<sup>-</sup>12\_] H. Will, W. Żyszkowski - Thermal explosion during copper-water thermal interaction, GfK Karlsruhe, IRE, June 1975. Sound film.
- [<sup>-</sup>13\_] W. Żyszkowski - On the Mechanism of Heat Transfer at a Strong Accident in the Reactor Core, Int. Meet. on Reactor Heat Transfer, ANS Local Section in Central Europe, Karlsruhe, Oct. 9-11, 1973, Paper 46, pp. 962-974.
- [<sup>-</sup>14\_] W. Żyszkowski - Experimental-Theoretical Investigation of the Thermal Explosion, Second Specialist Meeting on Sodium Fuel Interaction in Fast Reactors, Ispra, 21-23 Nov., 1973.
- [<sup>-</sup>15\_] W. Żyszkowski - On the Initiation Mechanism of the Explosive Interaction of Molten Reactor Fuel with Coolant, ANS Topical Conf. on Fast Reactor Safety, Beverley Hills, Calif., Apr. 2-4, 1974, pp. 897-909.
- [<sup>-</sup>16\_] W. Żyszkowski - Hipoteza mechanizmu eksplozji cieplnej, Symp. PAN n.t. Termodynamiki, Jablonna 1974 (in Polish) pp. 357-363.
- [<sup>-</sup>17\_] W. Żyszkowski - Thermal Interaction of Molten Copper with water, Int. J. Heat Mass Transfer, Vol. 18, No. 2, (1975), pp. 271-287.

- [<sup>-</sup>18\_] W. Żyszkowski - On the transplosion phenomenon and the Leidenfrost temperature for the molten copper-water thermal interaction, Int. J. Heat Mass Transfer, in preparation.
- [<sup>-</sup>19\_] W. Żyszkowski - Study of the thermal explosion phenomenon for the molten copper-water system, in preparation.
- [<sup>-</sup>20\_] M. Andoux, F.W. Katz, W. Olbrich, E.G. Schlechtendahl - SEDAP. An Integrater System for Experimental Date Processing, KFK 1594 (EUR 4730e), (1973), pp. 1-242.

## Appendix 1 Levitation heating

The levitation force in the levitation coil is described by the following formula [5, 6]:

$$F_L = 1.5 \pi \mu I^2 r^3 G(x) L_F \quad (\text{A.1})$$

where I - electric current in the levitation coil;

$\mu$ , r - permeability and radius of the levitating particle, respectively;

G(x) - function which describes "skin effects" of the electric current in the levitating particle [6] ( $x = r/\delta$ , where  $\delta$  is the depth of the "skin effects" and  $\delta = \sqrt{\rho_0 / \pi \mu f}$ ,  $\rho_0$  is the electric resistance of the levitating particle, and f is the electric current frequency);

$L_F$  - parameter which describes the geometrical relation between the levitating particle and the levitation coil (determined experimentally).

The power input to the particle in the levitation coil is described by the following formula [5]:

$$P = 3 \pi \rho_0 I^2 r F(x) L_N \quad (\text{A.2})$$

where F(x) and  $L_N$  are analogous to the G(x)-function and  $L_F$  in the foregoing formula [5].

The levitation force and the power input to the particle in the levitation coil can be varied by changing the size of the levitating particle, the current frequency, the current intensity or the form of the levitation coil. A disadvantage is that both quantities change simultaneously. This causes problems with respect to the stability of the particle in the levitation coil and/or

problems regarding the temperature of the particle. The most important advantage of the method is that the particle is heated homogeneously and without a contact with a crucible.

This method has been successfully applied to the production of small homogeneous samples of extremely pure alloys. Many substances, mainly metals, have been levitated and molten [1,2,5,6,7]. In this experiment, the levitation technique was used to study heat transfer phenomena.

## Appendix 2: Temperature lag of thermocouples

The measurement of the fast temperature changes should be proportional to the signals, i.e.

$$x_a (\tau) = \text{Const. } x_e (\tau) \quad (\text{A.3})$$

where  $x_a (\tau)$ ,  $x_e (\tau)$  are measured and real values respectively of the temperature as a function of the time  $\tau$ . The temperatures recorded during fast changes are nevertheless liable to be erroneous to a considerable extent. The thermal behavior of the inertia of the thermocouples, a quantity strongly dependent on the element, is responsible for this error.

Assuming linearity, the dynamic dependence

$$x_a (\tau) = f (x_e (\tau)) \quad (\text{A.4})$$

can be described by the following differential equation with constant coefficients:

$$\begin{aligned} A_n x_a^{(n)} + A_{n-1} x_a^{(n-1)} + \dots + A_2 \ddot{x}_a + A_1 \dot{x}_a + A_0 x_a &= \\ &= B_0 x_e + B_1 \dot{x}_e + B_2 \ddot{x}_e + \dots + B_m x_e^{(m)} \end{aligned} \quad (\text{A.5})$$

where the point means differentiation for time  $\tau$ .

For practical calculations, the foregoing equation was reduced to the simple form:

$$C_1 x_a = \tau_T \dot{x}_e + x_e \quad (\text{A.6})$$

where  $\tau_T$  means the temperature lag and  $C_1$  means a proportionality constant.

It should be mentioned, that in these equations the deadtime is neglected.

Table A.1 Experimental values of the thermometric lag of the thermocouples used in these experiments

Type of the thermocouple and the outside diameter		$T_u$ msec		$\tau_T$ msec		Scatter of results $S_p = \text{max/min}$		Remarks
		min	max	min	max	$T_u$	$\tau_T$	
TM	0.5	2.7	5.0	6.2	14.2	1.8	2.3	Thermocouple: Ni Cr - Ni
TM	1.0	4.7	7.0	20.6	31.8	1.5	1.35	Sheat material: DIN 4301
TI	0.5	5.1	12.0	17.3	25.5	2.35	1.47	Insulating material: MgO.
TI	1.0	11.5	16.2	44.8	57.2	1.4	1.27	All values measured in sodium.

The values of  $\tau_T$  depend to the type of thermocouple and are given in table A.1 for thermocouples used in this experiment. The table also indicates the values of the thermometric lag  $T_u$ . It should be mind, that the given values are from measurements in liquid sodium (about 300°C). The values for thermocouples in copper may be different.

The transient character of the phenomenon and the temperature lag of the thermocouple influence the temperature readings. The nature of contact between the thermocouple and the hot material changes during thermal interaction (At first, wetting of the thermocouple by the hot material; after fragmentation, contact with the thermal explosion zone) and it is difficult to define one single constant thermometric lag for the whole period of thermal interaction.